

THE ROLE OF MAPK AND AKT SIGNALING DURING ZEBRAFISH
OLFACTORY EPITHELIUM REGENERATION

by

Zeynep Dokuzluođlu

B.S., Molecular Biology and Genetics, Bođaziđi University, 2020

Submitted to the Institute for Graduate Studies in
Science and Engineering in partial fulfillment of
the requirements for the degree of
Master of Science

Graduate Program in Graduate Program in Molecular Biology and Genetics
Bođaziđi University

2022

ACKNOWLEDGEMENTS

I might be the sole official author of this work, but it is far from reality. I was incredibly lucky to be supported by many people that surrounded me. Among all people, I'm grateful to my thesis advisor Stefan Fuss, who is an excellent role model as a researcher and as a lecturer for pushing me to become a better writer, presenter, and thinker not only in the thesis process but from the very beginning when I joined the lab as an undergraduate student. In those days, I was lucky to have Yiğit as a very patient guide who has been there in the late hours of experimenting while I was being clumsy and even intolerable. I was also lucky to have Mehmet Can, and I knew I can ask whatever stupid question and still get an answer anytime I needed it. I'd also like to thank Aysu for sharing her expertise for injections with me multiple times and being there for my weirdest formatting questions for the thesis. I cannot overstate the mental support I've gotten from Şiran both as a friend who always provides sugary treats and as a lab mate whom I can always discuss my results with during my time at the lab, without her, the lab could've easily been unbearable for me. I'm also thankful to past and current lab members Sinay, Hatice, Ebru, Su, Ecem, Gökberk, and Kardelen for their friendship and help with all the tiring lab errands. Finally, I'd like to thanks to all the MBG members, and specifically Emre for his friendship when I needed a breath from everything. I'm also thankful to my family that supported me no matter how negligent I was getting during the process and to my mom for being a model of the strong independent woman I'm trying to be. Last but not least, I'm indebted to my partner in life Kübra for her smile, her positive attitude when I never came at the time I promised because of all the chaos in the lab, for believing me and motivating me when I did not have the energy, and making life an absolute joy despite whatever goes on in the world.

The work presented in this thesis has been supported by The Scientific and Technological Research Council of Turkey (TÜBİTAK) through research grant 119Z081 to SHF.

ABSTRACT

THE ROLE OF MAPK AND AKT SIGNALING DURING ZEBRAFISH OLFACTORY EPITHELIUM REGENERATION

The zebrafish olfactory epithelium (OE) is a neuroepithelium that is able to regenerate neurons. The ability of the OE for neuron regeneration stems from the presence of a dual progenitor system that persists to the adulthood and consists of globose basal cells (GBC) and horizontal basal cells (HBC). In this dual system, GBCs compensate for daily loss of neurons while HBCs are dormant but activated upon injury to regenerate neurons. Transcriptome profiling of the damaged OE revealed upregulation of the HB-EGF in an early phase of regeneration and suggested a regulatory role in OE regeneration. Pharmacological inhibition of HB-EGF signaling and its receptor EGFR in addition to exogenous stimulation of HB-EGF confirmed the regulation of regeneration by HB-EGF:EGFR interaction. However, cell types regulated by the binding of HB-EGF to EGFR, and cellular signaling pathways that mediate its pro-regenerative effect needed further investigation. In this work, roles of MAPK/ERK and PI3K/AKT signaling pathways which are both well-established to regulate cell fates were studied in the context of OE regeneration. For this purpose, loss of function approaches with pharmacological inhibitors of these pathways were followed by investigating their activity in regenerating OE through phosphorylated isoforms. These experiments revealed that MAPK/ERK signaling is the downstream effector of HBEGF:EGFR interaction in cells most likely to be HBCs and it is necessary for recovery of neurons. Despite the fact that PI3K/AKT pathway was also active in these cells, PI3K/AKT signaling was not found to be necessary for functional OE regeneration and it is proposed to stimulate cell cycle progression by promoting cellular growth.

ÖZET

MAPK VE AKT SİNYAL YOLAKLARININ ZEBRABALIĞI OLFAKTÖR EPİTELİ REJENERASYONUNDAKİ ROLLERİ

Zebrabalığı olfaktör epitel (OE) nöro-epitel bir doku olup ölen nöronlarını yenileyebilme edebilme kapasitesine sahiptir. OE bu gücünü iki tip öncül hücrelerin yetişkinlikte var olmasından almaktadır. Bu hücrelerden yuvarlak bazal hücreler rutin bir şekilde ölen nöronları telafi ederken, yatay bazal hücreler yalnız ağır hasar durumlarında uyanıp yeni nöron üretimine önemli katkılar sağlamaktadır. Hasarlı OE'lerin transkript analizi, heparin-bağlayıcı epidermal büyüme faktörünün erken bir safhada arttığını göstererek, HB-EGF'nin OE rejenerasyonunda düzenleyici bir rolü olması ihtimalini doğurmuştur. Bu ihtimal önceki araştırmalarda HB-EGF ve onun reseptörü EGFR'nin engellenmesiyle rejenerasyonun da engellendiğini göstererek bu hipotezi doğrulamıştır. Fakat HB-EGF'in hangi hücrelerdeki EGFR'a bağlanarak ve hangi sinyal yollarını aktive ederek bu rejeneratif etkiyi yarattığı bilinmemektedir. Bu çalışmada MAPK/ERK and PI3K/AKT sinyal yolları farmakolojik olarak inhibe edilmiş ve rejenerasyon sürecinde olan OE'lerde aktiviteleri fosforile olmuş versiyonları üzerinden araştırılmıştır. Buna göre MAPK/ERK yolağı HB-EGF ve EGFR'nin interaksiyonu üzerine büyük olasılıkla yatay bazal hücrelerde aktive olduğu ve bunun rejenerasyon için bir önkoşul olduğu bulgusuna ulaşılmıştır. Her ne kadar PI3K/AKT yolağı da bu hücrelerde aktif olarak gözlemlense de, fonksiyonel OE rejenerasyonu için bir önkoşul olmadığı görülmüş yine de yatay bazal hücrelerin büyümesini sağlayarak rejenerasyona katkılar yapabileceği düşünülmüştür.

TABLE OF CONTENTS

ACKNOWLEDGEMENTS	iii
ABSTRACT	iv
ÖZET	v
LIST OF FIGURES	ix
LIST OF TABLES	xi
LIST OF SYMBOLS	xii
LIST OF ACRONYMS/ABBREVIATIONS	xiii
1. INTRODUCTION	1
1.1. Maintenance and Regeneration of Adult Epithelial Tissues	1
1.1.1. Skin Epithelium	1
1.1.2. Intestine Epithelium	4
1.1.3. Respiratory Epithelium	6
1.2. Adult Neurogenesis	7
1.3. Olfactory Epithelium	11
1.3.1. General Overview of the Olfactory Epithelium	11
1.3.2. Regeneration of the Olfactory Epithelium	14
1.3.3. Zebrafish Olfactory Epithelium	16
1.4. HB-EGF/EGFR Signaling	19
1.4.1. MAPK/ERK Signaling Pathway	21
1.4.2. PI3K/AKT Signaling Pathway	23
2. PURPOSE	26
3. MATERIALS AND METHODS	28
3.1. Materials	28
3.1.1. Adult Zebrafish	28
3.1.2. Equipment and Supplies	28
3.1.3. Solutions and Buffers	28
3.2. Methods	28
3.2.1. Maintenance of Zebrafish	28
3.2.2. BrdU and EdU Incorporation	29

3.2.3.	Chemical injury of OE	30
3.2.4.	Intraperitoneal Injection of Inhibitors	30
3.2.5.	Dissection of the Olfactory Epithelium	31
3.2.6.	Cryosectioning of the Olfactory Epithelium	31
3.2.7.	Immunohistochemistry of Olfactory Epithelium	32
3.2.7.1.	Immunohistochemistry against BrdU and HuC/D	32
3.2.7.2.	Immunohistochemistry against pERK and pAKT	33
3.2.8.	Imaging by Confocal Microscopy	34
3.2.9.	Positional Profiling	34
3.2.10.	Area Analysis of HuC/D	35
3.2.11.	Statistical Analysis of Results	36
4.	RESULTS	37
4.1.	The Role of MAPK/ERK Signaling in OE Regeneration	38
4.1.1.	Early Phase of OE Regeneration by ERK Inhibition	38
4.1.2.	Late Phase of OE Regeneration with ERK Inhibition	42
4.1.3.	Activation Pattern of ERK Signaling During OE Regeneration	48
4.1.4.	Activation of ERK in Dividing Cells During Regeneration	53
4.2.	Upstream Regulators of ERK	57
4.2.1.	Activation of ERK Under MEK1/2 Inhibition	57
4.2.2.	Activation of ERK under HB-EGF Inhibition	58
4.2.3.	Activation of ERK under EGFR Inhibition	60
4.2.4.	Activation of ERK under EGFR Inhibition	62
4.3.	The Effect of Inhibition of PI3K/AKT Signaling on OE Regeneration	63
4.3.1.	Early Phase of OE Regeneration with AKT Inhibition	64
4.3.2.	Late Phase of OE Regeneration with AKT Inhibition	67
4.3.3.	Activation of AKT During OE Regeneration	70
5.	DISCUSSION	72
5.1.	An Overview of Regeneration	73
5.2.	MAPK/ERK Signaling Is Active in Proliferating Progenitor Cells of the OE	74
5.3.	Survival of Neurons and MAPK/ERK Signaling	77

5.4. MAPK/ERK Signaling Is The Downstream Mediator of HB-EGF:EGFR	78
5.5. AKT Regulates Mitosis but Not Regeneration in the OE	79
5.6. Updated Model of OE Regeneration	80
REFERENCES	82
APPENDIX A: EQUIPMENT AND SUPPLIES	83
APPENDIX B: SOLUTIONS, BUFFERS, ANTIBODIES	84

LIST OF FIGURES

Figure 1.1.	A detailed overview of Zebrafish OE	18
Figure 1.2.	Potential downstream signaling pathways of binding of HB-EGF to EGFR	21
Figure 4.1.	Effect of inhibition by U0126 on cell proliferation at 1 dpi	40
Figure 4.2.	Positional profiles and quantitative comparisons of BrdU ⁺ cells in the OE of control and U0126	41
Figure 4.3.	Effect of inhibition by U0126 on cell proliferation and OSN regeneration at 5 dpi	43
Figure 4.4.	Positional profiles and quantitative comparisons of HuC/D ⁺ /BrdU ⁺ and BrdU ⁺ cells in control and U0126	45
Figure 4.5.	Analysis of HuC/D covered area in DMSO and U0126 by 5dpi	47
Figure 4.6.	pERK-positive cells at 1 dpi	49
Figure 4.7.	pERK-positive cells at 3 dpi	51
Figure 4.8.	pERK-positive cells at 5 dpi	52
Figure 4.9.	PCNA/pERK double-positive cells of OE at 1 dpi	54
Figure 4.10.	PCNA/pERK double-positive cells of epithelial fold at 1 dpi	55

Figure 4.11. Positional profiles and quantitative comparisons of pERK ⁺ /PCNA ⁺ and PCNA ⁺ cells	56
Figure 4.12. pERK ⁺ cells under MEK1/2, HB-EGF, EGFR inhibition	59
Figure 4.13. Positional and quantitative comparisons of pERK ⁺ cells with MEK, HB-EGF, EGFR inhibition	60
Figure 4.14. Effect of inhibition by Ly294002 on cell proliferation at 1 dpi . . .	65
Figure 4.15. Positional profiles and quantitative comparison of BrdU ⁺ cells in the OE of control and Ly294002	66
Figure 4.16. Effect of inhibition Ly294002 U0126 on cell proliferation and OSN regeneration at 5 dpi	68
Figure 4.17. Positional profiles and quantitative comparisons of HuC/D ⁺ /BrdU ⁺ cells in the OE of control and Ly294002	69
Figure 4.18. Analysis of HuC/D covered area in control and Ly294002 by 5dpi	70
Figure 4.19. pAKT ⁺ and proliferating cells at 1 dpi	71
Figure 5.1. A proposed model of MAPK/ERK activation by HBEGF:EGFR along with PI3K/AKT/mTOR activity during OE Regeneration .	81

LIST OF TABLES

Table A.1.	Equipment and Supplies.	107
Table B.1.	Solutions, Buffers, Antibodies.	108

LIST OF SYMBOLS

g	Gram
L	Liter
M	Molar
mL	Mililiter
ng	Nanogram
μL	Microliter
μg	Microgram
μm	Micrometer
$^{\circ}\text{C}$	Degree Celcius

LIST OF ACRONYMS/ABBREVIATIONS

AHN	Adult Hippocampal Neurogenesis
AKT	AK Strain Transforming
AN	Adult Neurogenesis
ANOVA	Analysis of Variance
Ascl1	Achaete-Scute Family BHLH Transcription Factor 1
BrdU	5-Bromo-2-deoxyuridine
BSA	Bovine Serum Albumin
BSC	Basal Stem Cell
CBC	Crypt Base Columnar Cell
DG	Dentate Gyrus
dpi	days post injury
EdU	5-Ethynyl-2-deoxyuridine
EGF	Epidermal Growth Factor
EGFR	Epidermal Growth Factor Receptor
ERK	Extracellular Regulator Kinase
FGF	Fibroblast Growth Factor
GBC	Globose Basal Cell
HB-EGF	Heparin-Binding Epidermal Growth Factor
HBC	Horizontal Basal Cell
HFSC	Hair Follicle Stem Cell
hpi	hours post injury
HuC/D	Hu Protein C / D
IFE	Interfollicular Epidermis
ILC	Inter Lamellar Curve
IPC	Intermediate Progenitor Cell
Int	Intact
Krt5	Keratin 5
MAPK	Mitogen Activated Protein Kinase

MMP	Matrix Metalloprotease
mTOR	Mammalian Target of Rapamycin
NEC	Neuroepithelial Cell
NS	Non-Sensory
NSC	Neural Stem Cell
OE	Olfactory Epithelium
OP	Olfactory Placode
OSN	Olfactory Sensory Neuron
pAKT	phospho-AK Strain Transforming
PBS	Phosphate Buffered Saline
PBST	Phosphate Buffered Saline with Tween 20
PCNA	Proliferating Cell Nuclear Antigen
pERK	phospho- Extracellular Regulator Kinase
PFA	Paraformaldehyde
pH	Potential Hydrogen
PI3K	Phosphoinositide 3-Kinase
PTEN	Phosphatase and Tensin Homolog Protein
RGC	Radial Glia Cell
SEM	Standard Error of Means
SGZ	Subgranular Zone
SNS	Sensory Non-sensory Border
Sox2	Sex Determining Region Y-box 2
Sus	Sustentacular Glia Cell
T(r)p63	Tumor Protein 63
TrX	1% Triton X-100 Damaged
V-SVZ	Ventricular Sub-Ventricular Zone

1. INTRODUCTION

1.1. Maintenance and Regeneration of Adult Epithelial Tissues

Epithelial tissues are layered cell structures that cover the outer and inner surfaces of the body, organs, and glands. As a protective coating, epithelium faces the outside threats to the underlying tissue beforehand and also frequently wears off or gets injured. In addition to its protective function, epithelial tissues have many roles that are important for the life of the organism such as the regulation of body temperature by the skin epithelium, absorption of nutrients by the epithelium of intestine, and providing moisture for airways by the respiratory epithelium. Loss of such functions would have deadly consequences for the organism, and epithelial tissues evolved to contain progenitor pools to cope with the loss of cells that occur during its function. Of those, one progenitor pool divides frequently to compensate for routine cell loss due to wear off, while another pool of cells that does not usually divide, replenishes the lost cells in cases of traumatic injuries. Skin, intestine, and respiratory epithelium are some of the best-studied epithelial tissues of the human body. These epithelia have many similarities and distinctions regarding the composition of their progenitor and stem cell populations and the regulation of those cells for maintaining and regenerating lost and damaged tissue.

1.1.1. Skin Epithelium

The skin wraps the surface of the whole body with its appendages such as hair follicles and glands and protects from external threats to the organism such as UV lights, heat, injuries, and infections. The main layers of the mammalian skin are the epidermis, dermis, and hypodermis. The epidermis is also known as the interfollicular epidermis (IFE), and it consists of a stratified epithelium with the majority of the cells

being keratinocytes. Other cell types of the epidermis are Langerhans cells that provide immunity, melanocytes that synthesize pigments, and different sensory neurons to encode touch stimuli (Kanitakis, 2002). Layers of the IFE are generally categorized as the basal layer, the spinous layer, the granular layer, and finally, the cornified layer which are established by a differentiation program (Yousef *et al*, 2019). In the mature epithelium, Keratin 5 (Kr5) and Keratin 14 expressing cells in the basal layer are continuously dividing and they secrete laminin and integrin proteins to assemble the extracellular matrix (Kanitakis, 2002). As keratinocytes exit the basal layer by detaching from the basal lamina and move towards the spinous and granular layers, they terminally differentiate, and switch their expression of keratin proteins and stop the secretion of laminin and integrins. This migration and differentiation of keratinocytes is finalized with their apoptosis around the corneous layer. In this layer, flattened dead cells devoid of nuclei called squames form the protective barrier (Alonso & Fuchs, 2003). Shed cells are continuously replaced with new cells and the skin epidermis is found to be renewed completely about every four weeks (Potten, 1975). This high turnover of the skin is attributed to a subpopulation of keratinocytes from the epidermis that can be grown in culture for many passages and generate clones. Moreover, label retention assays that look for proliferation markers revealed the existence of slowly dividing Transformation Related Protein 63 (TRP63) positive stem-like cells in the bulge of the hair follicles and in the basal layer of the IFE (Alonso & Fuchs, 2003). In a separate study, it has been reported that TRP63-deficient mice showed abnormal development of squamous epithelia along with appendages highlighting the importance of TRP63 for the maintenance of stem and progenitor cells (Yang *et al*, 1999). Since cells in the bulge are dividing less and have the capacity to generate more lineages of the skin compared to basal IFE cells, these cells are referred to as multipotent hair follicle stem cells (HFSCs) while basal IFE cells are referred to as unipotent progenitors (Blanpain & Fuchs, 2006). However, later studies showed that another molecularly distinct and more quiescent stem-like cell population exists that can give rise to basal IFE cells in some of the skin compartments, and which were named IFE stem cells (Mascré *et al*, 2012). As the major source of homeostasis and regeneration, the division and differentiation of skin stem cells are tightly controlled by

various signaling pathways and transcription factors. For stratification, which provides a physical barrier, Notch signaling is involved in the commitment of basal IFE cells to spinous keratinocytes and regulates the balance between cells of spinous and basal layers (Blanpain & Fuchs, 2009). Other than Notch, mitogen-activated protein kinase (MAPK) and nuclear factor- κ B signaling pathways, along with transcription factors such as IRF6, GRHL3, and KLF4, were found to be involved in the differentiation of epidermal progenitors (Koster & Roop, 2007). Hair follicles in the skin also undergo a turnover process called the hair cycle and it is fueled by HFSCs. HFSCs only leave dormancy at the beginning of the hair cycle and during wound healing (Alonso & Fuchs, 2009). Wnt and BMP signaling have been shown to be involved in the regulation of HFSCs activation (Blanpain *et al.*, 2007). HFSCs lacking β -catenin cannot differentiate into follicular keratinocytes (Huelsken *et al.*, 2001) while BMP signaling regulates the quiescence of HFSCs through the expression of transcriptional repressor nuclear factor of activated T cells C1 (NFATC1), a transcriptional repressor of a cell cycle gene *Cdk4* (Horsley *et al.*, 2008). Finally, Notch signaling found to be required for the commitment of HFSCs to generate specialized hair follicle cells (Alonso & Fuchs, 2009). Healing of skin injuries can be divided into stages of hemostasis, inflammation, proliferation, and remodeling (Gantwerker & Hom, 2011). During hemostasis, blood clots form to avoid blood loss. This leads to the inflammation stage which includes the recruitment of neutrophils, macrophages, and lymphocytes for the generation of an accurate immune response against microbes, and for cleaning out damaged cells and matrix. Transition to the proliferation stage is assisted by macrophages that secrete chemokines and growth factors such as interleukin-1, platelet-derived growth factor, fibroblast growth factor, vascular endothelial growth factor, and transforming growth factor to induce cell division and migration of epidermal stem cells. Epidermal stem cells are activated in this phase and the epidermal stratification program starts. Once stratification is established, collagen remodeling is performed by matrix metalloproteases (MMPs; Sun *et al.*, 2014). In the proliferation phase, HFSCs and IFE stem cells are mobilized to the damaged area. The major stem cell type contributing to the regeneration depends on the severity of the injury and there are no lineage constraints for HFSCs and IFE stem cells during the proliferation phase since they produce all cell

types of the skin epithelium. Once healing is completed, plasticity is succeeded with lineage constraints and stem cells revert to dormancy and usual locations within the skin epithelium (Dekoninck & Blanpain, 2019).

1.1.2. Intestine Epithelium

The human small intestine epithelium is a single-layered epithelium facing the intestinal cavity that covers villi and protects the blood and lymphatic vessels and muscles required for the nutrient absorption of the intestine. As a structure facing the inside of the intestinal cavity, it is vulnerable to potential insults such as low pH, bacteria, and toxic by-products of digestion in addition to the mechanical stress of bowel movements. Probably due to these challenges, there is a constant turnover of the intestine epithelium fueled by resident stem cells. In fact, the intestine epithelium of most adult mammals is completely renewed every 2 to 6 days (Beumer & Clevers, 2016). Crypt-Villus structures are the units of the intestine epithelium responsible for efficient nutrient uptake. While villi are finger-like protrusions toward the lumen whose length varies within the intestine, crypts are cavities invaginating deeper into the intestinal mucosa. A villus is mostly composed of differentiated, non-dividing enterocytes that absorb water and nutrients, along with goblet cells that secrete mucous, and enteroendocrine cells that produce appetite-regulating hormones. In contrast, the crypt is composed of G-protein-coupled receptor 5 positive Crypt Base Columnar cells (CBCs) which function as stem cells in the intestine epithelium (Clevers, 2013). The transit-amplifying progeny of these stem cells migrate towards the villus and differentiate into the various villus cell types. Paneth cells are another group of cells that reside within the intestinal crypt that express factors such as ligands for Wnt, Notch, and epidermal growth factor (EGF) receptors that are required for the maintenance of stemness in addition to the secretion of antimicrobial proteins that protect stem cells (Clevers & Bevins, 2013). Under normal conditions, CBCs of the intestine epithelium divide symmetrically, which results in two $Lgr5^+$ CBCs. With many dividing cells in the crypt center and only a limited amount of space within the crypt region, CBCs located more towards the periphery of crypt center are pushed out to the villus. Once

this happens, pushed-out CBCs lose contact with the PCs and the growth factors that are secreted by PCs, which help CBCs to maintain their stemness (Clevers & Bevens, 2013). During this process, *Lgr5* expression decreases, and the expression of genes required for lineage differentiation increases. In accordance with the contact-dependent nature of this differentiation, Notch signaling which is activated ligands that are presented in the membrane of Paneth cells is shut down, which initiates the differentiation of the CBCs (Clevers, 2013). Some of the other canonical pathways that regulate the differentiation of CBCs are Wnt, BMP, and Epidermal Growth Factor (EGF) pathways. Agonists and antagonists of Wnt and BMP pathways are also secreted in a way that establish gradients of higher Wnt activity (activation of cell division) towards the crypt and higher BMP activity (suppression of cell division) towards the villus (Beumer & Clevers, 2016). The changing gradients of Wnt and BMP, in addition to whether the Notch pathway is active or not, also defines the cell fate during differentiation. For example, loss of Wnt results in a commitment to enterocyte lineage, inactive Notch but high Wnt results in differentiation of CBCs into Paneth cells, inactive Notch and low Wnt with high MAPK signaling leads to differentiation into goblet cells in villus, and finally, absence of Notch, Wnt, and MAPK with the presence of BMP signaling leads to differentiation to EECs. In the end, mature cells reaching the tip of the villus undergo apoptosis approximately five days after birth and are shed from the epithelium (Beumer & Clevers, 2021). Under damage conditions, a temporary epithelium without the absorptive capacities covers the wound depending on the nature of the injury (Hageman *et al*, 2020). After about one week, the temporary epithelium is replaced with crypts that fuel the functional regeneration. Because of the high plasticity of intestine epithelium cells, committed progenitors and fully matured cell types re-acquire stemness in the crypt region. This high plasticity is, in part, achieved by an open chromatin architecture that could be remodeled thanks to the help of mesenchymal cells who secrete BMP inhibitors and Wnt ligands for regulating and improving the efficiency of regeneration. Meanwhile, M2 macrophages are recruited to the injury zone and secrete cytokines such as IL-6 and can further regulate Hippo and Notch signaling (Hageman *et al*, 2020). Moreover, shortly after injury, hippo signaling, a pathway known for regulating the size of organs, is also activated in the crypt. A clusterin-

positive cell population with high hippo signaling contributes to the regeneration of the IE but not to its maintenance. These cells are also able to produce new Lgr5⁺ CBCs when their lineage was genetically traced (Ayyaz *et al*, 2019). Finally, EGF is produced by the enteric glial cells and it enhances the recovery through mucosal healing (Van Landeghem *et al*, 2011).

1.1.3. Respiratory Epithelium

The respiratory system is exposed to external threats through continuous air intake and, therefore, is also covered with an epithelial barrier, which secretes mucous necessary for respiration. Despite the lesser turnover of respiratory epithelium compared to skin or intestine epithelium under normal conditions, the respiratory epithelium is capable of regeneration following injuries (Zepp & Morissey, 2019). The respiratory system is divided into upper and lower tracts which encompasses the nose, the throat, trachea, and lungs and each of these units have distinct cell and progenitor types in an epithelial structure specialized for respiration and function together with the nearby mesenchymal and endothelial cells for proper gas exchange. In humans, main epithelial cell types of the trachea and proximal airways of the lungs are Tp63⁺/Krt5⁺ double-positive Basal Stem Cells (BSCs), Secretory Cells, Ciliated Cells, Brush Cells, Goblet Cells, Ionocytes and Pulmonary Neuroendocrine Cells (PNECs) injuries (Davis & Wypych, 2019). During development, Wnt ligands and Fibroblast Growth Factors (FGFs) secreted from the mesenchyme induce lung progenitors from the endoderm. In addition to Wnts and FGFs, BMPs, Retinoic Acid (RA), and TGF- β were found to play roles in the generation of bronchiole branching in the lung (Zepp & Morissey, 2019). Cells expressing TRP63 and Krt5 also exist in developmental stages and they are capable of generating all epithelial lineages of lung. Notch signaling is also involved in commitment to fates such as secretory or ciliated cells in combination with transcription factors required for further lineage specification. Regular turnover of these BSCs that mostly exists along the entire airway of humans are also found to be regulated by FGF and BMP signaling in the adult tissue (Zepp & Morissey, 2019). Upon SO₂ inhalation, which destroys the tracheal epithelium, remaining BSCs start

to proliferate on the first day after injury (Basil *et al*, 2020). Under normal conditions, these cells differentiate into secretory cells and then further differentiate into the ciliated lineage (Watson *et al*, 2015). However, with injury, these BSCs demonstrate plasticity by directly differentiating into ciliated cells with the presence of myeloblastosis oncogene transcription factor (Zepp & Morissey, 2019) into secretory cells as usual with the expression of the NOTCH2 transcription factor. Loss of Notch signaling in BSCs results in a shift of bias toward producing ciliated cells and emphasizes the importance of Notch signaling for balancing distinct cell populations (Rock *et al*, 2011). In the distal airways, injury also induces the FGF10 expression through Hippo signaling in the nearby smooth muscle cells which in turn activates Wnt signaling in the injured epithelium (Lee & Rawlins, 2018). In cases with excessive tissue loss, regions that could not reach oxygen for prolonged periods have been shown to create skin-like keratinized epithelium composed of Krt5⁺ cells lacking the respiratory properties (Basil *et al*, 2020).

1.2. Adult Neurogenesis

Nervous tissues in vertebrates form the organs of the central nervous system such as the brain, the spinal cord, and present in peripheral sensory organs such as eye, nose, ears, tongue and skin. While neurons in nose, tongue and skin are prone to external threats and have greater ability to regenerate, neurons of central nervous system are generally well-protected by surrounding tissues and they are even capable of outliving the organism itself if they were to be transplanted into a younger host (Magrassi *et al*, 2013). Thus, the maintenance of the neuronal tissue does not rely on the turnover of neurons but rather on their protection once they are generated during their development. According to Santiago Ramón y Cajal, who is considered to be the father of modern neuroscience, “once the development ends the nerve paths are fixed” and there is no birth or integration of new neurons into the system. These claims resulted in a dogma that remained unchallenged until the 1950s. One of the first researchers, who contested the dogma was Joseph Altman in the 1960s. He argued that the observation that neurons usually do not divide does not rule out the possibility that progenitor

cells may be present that could do so under different circumstances. During his experiments, he lesioned the brain of adult rats and supplied a radioactive thymidine analog that is incorporated into newly synthesized DNA of dividing cells and passed on to their progeny. After analyzing the results from varying time points between 1 day to 1 month-post-injury, he discovered the presence of cells that incorporated the proliferation marker in the dentate gyrus (DG) of the hippocampus, the cortex, and in another study in the olfactory bulb (OB), all of which were areas independent from the site of lesion. He also suggested that cells proliferate within the subependymal zone (SEZ) of the lateral ventricles and migrate to the OB. Even though these findings are accepted facts today, unfortunately, he was too ahead of his time and the scientific community was not convinced that neurons could be born during adulthood. In the 1970s, Michael Kaplan found further supportive evidence for the dividing granule cells of the DG and in the OB to be neurons. In the 1980s, Fernando Nottebohm and colleagues also used radioactive thymidine tracers in canary birds to reveal cells that were found later to be radial glia (Alvarez-Buylla *et al*, 1990) in the ventricular zone (VZ). In addition, newborn neurons occur seasonally in the higher vocal center, which ultimately proved that adult neurogenesis (AN) does occur routinely in songbirds (Goldman and Nottebohm, 1983). Progenies of radial glia cells in the VZ are integrated into an existing neural network in the higher vocal center, which correlates with seasonal song learning during the mating period of the birds (Paton and Nottebohm, 1984). However, these studies were still criticized for the fact that birds are not mammals and that the observed adult neurogenesis may be a specialty of these analyzed species but could not be generalized. Conclusive evidence for AN in mammals was provided by Elizabeth Gould in 1999, when she used a superior non-radioactive thymidine analog called Bromodeoxyuridine (BrdU) for the labeling of dividing cells in the adult monkey brain. With fluorescence microscopy, she clearly revealed the presence of BrdU in the nucleus of cells that were positive for a mature neuron marker in DG. Meanwhile in 1998, Eriksson examined the post-mortem brain of cancer patients who priorly received BrdU injections to track their tumors, and found newborn neurons in the human DG. Even though the controversy about AN in humans still persists, it is proved through murine models that new neurons are born in predominantly within two brain regions, the subgranular zone

(SGZ) of the DG in the hippocampus and in the ventricular-subventricular zone (V-SVZ; also called subependymal zone) during adulthood. However, as the organism ages, neurogenesis declines in these areas. The current theory in the field is that a pool of neural stem cells (NSCs) is set aside during development and since their number is limited, they are exhausted over time or become increasingly quiescent (Babcock *et al.*, 2021). Exhaustion of neurogenesis also correlates with age-related cognitive decline as the hippocampus is involved in many cognitive tasks such as memory formation, navigation, and learning. According to current evidence, neurogenesis in the DG of the hippocampus (adult hippocampal neurogenesis or AHN) contributes to specialized tasks such as pattern separation and the spatial navigation through the addition of new neurons to an existing circuitry, which further increases the plasticity of neuronal networks without neuronal turnover (Kempermann, 2022). In tasks that require complex spatial learning, AHN is involved in integrating new information in an already known context as an example of cognitive flexibility (Garthe *et al.*, 2009). AHN is also involved in the ordering of the knowledge in time which relates to the sequential or autobiographical memory function of the hippocampus (Aimone *et al.*, 2006). Moreover, as a major source of plasticity, there have been implications that AHN drives the individualization of brains (Zocher *et al.*, 2020). Mechanisms regulating neurogenesis are complex and depend on the tissue environment as they differ during development and adulthood. NSCs are generally located close to astrocytes, a glial cell type in the central nervous tissues, and to the blood vessels. When NSCs divide, they typically give rise to intermediate progenitor cells (IPCs), which undergo several rounds of cell divisions before further differentiating into neurons (neurogenesis) or glial cells such as astrocytes, oligodendrocytes, ependymal cells, and microglia (gliogenesis). During early development they have a higher tendency to generate neurons while they generate more glial cells at later postnatal stages (Götz *et al.*, 2009). As development finishes, two quiescent NSC pools with distinct origins persist in the V-SVZ and in the SGZ. Whether these stem cells will stay quiescent or divide and generate neurons depends on a combination of factors. Among those, one of the most potent regulators are the ligands of the Notch signaling pathway, which are expressed by granule neurons in the DG and by IPCs in the V-SVZ. The Notch pathway is active in quiescent NSCs and

experimental manipulations that shut off the pathway leads to transient activation of all NSCs for neurogenesis and loss of the pool (Ehm *et al*, 2010). Moreover, Notch and EGFR signaling pathways regulate the balance between IPCs and NSCs in the V-SVZ (Aguirre *et al*, 2010). Wnt and BMP pathways also regulate the maintenance of NSCs both during development and adulthood with varying ligands and downstream targets. In the adult SGZ, BMPs are provided by granule neurons to keep NSCs quiescent, while noggin, an antagonist of BMP, induces proliferation (Mira *et al*, 2010). On the other hand, Wnt signaling in both the V-SVZ and the SGZ boosts renewal (Lie *et al*, 2005) and differentiation to neurons and granule neurons secrete inhibitors of Wnt to keep NSCs quiescent (Seib *et al*, 2013). Interestingly, physical exercise has been shown to increase the adult neurogenesis and the effect of it is thought to be mediated through insulin-like growth factor 1 (IGF1; Trejo *et al*, 2001). The main downstream event of these pathways that regulate the proliferation of NSCs is the activation of a transcription factor called achaete scute-like 1 (Ascl1). Intriguingly, deletion of Ascl1 completely abolishes the differentiation of adult NSCs into neurons but has no effect on developmental NSCs. For the expression of Ascl1, Notch signaling has to be switched off which coincides with the exit of NSCs from quiescence (Sueda *et al*, 2019). Another intrinsic regulator is the AKT pathway which is suppressed by phosphatase and tensin homolog protein (PTEN) activity in the quiescent NSCs and NSCs are lost if PTEN is knocked-out (Bonaguidi *et al*, 2011). Moreover, another growth factor known to regulate quiescence called milk fat globule-epidermal growth factor 8 (MFGE8) has been shown to exert its effect through AKT-mTOR pathway (Zhou *et al*, 2018). Despite being a stem cell population and sharing regulatory aspects with other stem cell populations known for their capabilities to contribute to regeneration, NSCs are not efficiently activated when it comes to recovering from injuries in mammals. However, in lower vertebrates such as zebrafish, NSCs have greater potential for brain regeneration. The key difference between mammalian and non-mammalian vertebrate NSCs relies in their development. In mammals, all radial glial cells (RGCs) and neuroepithelial cells (NECs) which function as NSCs during the development period are differentiated into astrocytes in adulthood. The zebrafish brain lacks astrocytes while RGCs are sustained in the telencephalon, and express some of the astrocyte markers. Zebrafish brain lacks

astrocytes while RGCs are sustained in the telencephalon, and carry some of the astrocyte markers (Ganz & Brand, 2016). Hence, RGCs are thought to have evolved into astrocytes with new responsibilities in mammals while, at the same time, losing their neurogenic potential. In mammals, traumatic injuries results in excessive production of astrocytes causing formation of scars, while zebrafish NSCs are able to generate functional and integrating neurons, thereby achieving scar-free regeneration of brain (Diotel *et al*, 2020).

1.3. Olfactory Epithelium

1.3.1. General Overview of the Olfactory Epithelium

The olfactory epithelium (OE) is a peripheral sense organ that detects environmental chemicals, also called odorants, with specialized olfactory sensory neurons (OSNs). It is positioned in the nasal cavity and connected to the olfactory cortex in the brain via the olfactory bulb. Just like the skin, intestine, and respiratory epithelium, it is exposed to external threats and routine wear-off, and probably due to these reasons, uniquely for a tissue occupied largely by neurons, life-long continuous replacement of dying OSNs with the new-born OSNs exists. This makes the OE an attractive candidate for the study of adult neurogenesis since progenitor cells frequently differentiate into neurons that are continuously integrated into existing circuits and can even be regenerated at high rate in cases of injury. To achieve these unusual properties, the OE has a dual stem/progenitor cell system that is intricately regulated by many factors and signaling pathways. Overall, the OE is a tissue that combines the plasticity of other epithelia with high-specialization of the nervous tissues, and studies on the OE can shed light on the nature and identify of signals that trigger adult neurogenesis to directly replace dying neurons, which is different from adult neurogenesis in the brain. Therefore, lessons from OE neurogenesis can contribute to the development of strategies to replenish degenerating neurons that are observed in numerous neurological diseases. During mouse development, OE formation starts early around embryonic day 10 with the thickening of the ectoderm to generate the olfactory placode (OP).

Initially, the OP is mostly homogeneous and consists of olfactory neural stem and progenitor cells with no mature OSNs. Later during development, compartmentalization occurs along the baso-apical axis and differentiation of the progenitors into sustentacular glia cells (Sus) and neurons towards the apical can be observed (Cuschieri & Bannister, 1975; Sokpor *et al*, 2018). Once development is complete, complete, the mature OE is characterized by the presence of mature neurons and Sus cells in apical layers, immature neurons in intermediate layers along with Bowman’s gland cells and microvillar cells, and finally a basal layer, which contains horizontal basal cells (HBCs) and globose basal cells (GBCs). HBCs and GBCs are the sources of lifelong neurogenesis in the OE (Graziadei & Graziadei, 1979). Interestingly, not all HBCs are placode derived and have been shown to originate from the neural crest. Their presence in the OE can be observed at later post-natal stages (Suzuki *et al*, 2013). As the name suggests, HBCs have horizontally flattened profiles and are attached to the basal lamina. They express epithelial stem cell markers such as Krt5 and integrins (Holbrook *et al*, 1995) in addition to neural stem cell markers such as Pax6 and Sox2 (Guo *et al*, 2010). They also express EGFR (Mahantappa & Schwarting, 1993) and TRP63 which have regulatory roles for their quiescence (Packard *et al*, 2011). As TRP63 expressing stem cells, they are mostly quiescent and only divide under injury conditions with the capacity to generate GBCs, neuronal and non-neuronal cells (Leung *et al*, 2007). GBCs are the progenitor pools of the OE which divide frequently to generate OSNs on a continuous basis. They are a heterogeneous population including a recently identified Lgr5⁺ quiescent-multipotent subset (Chen *et al*, 2014), a Sox2⁺, Pax6⁺, and Six1⁺ multipotent subset, an Ascl1⁺ transit-amplifying subset, and a Neurod1⁺/Neurog1⁺ double-positive immediate-precursor subset. While Ascl1⁺ and Neurod1⁺ GBCs are committed to neuronal fate, Neurod1⁺ GBCs further lose the expression of Sox2 and Pax6 (Krolewski *et al*, 2013). In line with their function as the main neurogenic progenitors of the OE, loss of GBCs also results in a loss of neurogenesis. Moreover, these subsets of GBCs also accurately represent the transcriptional programs that are necessary to drive neurogenesis forward. Generation of neurons from GBCs both during development and adulthood depends on a cascade of activation of the transcription factors Sox2, Ascl1, Neurod1, and Neurog1 in the given order (Krolewski *et al*, 2013)

Regulation of differentiation with TFs is accompanied by epigenetic changes such as chromatin remodeling by polycomb (Goldstein *et al*, 2016) and BAF complexes (Bachman *et al*, 2016), and regulatory RNA activities for the development of the OE (Choi *et al*, 2008). Finally, signaling through ATP has been shown to generate Ca^{++} responses in the GBCs of zebrafish OE, which enhances their neurogenic activity (Demirler *et al*, 2020). Immature neurons produced by GBCs are found in more apical layers than GBCs and complete their maturation once they can establish their axon outgrowths and dendrites in basal lamina and apical surface, respectively. As they mature they move towards apical layers and change their expression of GAP43 to OMP (Verhaagen *et al*, 1989; Farbman & Margolis, 1980). Because of their exposed nature, the average lifespan of a mature OSN ranges only between 30 to 90 days (Mackay & Kittel, 1991). Mature neurons are bipolar and detect odors on the apical surface with GPCR-like olfactory receptors expressed in their cilia. Each OSN stochastically expresses only one type of olfactory receptor from approximately 400 genes in humans, and 1100 genes in the mouse (Niimura & Nei, 2005). Moreover, OSNs expressing the same olfactory receptor are organized into expression domain within the OE and they send their axons to the same glomerulus in the OB which is a spherical central for synapse formation with the olfactory bulb neurons (Strotmann & Breer, 2006). Genetic mechanisms for choosing one olfactory receptor gene among the large genomic repertoire and convergence of axons of OSNs with the same type of olfactory receptor to a glomerulus are ongoing topics of research. Sustentacular cells are the resident glial cells of the OE with elongated cell bodies that help the OSNs by taking up toxins, odorants, and dead cells, and balancing the ionic composition of the OE in addition to providing structural support. Intriguingly, these cells are also Pax6⁺ and Sox2⁺ (Guo *et al*, 2010) in addition to being K8⁺ and K18⁺. They also have a slow proliferation rate which might suggest neural stem cell properties but further research is required to investigate their capacity for neurogenesis (Weiler & Farbman, 1998). Other supporting cell types of mammalian OE are microvillar cells and Bowman's glands which secrete neuropeptide-Y and mucus respectively, and finally, olfactory ensheathing cells (Doyle *et al*, 2008; Chen *et al*, 2014). Olfactory ensheathing cells are glial cells thought to have a dual origin of OP and neural crest. As their name suggests, they wrap the axons of OSNs exiting the

OE towards the olfactory bulb underneath the basal lamina (Tennent & Chuah, 1996). Wrapping of OECs does not include myelination in the olfactory system, however, when transplanted into the spinal cord they can rescue myelination defects and in vitro, they have the pluripotency to differentiate into Schwann cells and astrocytes (Chehrehasa *et al.*, 2010). To maintain the OSNs in the OE, *Ascl1* is critical. Knock-out experiments with *Ascl1* resulted in less neurons but did not affect the composition of other cells, which puts *Ascl1* forth as the driver of neural fate. *Ascl1* is also regulated by the Notch pathway through a downstream effector called *Hes1* and suppression of neural transcription factors by *Hes1* results in a bias for producing glial cells (Cau *et al.*, 2000). Another important factor is *Runx1* which is required for maintaining *Neurod1* and the corresponding GBC subset (Theriault *et al.*, 2005). For the maturation of immature OSNs, *Olf/Ebf* family of transcription factors, Nuclear Factor I, STAT3, and *Klf4* have been shown to be important (Sokpor *et al.*, 2018).

1.3.2. Regeneration of the Olfactory Epithelium

The olfactory system and specifically the OE is a remarkable exception to the inability of nervous tissues to regenerate upon injury. Most probably due to exposure to the toxins and microbes in its vulnerable location compared to the brain in the skull and the spinal cord in the spine, the need arose for the OE to maintain post-development plasticity and neurogenic potential. Both the type and severity of injury affect the regenerative response of the OE (Brann & Firestein, 2014). Approaches to study the phenomenon of OE regeneration can be categorized as techniques that involve damaging the OE as a whole with a toxic gas or solution such as MeBr, ZnSO₄, and triton X-100 or techniques that will selectively kill the neurons of OE by degenerating its axons such as axotomy or bulbectomy (Schwob, 2002). In the bulbectomized OE lacking only OSNs, an acceleration in neurogenesis is observed. Interestingly, under these conditions GBC activation is increased with no change in HBC activity (Schwartz Levey *et al.*, 1991). Among other techniques, MeBr inhalation is widely used in rodent models because of its ease of delivery and removal in addition to the effective elimination of neurons and sustentacular cells while sparing the basal cells such as GBCs and HBCs.

Studies on OE regeneration after injury are facilitated by lineage tracing approaches with replication-incompetent retroviral vectors containing markers heritable with division. These vectors are transduced into the injured OE and enable the tracking of progenitors with their progeny in resulting clones. Such experiments showed clones composed of OSNs, sustentacular cells, Bowman's gland cells, microvillar cells, GBCs, and HBCs or alternatively clones of Sus cells and bowman glands in the MeBr lesioned OE (Huard *et al*, 1998). Direct differentiation of GBCs into Sustentacular cells was also observed in later studies (Mangplaus *et al*, 2004) and since GBCs were the most mitotically active cell type after injury, the clonal analysis was interpreted such that GBCs constitute a multipotent OE stem cell population, which mainly contributes to the regeneration of the OE (Huard *et al*, 1998). The hypothesis of GBCs being the multipotent stem cells of the OE was further confirmed by transplantation studies where GBCs were isolated from an intact OE and engrafted into MeBr lesioned OE and gave rise to clones including all cell types of the OE while HBC transplantation was not successful and sustentacular and Bowman's gland cells can generate clones of themselves (Chen *et al*, 2004). Currently, it is widely accepted that at least a subset of GBCs are multipotent and have a similar capacity as the progenitors of OP during early development to generate OE cells (Schwob *et al*, 2017). Since HBCs are presumed to arrive at the OE post-developmentally and did not yield clones when collected and grafted into intact OEs, their contribution to regeneration was overlooked in earlier studies. However, lesions that kill Sustentacular cells, such as MeBr inhalation in rodents (Chen *et al*, 2004) and Triton X-100 irrigation in zebrafish (Demirler *et al*, 2020; Kocagöz *et al*, 2022) have been found to cause increased proliferation of HBCs. In rodents, they also give rise to OSNs, sustentacular cells, Bowman's gland cells, GBCs, and even ciliated cells of the respiratory epithelium in the injured OE (Leung *et al*, 2007; Schnittke *et al*, 2015). Moreover, the issue of not generating clones when transplanted to an injured OE can be overcome when HBCs are activated by retinoic acid *in vitro* and engrafted afterward (Peterson *et al*, 2019). However, in severe damage conditions that further eliminates GBCs but spares only HBCs, respiratory metaplasia is observed suggesting that HBCs by themselves cannot regenerate the OE. When they are closely examined during regeneration, proliferating HBCs lose the TRP63 expression which is restored

after regeneration. Overexpression of TRP63 during early injury hinders the proliferation of HBCs while Tp63 knock-out in the intact OE causes them to generate neurons and glial cells, demonstrating that TRP63 is necessary and sufficient for HBCs to leave dormancy and to contribute to neurogenesis (Schnittke *et al*, 2015). Moreover, Notch ligands were found to be present on sustentacular cells while HBCs express the Notch1 receptor. Notch signaling keeps the HBCs dormant in the intact OE by upregulating Tp63. Consistently, selective depletion of sustentacular cells was sufficient to activate HBCs in an otherwise uninjured OE (Herrick *et al*, 2017). A recent study also found out that hippo signaling regulates the regeneration and inhibition of this pathway reduces but does not prevent the regeneration of the OE in rodents (Wu *et al*, 2022). Injury not only activates HBCs but also induces plasticity in $Ascl1^+$ transit-amplifying GBCs and $Neurog1^+$ immediate precursor GBCs to revert to $Sox2^+$ multipotent type (Lin *et al*, 2017).

1.3.3. Zebrafish Olfactory Epithelium

The zebrafish OE consists of sheets of neuroepithelium that fold onto itself to form double-layered structures called lamellae emanating from the median raphe in a way that resembles an ellipse-like flower with a medial-lateral symmetry. Approximately two-thirds of the each lamellae starting from the median raphe is inhabited by OSNs and referred to as the sensory region while the rest of the structure forms the non-sensory region that is composed of ciliated cells with high $Krt5$ expression (Hansen & Zeiske, 1998; Demirler *et al*, 2020). New lamellae are added to the anterior side of the OE post-developmentally and lead to the continuous growth of the tissue in the adult zebrafish (Hansen & Zeiske, 1998) which is a process that is limited to one year after birth in rodents (Weiler & Farbman, 1997). A lamella refers to two neuroepithelial sheets anchored to a common lamina propria which is close to the basal layers of each neuroepithelium and at the center of the lamella structure. One epithelial fold refers to one neuroepithelium folded on itself that has the water-facing apical surface of the neuroepithelium in the center of the structure (Calvo-Ochoa *et al*, 2021). The epithelial fold, which will be referred to simply as fold from now on, can be subdivided

radially into four distinct parts: the interlamellar curve (ILC), the core-sensory region (CS), the sensory non-sensory (SNS) border, and finally the non-sensory (NS) region (Bayramli *et al*, 2017). Each side of the fold is composed of OSNs, sustentacular cells in the apical, and GBCs, and HBCs on top of the lamina propria in the basal of the sensory region, while goblet (analogous to BG cells in rodents) and ciliated cells span the whole non-sensory (Demirler *et al*, 2020; Hansen & Zeiske, 1998). While the organization of HBCs, Sus cells, and OSNs are similar to the mammalian OE in terms of location in the neuroepithelium, $Ascl1^+$ GBCs are restricted to the ILC and SNS in the zebrafish OE. Accordingly, presence of immature $Gap43^+$ neurons is also limited to the ILC and SNS. A representational summary of the zebrafish OE can be found in Figure 1.1. In the intact OE, the majority of BrdU-positive dividing cells originate from dedicated growth regions at the ILC and SNS. Hence, neurogenesis required for the turn-over of dying neurons distinctly occurs in these regions. Neurons born in these zones are found to migrate towards the center of the sensory as they age (Bayramli *et al*, 2017). The majority of mature OSNs of the zebrafish OE are Omp^+ ciliated cells, $TrpC2^+$ microvillus cells which are normally found in the vomeronasal organ of rodents, and crypt, kappa, and pear cells which are a minor fish-specific group of sensory neurons. Analysis of the localization of the OR types also found zones of expression similar to mammalian OE (Calvo-Ochoa *et al*, 2021). Zebrafish Sus cells are positive for the markers $Sox2$ and $cytokeratin14$ and they have cell bodies in the basal layer and extensions in close contact with the dendrites of OSNs, thus, spanning the whole apico-basal axis of the tissue (Demirler *et al*, 2020). Zebrafish HBCs span the whole basal lining of the fold and are not limited to zones like GBCs. Like their rodent counterparts, zebrafish HBCs are also positive for $Sox2$, $Krt5$, and $Tp63$. They are typically dormant but start to divide more frequently upon damage, however, their baseline mitotic activity appears to be higher in the zebrafish OE compared to rodent HBCs (Kocagöz *et al*, 2022). The embryonic origin or the arrival of zebrafish HBCs to the OE is not well understood, however, current data suggests that all cells of the OE are derived from the OP adjacent to the neural plate in early development, and endogenous expression of the NC markers was not found (Torres-Paz & Whitlock, 2014).

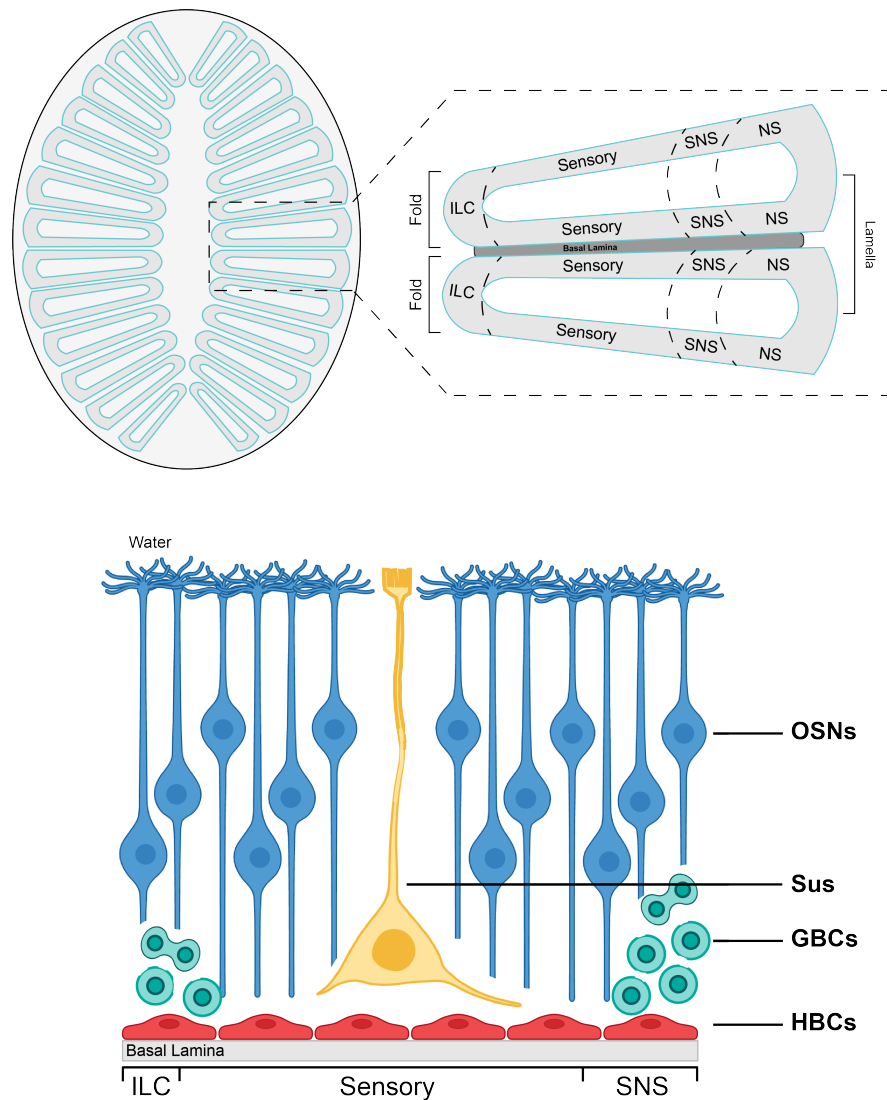


Figure 1.1. A detailed overview of zebrafish OE.

While complete recovery from MeBr lesion takes up to 6 weeks in rodents (Schwob *et al*, 1995), it only takes a week for zebrafish to regenerate the OE after Triton X-100 injury (Iqbal & Byrd-Jacobs, 2010). As mentioned above, in the intact OE, dividing cells have a bimodal distribution along the radial dimension of the fold and are mostly observed in the ILC and SNS. When the OE is injured with Triton X-100, the bimodality is disturbed and a homogeneous presence of dividing cells along the whole fold can be observed. The change in proliferation pattern is mostly due to the activation of otherwise dormant HBCs within the sensory OE (Kocagöz *et al*, 2022). Their activity

peaks during the 3rd day of post-injury (dpi), and they revert to dormancy during the 5th day post-injury. Pharmacological agents stimulating the Wnt signaling were found to enhance the mitotic activity of HBCs in the intact OE, however, inhibition of the Wnt did not completely prevent the activation of HBCs, suggesting the presence of additional regulators for the activation of HBCs during injury (Kocagöz *et al*, 2022). Axotomy of the zebrafish OE also increases the HBCs activity with a bias towards the neurogenic zones. However, their activity does not give rise to OSNs at least during the early phases of recovery (Kocagöz *et al*, 2022). A recent transcriptome analysis revealed the upregulation of heparin-binding epidermal growth factor (HB-EGF) and EGF receptors as early as 4 h post-injury (hpi). Importantly, HB-EGF stimulation also increases neurogenesis and divisions of Sox2⁺ stem cells in the intact OE. Administration of inhibitors for the HBEGF and EGFR signaling significantly prevents the regeneration of the zebrafish OE by 5 dpi. (Şireci, Alkiraz, unpublished). Although there is substantial evidence pointing out that HB-EGF/EGFR signaling regulates OE regeneration and the activation of HBCs upon damage, downstream effectors of this pathway remain to be investigated.

1.4. HB-EGF/EGFR Signaling

HBEGF is a member of the epidermal growth factor family that can bind to EGFR (ErbB1 homodimers and ErbB1/4 heterodimers) which are members of the receptor tyrosine kinase family. HB-EGF can function as a paracrine signal once it is cleaved by proteases such as ADAM family of metalloproteases, and matrix metalloproteinases (MMPs). It is expressed in a pro-HBEGF form, which is a transmembrane protein, its intracellular domain can interact with apoptotic proteins which regulate the survival of HB-EGF expressing cells (Hung *et al*, 2014). The process of cleaving the extracellular domain of pro-HB-EGF is called ectodomain shedding and results in the release of HBEGF that has been shown to contribute to the recovery from injury in a range of tissues (Dao *et al*, 2018). Although the ectodomain shedding and autocrine and paracrine signaling are canonical for HB-EGF signaling, pro-HB-EGF can also activate EGFRs of adjacent cells without shedding (Dao *et al*, 2018). Ectodomain shedding is

positively regulated by the p38 MAPK pathway and Protein kinase C (Gechtman *et al*, 1999; Izumi *et al*, 1998), and inhibition of metalloproteases required for shedding impaired the regeneration of zebrafish and rodent OE (Şireci *et al*, unpublished; Chen *et al*, 2020). In our laboratory we have shown that inhibition of HB-EGF or its receptor EGFR also significantly prevented regeneration in the zebrafish OE. When skin is burned, HB-EGF becomes abundant in the hair follicle and at the edges of the wound, which is normally confined to the basal layer. Keratinocyte-specific gain and loss of function experiments revealed that HB-EGF contributes to the mobilization of cells during injury and is regulated by retinoic acid (Shirakata *et al*, 2005; Xiao *et al*, 1999). In the cornea epithelium, injury causes the activation of p38 MAPK activity, which in turn increases the shedding of pro-HB-EGF by ADAM17 (Hollborn *et al*, 2006; Yin & Yu, 2009). A similar proliferative effect of HB-EGF dependent on MAPK/Erk and PI3K/AKT activity has also been observed in the intestine epithelium and respiratory epithelium regeneration (El-Assal & Besner, 2005; Dao *et al*, 2018) HB-EGF levels also rise in the brain upon ischemic injury and supplying more HB-EGF to a rat ischemic model increased neurogenesis and improved recovery of motor functions (Oyagi *et al*, 2011; Jin *et al*, 2004). Proliferative effects of HB-EGF observed on cortical cultures were also mediated through EGFR and MAPK/ERK and PI3K/AKT pathways were the main downstream effectors (Jin *et al*, 2005). Another neurogenic effect of HB-EGF was described in studies on retina regeneration in zebrafish, which reveal HB-EGF as the driving factor of de-differentiation of resident Müller glial cells called Müller glia into neuro-competent stem cells. They also show that HB-EGF is part of a signaling loop with *Ascl1* and Notch and simultaneously acts as an upstream regulator of the Wnt pathway which is also important for the proliferation of retinal progenitors (Wan *et al*, 2012). The binding of HB-EGF to a receptor from the EGFR family can induce several signaling cascades such as the Ras/Raf/MEK/ERK, PI3K/AKT, JAK/STAT, Nck/PAK, and Phospholipase C/PKC/JNK pathways (Schlessinger, 2000). Among these, ERK and AKT pathways are heavily involved in decisions of the cell fate and are also the focus of this study. Whether a cell will divide, die, or change its metabolism depends on the activity of these pathways (Normanno *et al*, 2006). A simplified scheme for the binding of HB-EGF to EGFR and leading to the activation of PI3K/AKT and

MAPK/ERK pathways is presented in the Figure 1.2. Further details of these pathways will be provided in the next sections.

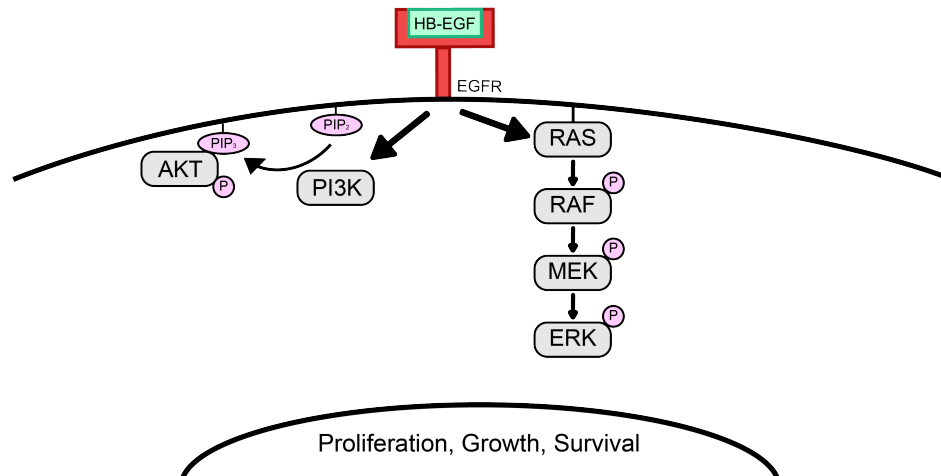


Figure 1.2. Potential downstream signaling pathways of binding of HB-EGF to EGFR.

1.4.1. MAPK/ERK Signaling Pathway

The Mitogen-Activated Protein Kinase (MAPK) pathway is a sequential cascade of phosphorylation performed by protein kinases and generally converges onto an effector such as ERK1/2, JNKs, and p38-MAPKs in mammals. Among these ERK1/2 is well studied and considered to be the classical MAPK pathway effector. As a general principle of MAPK pathways, the downstream kinase that regulates biological processes in the cell is called Mitogen-Activated Protein Kinase (MAPK). The kinase that phosphorylates the MAPK is called MAPK kinase (MAPKK). The most upstream kinase that phosphorylates the MAPKK is referred to as MAPKK kinase (MAPKKK). In the classical MAPK/ERK pathway, MAPK is the ERK1/2 module, MAPKK is the MEK1/2 module, and MAPKKK is the family of Raf proteins (Morrison, 2012). Induction of MAPK/ERK starts with the binding of a ligand such as FGF2, PDGF,

IGF-1, Neuroregulins, BDNF, neurotrophin-3, and TGF- α to its respective receptor on the cell surface which are generally members of RTK or GPCR families. However, intracellular events such as Ca^{++} signaling, the presence of reactive oxygen species, and damage to DNA can also cause ERK activation (Wen *et al*, 2022). Various adaptor and scaffold proteins in addition to components of the MAPK/ERK pathway localize around the intracellular domain of the receptor which increases the concentration of kinases of the pathway and contributes to the effectiveness of the MAPK pathway (Morrison, 2012). Afterward, Ras promotes the dimerization of Raf which phosphorylates a serine residue of MEK1/2. The kinase activity of MEK1/2 is specific for ERK1/2 and it phosphorylates ERK1/2 at residues of Tyr 204/187 and Thr 202/185. In the end, phosphorylation of ERK causes structural changes that enables the kinase activity of ERK which in turn further phosphorylates proteins in the membrane, other organelles, and cytoplasm (Chang & Karin, 2001). Moreover, dimerization leads to ERK entering the nucleus to phosphorylate transcription factors and change their structures in a way that alters their DNA-binding (Maik-Rachline *et al*, 2019). A well-known example is the regulation of the expression of the cyclinD1 by ERK, which contributes to the regulation of cell cycle progression from the G1 to the S phase, the critical step for cell division. MAPK/Erk activity not only regulates the expression of Cyclin D, but also the activity of cell cycle regulating proteins post-translationally in the cytoplasm such as Cdks and their regulator Cdc phosphatases and C-Myc which are all well-studied regulators of the cell cycle (Zhang & Liu, 2002). In addition to the cell cycle, ERK has also targets proteins involved in cell survival, differentiation, migration, metabolism, and growth, thereby regulating a host of cellular processes (Lavoie *et al*, 2020). Orchestrating all these processes which are all required and need to be thoroughly controlled for functional recovery of tissues from injury, brings the MAPK/ERK signaling forward as a potent regulator of regeneration. Examples of the MAPK/ERK activity during regeneration of vertebrate organs in regeneration-competent animals are rapidly expanding. In frogs, a critical step for regenerating limbs called blastema formation was found to be promoted by MAPK/ERK and PI3K/AKT activities (Suzuki *et al*, 2007). Another study on optic nerve regeneration also revealed that retinoic acid-dependent MAPK/ERK and STAT3 activity is required for the survival of retinal ganglion after

injury (Duprey-Díaz *et al*, 2016). In the fin regeneration of zebrafish, FGF-induced ERK1/2 was found to regulate Wnt and stimulate the initiation of regeneration and proliferation (Matthew *et al*, 2009). In bone regeneration, rhythmic waves of ERK1/2 activity moving through osteoblasts in a ring-like pattern were found to contribute to the growth of the bone and to be a key element for successful regeneration (De Simone *et al*, 2021). In the mouse model of spinal cord injury, MAPK/ERK activity is observed during the dedifferentiation, proliferation, and remyelination of Schwann cells in addition to the generation of inflammatory signals by Schwann cells (Napoli *et al*, 2012). MAPK/ERK activation also promotes the differentiation and myelination of oligodendrocytes in CNS which are analogs of Schwann cells in PNS (Najm *et al*, 2015). It also contributes to the survival of neurons in the CNS by interacting with the anti-apoptotic Bcl-2 (Jiao *et al*, 2005). Opposing to previous examples from other tissues, EGFR/ERK can also cause suppression of differentiation of neuronal progenitors after spinal injury (Xue *et al*, 2020).

1.4.2. PI3K/AKT Signaling Pathway

AKT (AK Strain Transforming; Xie & Weiskirchen, 2020) is also known as protein kinase B and it is a serine/threonine kinase from the AGC family of kinases. AKT has three isoforms in mammals and all have a PH domain that can bind to phosphatidylinositol (3,4,5) triphosphate (PIP3) and phosphatidylinositol (3,4) diphosphate (PIP2) lipids in the membrane. The kinase domains of the AKT proteins are heavily similar to PKA, PKC, and PDK1 which are some of the other members of the AGC family. The pathway can also be induced by RTKs, most commonly by the insulin receptor and EGFR, but also by GPCRs. Phosphoinositide 3-Kinase (PI3K) is recruited to an adaptor protein and phosphorylates inositol lipids abundant in the membrane to generate PIP2 and PIP3. PDK1 and Akt are recruited to the membrane through binding of their PH domain to PIP2 and PIP3. Phosphorylation by PDK1 and mTORC2 at different sites activates the AKT. Upon activation, AKT can phosphorylate many targets, most notably, GSK3 from glucose metabolism, TSC2 from the mTORC1 complex, and FOXO transcription factors, p27, and BAD. AKT promotes the survival

the survival of cells by inactivating pro-apoptotic proteins such as BAD. By phosphorylating the FOXO transcription factors that promote the expression of pro-apoptotic genes, AKT causes their export from the nucleus and further inhibits the expression of those pro-apoptotic genes. Akt also promotes the growth of cells through phosphorylating and inactivating TSC2. TSC2 is an inhibitory component of the mTORC1, so inhibition of TSC2 by AKT stimulates the activity of the mTORC1 complex (Inoki *et al*, 2002). Further downstream mTORC1 components are eukaryotic initiation factor 4E binding protein 1 (4E-BP1) which binds to eIF4E and prevents it from initiating the translation of mRNA. When mTORC1 is activated by AKT, 4E-BP1 is phosphorylated and released from the eIF4E which enables protein translation (Gingras *et al*, 1999). The cell cycle also relies on protein translation for sufficient protein synthesis and for the proper abundance of cell cycle proteins such as cycD that can trigger or prevent the progression of the cell cycle (Mamane *et al*, 2004). Accordingly, inhibition of mTOR can lead to arrest of the cell cycle (Skeen *et al*, 2006). AKT can also directly phosphorylate and regulate the regulators of the cell cycle such as p21 and p27 (Medema *et al*, 2000; Zhou *et al*, 2001), thus contributing to cell proliferation by regulating the cell cycle. AKT has also been shown to shut off the MAPK/ERK pathway by inhibiting c-Raf, the upstream kinase of the MEK/ERK (Zimmermann & Moeling, 1999) thereby preventing cell proliferation. Another target of AKT, Glycogen Synthase Kinase 3 (GSK3) inhibits the glycogen synthase which synthesizes glycogen when glucose becomes abundant in the cell. AKT phosphorylates and inhibits the GSK3 which results in increased glycogen synthesis. Activation of AKT also increases the number of glucose transporters on the cell surface and increases glycolysis by changing the activities of enzymes of the aerobic glycolysis (Elstrom *et al*, 2004; Hoxhaj & Manning, 2019). Although regulatory effects of AKT are generally studied within cancer biology, evidence for fates of the stem cells including neural stem cells and neurodegenerative diseases being closely linked to the PI3K/AKT pathway is accumulating. For example, upon activation by FGF, PI3K/AKT signaling suppresses Wnt and ERK pathways and it is required for preserving pluripotency of human embryonic stem cells (Singh *et al*, 2012). Axon repair in the brain is also regulated by multiple aspects of PI3K/AKT signaling. Oligodendrocyte cells have impaired myelination in multiple sclerosis, and

in the cuprizone-induced demyelination model of multiple sclerosis, can be overcome by promoting mTOR (mammalian target of rapamycin) signaling, which in turn increases remyelination (Jeffries *et al*, 2021). Failure of axon regeneration in CNS can also be reversed by inactivation of PTEN, a well-studied inhibitor of AKT/mTOR signaling, probably due to stimulation of axonal protein synthesis by mTOR (Lee *et al*, 2014). Another recent example comes from adult neurogenesis in murine models, which can be enhanced by exercise. A critical mediator for this effect is found to be miRNA 135-a which can interact with PIP3 and potentially interfere with PI3K/Akt signaling (Pons-Espinal *et al*, 2019). Moreover, the neurogenic potential of neuronal progenitors in the hippocampus can be categorized according to their level of reactive oxygen species (ROS) which are products of the aerobic glycolysis in cytoplasm and the oxidative phosphorylation in the mitochondria. Quiescent NPCs have the highest level of ROS among all progenitors while levels of PTEN, an inhibitor of both cell cycle and AKT, decrease towards committed NPCs from quiescent NPCs (Adusumilli *et al*, 2021). Apart from metabolic aspects, neurodifferentiation in zebrafish larvae is also mediated by AKT through interactions with Notch signaling (Cheng *et al*, 2013). Overall, PI3K/AKT pathway can directly regulate survival, metabolism, and proliferation of cells, and whether inhibition or stimulation of this pathway impacts the NSCs and potentially regeneration of nervous tissues remain to be investigated.

2. PURPOSE

The peripheral OE is an established model to study adult neurogenesis and nerve cell regeneration, which are limited processes in the mammalian brain. Understanding the extra- and intracellular signaling pathways that influence adult neurogenesis may provide a better understanding of how neural stem cells could be activated to replace dying or degenerating neurons and may contribute to the development of novel therapeutic strategies. A recent transcriptome analysis of the regenerating zebrafish OE that was performed in our research group revealed a significant and transient upregulation of the signaling factor *hbegfa* and its receptor *egfra* (*erbb1*) as early as 4 h post injury, which suggests that HB-EGF:EGFR signaling may trigger regenerative OSN neurogenesis. *In situ*-hybridization against *hbegfa* confirmed the transcriptome results at tissue level. Intranasal stimulation with recombinant HB-EGF protein resulted in increased mitotic divisions of Sox2⁺ progenitor cells and neurogenesis in the intact OE, while inhibition different stages of HB-EGF signaling with pharmacological agents impaired the regeneration process. However, the intracellular signaling pathways that are activated as a result of EGFR stimulation by HB-EGF and their contribution to the OE regeneration remain largely unknown. Among the candidate signaling pathways that can be transduced by EGFR, the MAPK/ERK and PI3K/AKT pathways are well-known for their role in regulating the cell cycle. Therefore, the main aim of the studies presented in this thesis was to reveal whether these signaling pathways are involved in the regeneration of the OE and their respective contributions to the process.

To understand whether activation of the MAP/ERK and PI3/AKT pathways are necessary for injury-induced progenitor cell proliferation and neurogenesis, they were pharmacologically inhibited in lesioned OEs with the small chemical inhibitors U0126 and Lys294002, respectively. The rate of cell proliferation and tissue distribution of dividing cells in intact and injured OEs was compared between vehicle-injected control animals and fish treated with the inhibitors at 24 h post lesion. To establish their im-

pact on the overall regeneration process, the efficiency of regeneration was analyzed quantitatively at 5 d post lesion by examining the number of newly generated OSNs.

To further validate the results that could be observed with the loss of function approaches using pharmacological inhibitors, the activation of the MAPK/ERK and PI3/AKT pathways in dividing cells were examined at tissue level at 24 h post lesion by co-immunostainings of the tissue with the PCNA S-phase marker of the cell cycle and the activated, phosphorylated isoforms of pERK and pAKT. The analysis was repeated at 3 and 5 d post injury to establish the time window of the regeneration process during which these regulators are activated. To provide a conclusive link between EGFR activation by HB-EGF and the MAPK/ERK pathway the number of pERK-positive cells was analyzed in intact and injured OEs in which the ERK phosphorylation, HB-EGF signaling, or EGFR signaling were inhibited by small molecule inhibitors.

3. MATERIALS AND METHODS

3.1. Materials

3.1.1. Adult Zebrafish

Adult zebrafish (*Danio rerio*) of at least 6 months of age from the AB/AB strain or wild type fish obtained from a local petshop that are bred in the facility were used in all experiments. All fish were kept in Vivarium Animal Facility of Boğaziçi University Center for Life Sciences.

3.1.2. Equipment and Supplies

A list of all equipment and disposable and non-disposable supplies are provided in appendix A.

3.1.3. Solutions and Buffers

A list of all solutions, buffers and antibodies used throughout this study with their respective manufacturer is given in appendix B.

3.2. Methods

3.2.1. Maintenance of Zebrafish

Adult zebrafish was kept at in a dedicated fishroom with constant temperature of 28 °C and a 14 hours light / 10 hours dark cycle at the AAALAC-accredited Vivarium of the Center for Life Sciences and Technologies at Boğaziçi University. Fish were maintained in three independent systems manufactured by Aquatic Habitats in tanks containing 1, 3, or 10 l fish-water. The system provides circulation, aeration and filte-

ring, in addition to heating and sterilization with UV light. System water is routinely changed with freshly made artificial fresh water by dissolving 2 g sea salt, 7.5 g sodium bicarbonate, and 0.84 g calcium sulfate in 100 liters of reverse osmosis water. Dirty fish tanks were cleaned weekly and filters of the systems were replaced weekly to ensure a pathogen-free environment for the fish. Fish were fed twice with dried & frozen egg yolk and flake food in the mornings, and with brine shrimp in addition to yolk and flake food in the evenings. The use of experimental zebrafish for this study was approved by the Institutional Ethics Board for Animal Experiments at Boğaziçi University (BUHADYEK) under title 2020-17 (“The role of heparin-binding epidermal growth factor (HB-EGF) signaling during regenerative neurogenesis in the zebrafish olfactory epithelium”). All relevant international, national, and institutional guidelines for the care and use of animals were followed, including the National Animal Protection Act (Turkish national law number 5199, “Hayvanları Koruma Konunu”, published 24.06.2004), the directive 2010/63/EU of the “European Parliament and the Council of 22. September 2010 on the Protection of Animals Used for Scientific Purposes” and the “Guide for the Care and Use of Laboratory Animals” (NRC2011) of the Association for Assessment and Accreditation of Laboratory Animal Care (AAALAC).

3.2.2. BrdU and EdU Incorporation

To label dividing cells, the thymidine analogs 5-Bromo-2-deoxyuridine (BrdU; AppliChem) and 5-ethynyl-2'-deoxyuridine (EdU ; Thermofischer) were used. For BrdU incorporation 30 mg/l of BrdU was dissolved in tank water. Fish were kept in the to ensure BrdU stability over the 24 hour period that will be analyzed for mitotic activity. For the detection of BrdU, a rat antibody against BrdU (Abcam Cat no:Ab6236) was utilized. For EdU, 25 μ l of 10 mM Edu in PBS solution were injected intraperitoneally to fish immediately prior to the period of analysis of mitotic cells. For the detection of EdU, a detection cocktail a 500 μ l of cocktail containing 431.4 μ l of sterile water, 43 μ l of 10X Click-iT EdU reaction buffer, 20 μ l of CuSO₄, 0.6 μ l Alexa-Fluor 647-azide or Alexa-Fluor 488-azide, and 5 μ l of 10X Click-iT EdU buffer additive was added to an eppendorf tube in the given order. This recipe provides sufficient detection solution

for two slides and was adjusted according to the number of slides used in the staining reaction. After preparation, the cocktail was immediately pipetted onto slides for thirty minutes of incubation and washed twice with PBS-T to stop the reaction. Detection of EdU was only performed once immunohistochemistry against other epitopes was completed.

3.2.3. Chemical injury of OE

To chemically lesion the OE, fish were anesthetized in 40 mL of tank water containing 160 mg/mL tricaine (Sigma) until fish lost the reflex against tactile stimuli to the tail and opercular movements slowed down. Anesthetized fish was placed ventral side-down onto the groove of a sponge to ensure that it will remain stationary during the procedure. A 1% Triton X-100 solution was prepared by adding 10 μ l of Triton X-100 and 200 μ l of phenol red solution to 790 μ l of 1X PBS. Approximately 1 μ l of this solution was administered to the left nasal cavity with a heat-pulled glass capillary tube for 90 s to ensure induction of degeneration. At the end of the incubation period, the damage solution was flushed out with tank water by a Pasteur pipette, and fish was put back into tank water for recovery.

3.2.4. Intraperitoneal Injection of Inhibitors

For ERK inhibition, 10 μ g of U0126 (Tocris) dissolved in 2.6 μ l of DMSO and 3 μ l of phenol red solution was added into 24.4 μ l of 1X PBS to prepare a 30 μ l injection solution. Each fish received injections 6 h before, during, and 6 h after the injury by nasal irrigation with 1% Triton X-100. For AKT inhibition, 25 μ g of Ly294002 (Caymann) dissolved in 2.5 μ l of DMSO and 3 μ l of phenol red solution was added into 24.5 μ l of 1X PBS to prepare a 30 μ l injection solution. Each fish received injections 4 h before, during, and 4 h after injury. For inhibition of HB-EGF signaling, 1 μ g of CRM-197 (Santa-Cruz) in 1 μ l of HEPES and 3 μ l of phenol red solution was added into 26 μ l of 1X PBS solution. Each fish received injections 6 h before and during the nasal injury. For inhibition of EGFR signaling, 27 μ g of PD153035 (Sigma) dissolved

in 10 μl of DMSO and 3 μl of phenol red solution was added into 17 μl of 1X PBS to prepare a 30 μl injection solution. Each fish received injections 4 h before, during, and 4 h after injury and an additional injection 4 h before dissection. During injection, the fish were anesthetized as described in section 3.2.2 and placed dorsal side down onto the groove of the sponge so that abdomen region is facing upwards. Injections of 30 μl inhibitor solution were administered with a 0.5 ml insulin syringe (Beckon Dickinson) with a 30G-sized needle. Injection point was just anterior of the anal fins and to the middle of abdomen. After injection, the fish were put back immediately to tank water for recovery.

3.2.5. Dissection of the Olfactory Epithelium

Prior to dissection, fish were euthanized with an overdose of the anesthetic tricaine, decapitated with a fine blade, and heads were put on a soft dissection pad containing drops of ice-cold PBS. Fine forceps (Dumont 5) were used for removal of other parts of the head to reach the OE. The head was cut into half from the midline to have the left OE in the left half and right OE in the right half of the head. Once the skin of the OE was removed, OEs were removed from the nasal cavity by detaching it from underlying nasal bones with the help of the forceps. After dissection, OEs were either embedded in OCT medium (Sakura Finetek), ventral side facing upwards and frozen to $-20\text{ }^{\circ}\text{C}$ or collected into 4% ice-cold PFA solution. Once frozen OCT-embedded OEs were stored at $-20\text{ }^{\circ}\text{C}$ fridge.

3.2.6. Cryosectioning of the Olfactory Epithelium

Frozen OEs embedded in OCT were transferred into the cryostat that was set to $-20\text{ }^{\circ}\text{C}$ for chamber temperature and $-18\text{ }^{\circ}\text{C}$ for object temperature for equilibration. Frozen OEs were mounted onto stage and trimmed to get rid of additional OCT prior to sectioning. During sectioning, section thickness was set to 12 μm and each section was collected onto a Superfrost[®] Plus slide manufactured by ThermoFisher Scientific. Slides were heat-fixed for at least one hour in an oven set to $60\text{ }^{\circ}\text{C}$. To ensure the sta-

bility of sections during the antigen retrieval procedure for pERK and pAKT stainings, sections were heat-fixed for two hours. Afterwards, slides were stained and additional back-up slides were stored at -80°C . Before staining of slides stored in -80°C , an additional heat-fixation was performed for 30 minutes in 60°C , to avoid detachment of sections.

3.2.7. Immunohistochemistry of Olfactory Epithelium

3.2.7.1. Immunohistochemistry against BrdU and HuC/D. After heat-fixation, edges of the slides were marked with PAP pen (Sigma) to create a hydrophobic seal that will keep the solutions on the slides inside the marked area. Afterwards, sections were allowed to rehydrate with PBS for 5 minutes. To fix the OE sections, 1 ml of 4% paraformaldehyde (PFA) solution in PBS (pH = 7.4) was used to cover the whole slide for 15 minutes in a moist chamber. To ensure removal of PFA on sections prior to next steps, slides were washed with PBS-T (pH = 7.4) for 10 minutes in a jar for three times. Between each wash, PBS-T in the jar was renewed. To improve nuclear staining, as required for BrdU and HuC/D, a 15 min treatment with 4 N HCl was performed. To remove excess HCl that can interfere with efficient blocking, slides were washed three times with PBS-T for 10 min. Afterwards, slides were put back to the incubation chamber for blocking with 3% bovine serum albumin (BSA) solution in PBS-T at room temperature for one h. Once blocking was finished, primary antibody cocktails were added onto slides and covered with plastic coverslips. For one slide, 250 μl of antibody solution were prepared in 3% BSA blocking solution. HuC/D (mouse anti HuC/D; Life Technologies, 16A11, 1661237) and BrdU (rat anti-BrdU; Abcam, ab6326) antibodies were diluted 1:500 in blocking solution. Incubation with the primary antibody cocktail was performed overnight at 4°C . To avoid drying or evaporation of the antibody solution, the base of the staining chamber was covered with tissue paper and soaked with water or PBS to provide moisture to the chamber. In the following day, the primary antibody solution was recovered and stored at -20°C for future reuse. After primary antibody incubation, slides were washed with PBS-T for at least three times 15 min each. A secondary antibody s containing Cy2- (mouse anti-rat;

Jackson Immuno) and Cy5-labeled (rabbit anti-mouse; Jackson Immuno) antibodies at 1:250 dilution in 250 μ l of blocking solution was prepared and added onto the slides. Incubation of secondary antibody cocktail was performed at room temperature for two h. After secondary antibody incubation, slides were washed with PBS (pH = 7.4) three times for 10 minutes, each, and slides were imaged under a confocal microscope.

3.2.7.2. Immunohistochemistry against pERK and pAKT. Since capturing a phosphorylated residue on a protein can be challenging, a different staining protocol was used to observe pERK and pAKT-positive cells. According to this protocol, intact and damaged OE were collected into separate 1.5 ml Eppendorf tubes containing 1 ml 4% ice-cold PFA with their nasal bones and upper-skin immediately after dissection to avoid delays in the dissection that might cause protein degradation. Collected OEs were fixed in 4% PFA overnight. On the following day, OEs were washed with PBS-T in the Eppendorf tubes for three times, fifteen min, each. To recover epitopes that might have been masked during the long fixation period, an antigen-retrieval protocol was performed at 70°C on a thermomixer for 15 minutes. The buffer used for antigen-retrieval was 150 mM Tris-HCl (pH = 9). Once the tubes cooled down to room temperature, the OEs were washed with PBS-T three times for fifteen min to completely remove the antigen retrieval buffer. After the washing steps, the OEs were transferred to the dissection pads and further dissected out from other tissue remnants and embedded into OCT medium for cryosectioning. After sectioning and heat-fixing at 60°C of 2 h in the oven, sections of OE were briefly rehydrated with PBS and immediately afterwards, blocked with the 3% BSA in PBS-T for one hour. A pERK antibody (rabbit anti pERK; Cell signaling; 4370S), PCNA antibody (mouse anti PCNA; Sigma-Aldrich; O84M4776), and pAKT antibody (rabbit anti-pAKT; Cell Signaling; 2965S) was used with this protocol with each of them diluted at 1:500 in blocking solution. Primary antibody incubation was performed overnight in the moist chamber. The following day, slides were washed in jars filled with PBS-T three times for 15 min and secondary antibody incubation was performed for 3 h at room temperature. For the detection of pERK and pAKT antibodies, Alexa488-anti-rabbit secondary antibodies were used at 1:800 while a Cy3-anti-mouse was used at 1:250 for detection of anti-PCNA and anti

-HuCD antibodies. After secondary antibody incubation, slides were washed in PBS three times for 10 min. Once the immunostaining was completed, the EdU detection cocktail was prepared as mentioned in the section 3.2.2 and slides were incubated in the chamber at room temperature for 30 minutes. To stop the reaction, slides were washed in PBS-T for 5 minutes and 10 minutes. If nuclear staining with PCNA antibody was not preferred, cell nuclei were stained with DAPI (0.1 g/l ; Thermo Fisher) by another 20 minute incubation with DAPI solution at room temperature in the dark that was followed by three 10 minutes washes in PBS. At this stage sections were ready for imaging with the confocal microscope.

3.2.8. Imaging by Confocal Microscopy

Images of whole OE sections were taken on a Leica SP5-AOBS confocal microscope using a 20X water immersion lens, while Hemi-OEs were taken with a Leica TCS SP8 system using a 40X water immersion lens. All images were taken with a resolution of 2048x2048 pixel at 400 Hz acquisition frequency. To filter out background, smart offset between 0 and 2% was used in the images taken with PMT detectors. pERK and pAKT stainings were specifically imaged with HyD detector of the Leica TCS SP8 to improve the signal to noise ratio. Each section was frame-averaged between 2 to 4 times to improve the quality of the image. 5 sections were chosen and imaged from each OE of each fish for further analysis.

3.2.9. Positional Profiling

Images stored as LIF files in the computers of the confocal microscope were adjusted and further analyzed using the FIJI software (Version 2.1, ImageJ). First, the image stacks were converted into a single maximum-projected tiff and saved. Afterwards, for the analysis of experiments presented in 4.1.1, 4.1.2, 4.3.1, and 4.3.2 whole OE images were cropped into left and right rectangular hemi-OEs with a width of the OE radius and a height corresponding to $2/3$ of the radius length. The radius of the OE was measured in FIJI from the center at the tip of the ILC to the peripheral edge

of the hemi-OE. Images obtained from left hemi-OEs were flipped horizontally to make sure that the ILC and non-sensory OE correspond to the beginning and the end of the x axis for both hemi-OEs during positional profiling. A custom-made FIJI macro was utilized to divide the images into ten equal compartments that correspond to the ILC in compartment 1, the entire sensory region in compartments 2 - 6, the SNS in compartments 7 and 8, and finally the NS region in compartments 9 and 10. In the FIJI macro, cells were manually marked with the multi-point tool and were counted into their respective bin according to their position along the x axis. The average cell numbers for each compartment is provided by an R script (Version 1.2, R Studio) that corrects the cell counts of the FIJI macro by equally distributing cells positioned on compartment borders to either side. For the positional profiling of other experiments, individual epithelial folds spanning the region between the ILC to the peripheral edge were cropped out instead of hemi-OEs and same custom FIJI macro that distributes the marked cells along the radial axis was used for the positional profiling.

3.2.10. Area Analysis of HuC/D

An area analysis was used to reveal the efficiency of regeneration in the injured OEs by judging how many new OSNs have been generated over the 5 day recovery period. For this purpose, 5 sections were collected for each condition and the HuC/D channel was converted to a binary image format and thresholded. The threshold was set onto the binary image to avoid any interference from differing brightness of HuC/D signals, which enabled inclusion of all HuC/D⁺ pixels without background. The area of HuC/D⁺ pixels was measured with the measure tool in addition to the area of the total OE, which was determined with polygon tool, and a ratio representing the area covered by HuC/D cells was calculated for each image. The mean of the HuC/D/total OE ratios of the intact OEs collected from control group of the experiment was considered as 100% occupation with a HuC/D area coefficient of 1, and used for normalization of other OE sections collected from damaged OE of control group and both intact and damaged OE of experiment groups.

3.2.11. Statistical Analysis of Results

For all experiments, ANOVA tests that will include comparisons of both intact and damaged OEs and their respective regions of the folds was carried out for both control and experimental groups. These ANOVA analyses were followed by Tukey's HSD test to be able to make comparisons between two conditions among all possible comparisons. These statistical analyses were conducted with PRISM software, and plotted graphs were organized in the Adobe Illustrator to generate figures presented in the results.

4. RESULTS

The OE is capable of regenerating dying and damaged neurons, a feature that is unique to the OE when compared to most other nervous tissues (Schwob, 2002). While the rat OE achieves complete regeneration by six weeks after injury (Schwob *et al*, 1995), regeneration of the zebrafish OE is mostly accomplished within 5 days after injury (Iqbal & Byrd-Jacobs, 2010; Kocagöz *et al*, 2022), which makes the zebrafish OE a powerful tool for studying adult neurogenesis and nerve cell regeneration. Investigating the cellular and molecular events that orchestrate the regeneration in the OE may provide valuable insights for replacing dying neurons in other parts of the nervous system. A transcriptome analysis of the injured zebrafish OE that was performed recently in our lab revealed a fifteen-fold increase in the levels of *hbegfa* at 4 hpi, which was confirmed by *in situ*-hybridization of injured and intact OEs (Güler, 2021). In addition to the OE, HB-EGF was also described as a critical regulator of regeneration in the injured zebrafish retina (Wan *et al*, 2012). HB-EGF binds to EGFR and, among other signaling pathways, can activate MAPK/ERK signaling, which in turn regulates the expression of genes required for neurogenesis such as *ascl1a* and *pax6b* (Wan *et al*, 2012). This signaling cascade is sufficient and necessary for reprogramming of mature Müller glia cells of the retina into neurogenic progenitors that are capable of generating neurons upon injury (Goldman, 2014). In the OE, expression of *egfra*, the respective receptor of HB-EGF was also found to be upregulated after injury and to be expressed by Tp63⁺ HBCs as confirmed by *in situ*-hybridization assays (Güler, 2021). While, exogenous stimulation of the intact OE with human recombinant HB-EGF triggers an increase in cell division and neurogenesis in the intact tissue (Kocagöz, 2021), inhibition of HB-EGF shedding and signaling through EGFR impairs regeneration of the injured OE (Şireci, unpublished; Alkiraz, 2022). Binding of HB-EGF to EGFR can activate many signaling pathways, most notably MAPK/ERK and PI3K/AKT signaling, which are both established master regulators of cell cycle progression and cell fate decisions and involved in regenerating bone, limbs, heart, and liver, in addition to promoting axon regrowth and proliferation of glial cells in CNS and PNS (Wen *et al*, 2022).

4.1. The Role of MAPK/ERK Signaling in OE Regeneration

To investigate whether the MAPK/ERK pathway is activated in the injured OE and if activated MAP/ERK signaling contributes to regenerative OSN neurogenesis, pharmacological inhibition with U0126 was used. U0126 inhibit the kinase of activity of MEK1/2, which is the immediate upstream kinase and activator of ERK (Duncia *et al*, 1998). As a selective inhibitor of MEK1/2, U0126 does not interfere with other MAPK pathways. The effect of inhibiting ERK activation on the regenerating OE was investigated at 1 and 5 dpi by staining the tissue for proliferation markers and the pan-neuronal marker HuC/D. The time course of ERK activation was further revealed by immunostaining against the phosphorylated form of ERK (pERK) at 1, 3, and 5 dpi. The successful inhibition of the ERK pathway by the U0126 was confirmed at tissue level by examining the number of pERK⁺ cells in inhibited OEs by immunostaining.

4.1.1. Early Phase of OE Regeneration by ERK Inhibition

Initially, effect of inhibition with U0126 was examined during the early phase of OE regeneration at 1 dpi. This phase has previously been characterized by a change in the spatial distribution of mitotic cells across the OE. In the intact tissue a bimodal distribution of mitotic cells with a strong preference to the ILC and SNS can be observed, which changes into a more uniform distribution of dividing cells along the sensory region in the damaged OE (Kocagöz *et al*, 2022). This change in pattern largely corresponds to a switch in mitotic activity from constitutively active GBCs that are located at the ILC and SNS to injury-activated HBCs that are positioned uniformly through the sensory region (Kocagöz *et al*, 2022). To inhibited ERK signaling during de- and early regeneration of the OE , intraperitoneal injections of 10 μ g U0126 were performed in fish in which the OE has been lesioned by nasal irrigation with 1% Triton X-100 as described in the section 3.2. A control group received intraperitoneal injections of 2.6 μ l of DMSO in 30 μ l PBS (vehicle of U0126) with the same timeline. Both the control and the experiment group consisted of 3 fish each. Each fish was incubated in tank water containing 30 mg/L BrdU to mark dividing cells between 0 and 24 hpi.

Following dissection and sectioning, the OEs were stained against the proliferation marker BrdU and the pan-neuronal marker HuC/D. For quantitative analysis of BrdU⁺ dividing cells and generation of positional profiles, images of whole-OEs were first cropped to rectangular hemi-OEs and positional profiles were generated in a way that describes the OE architecture and the occurrence of different cell types along epithelial folds. For this purpose, the total number of cells were counted into different regions along the radial dimension of the OE that correspond to the ILC (radial index 0.05), the sensory OE (radial index 0.15 – 0.55), the sensory/non-sensory border (SNS; radial index 0.65 – 0.75), and the non-sensory peripheral OE (NS; radial index 0.85 – 0.95). Cell counts from DMSO and U0126 groups were entered into PRISM software to carry out a one-way ANOVA followed up by Tukey HSD post-hoc analysis. Error bars represent standard error of mean (SEM) in all graphs. p-values below 0.05 are considered significant. This approach was followed for all statistical analysis of results throughout this study.

Representative images of the early response to Triton X-100 lesion experiment can be seen in Figure 4.1. Beginning from the left, the first and second columns contain images of the intact and damaged OEs that were collected from the control group that was injected with the vehicle DMSO. When the intact and injured OE of this group were compared, it can be seen that HuC/D⁺ neurons are efficiently ablated, except for occasional clusters of surviving cells in the ILC. As expected, the characteristic bimodal distribution of BrdU⁺ cells in the intact OE changes to a homogenous distribution of BrdU⁺ cells along the entire epithelial fold in the damaged OE and mitotically active cells appear to be randomly distributed. The third and fourth columns consist of representative images of intact and injured OEs collected from fish that have been injected with the MAP signaling inhibitor U0126. Similar to control OEs, HuC/D⁺ cells are almost completely lost at 1 dpi in the damaged OE and a loss of the bimodal distribution of mitotic cells can be seen. However, despite the apparent random distribution of dividing cells upon injury, BrdU⁺ cells were notably less in the damaged OE of U0126 fish when compared to the damaged OE of the control group.

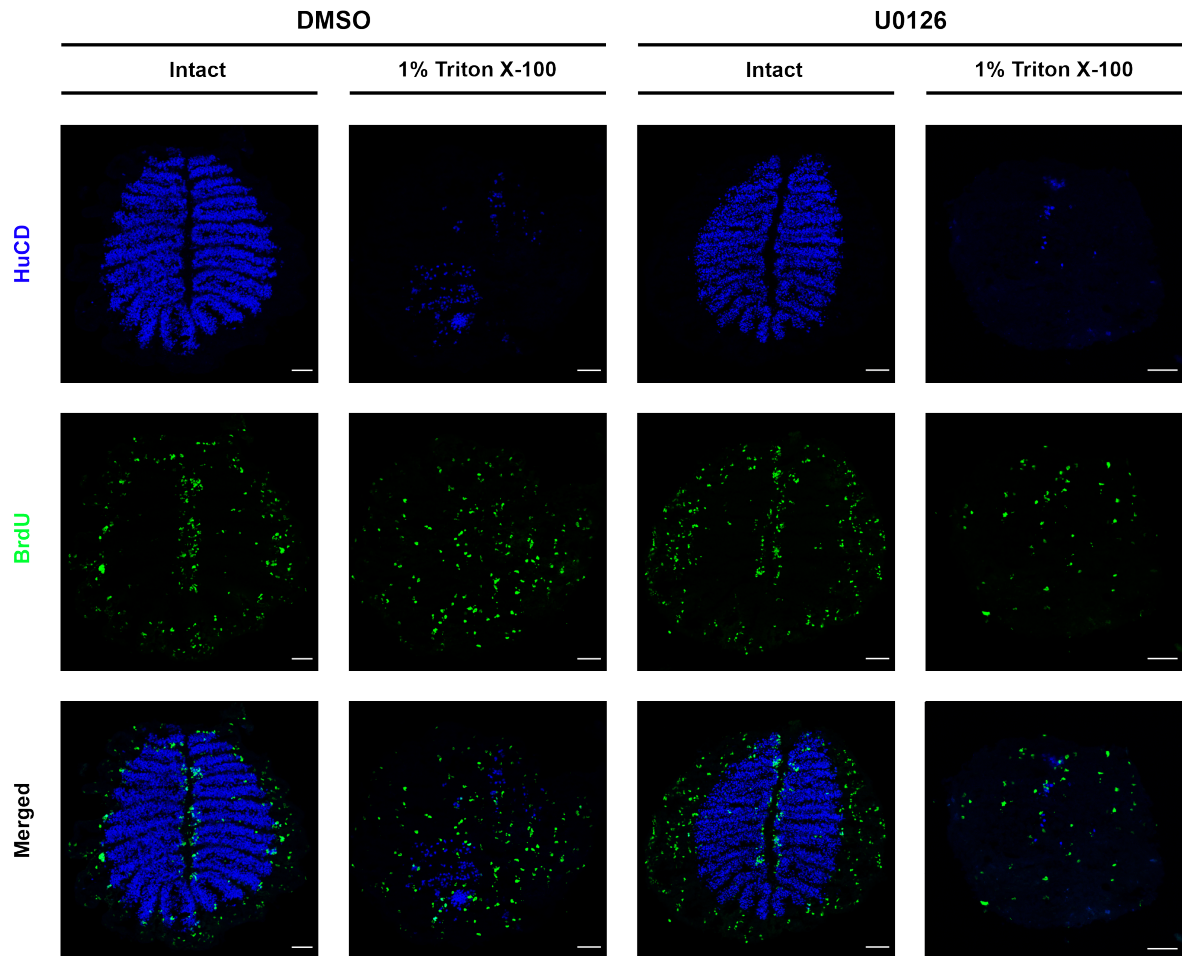


Figure 4.1. Effect of inhibition by U0126 on cell proliferation at 1 dpi. Immunohistochemistry against HuC/D (blue) and BrdU (green) in the intact and damaged OE of DMSO (left) and U0126 (right) groups. Scale bars are 50 μm .

A quantitative analysis of BrdU⁺ cells for the intact and damaged OE at 1dpi for the DMSO and U0126 groups is presented in Figure 4.2. In the Figure 4.2.a, positional profiles of BrdU⁺ cells that can be observed along epithelial folds of the intact OE of DMSO and U0126 fish are presented. As expected, BrdU⁺ cells can be found largely at the ILC and SNS in the intact OE of both groups. However, a minor decrease in the number of BrdU⁺ cells is observed in the ILC, sensory region and SNS for the intact OE of U0126 group when compared with DMSO-injected fish.

OEs of DMSO and U0126 groups was analyzed, significant decreases were found in the ILC, sensory region, and SNS. The most significant change occurs in the sensory OE, in which injury typically induces a strong proliferation response. In the DMSO-treated group, a 2.7-fold increase in the number of BrdU⁺ cells from 12.2 ± 1.6 to 33.4 ± 2.7 cells can be observed. While a 1.8-fold increase in the number of cells from 6.5 ± 0.8 to 11.8 ± 1.4 cells is still noticeable in the injured OE of the U0126 group, the overall number of dividing cells is similar to the number of cells in the intact OE of DMSO-treated animals (12.7 ± 1.6 cells/hemi-OE). The difference between the injured OEs of both experimental groups was highly significant (ANOVA $F_{(3,120)} = 28.48$ p-value <0.0001 , Tukey's p-value <0.0001). A significant reduction was also observed for the ILC (Tukey's p-value = 0.02) and SNS (Tukey's p-value = 0.01) but not for the NS (ANOVA $F_{(3,120)} = 33.32$ p-value <0.0001 , Tukey's p-value = 0.92). These observations suggest that inhibition of the MAP/ERK signaling pathway by U0126 strongly and significantly prevents activation and mitotic cell divisions of injury-responsive progenitor cells, predominantly within the sensory region of the OE.

4.1.2. Late Phase of OE Regeneration with ERK Inhibition

To further understand the impact of MAPK/ERK inhibition by U0126 on overall OE regeneration, a similar experiment was conducted with another set of 3 fish each for the DMSO control U0126 group that were injected again prior, at, and after OE damage. However, in this experiment, the animals were incubated in BrdU-containing fish water between 48 and 72 hpi, which corresponds to the middle phase of regeneration at which a peak activity of cell proliferation can be observed in the sensory region (Kocagöz *et al*, 2022). After 72 hpi, OEs were allowed to further regenerate until 120 hpi (5 dpi), at which regeneration is nearly complete and when most of the neurons have been restored (Iqbal & Byrd-Jacobs, 2010; Kocagöz *et al*, 2022).

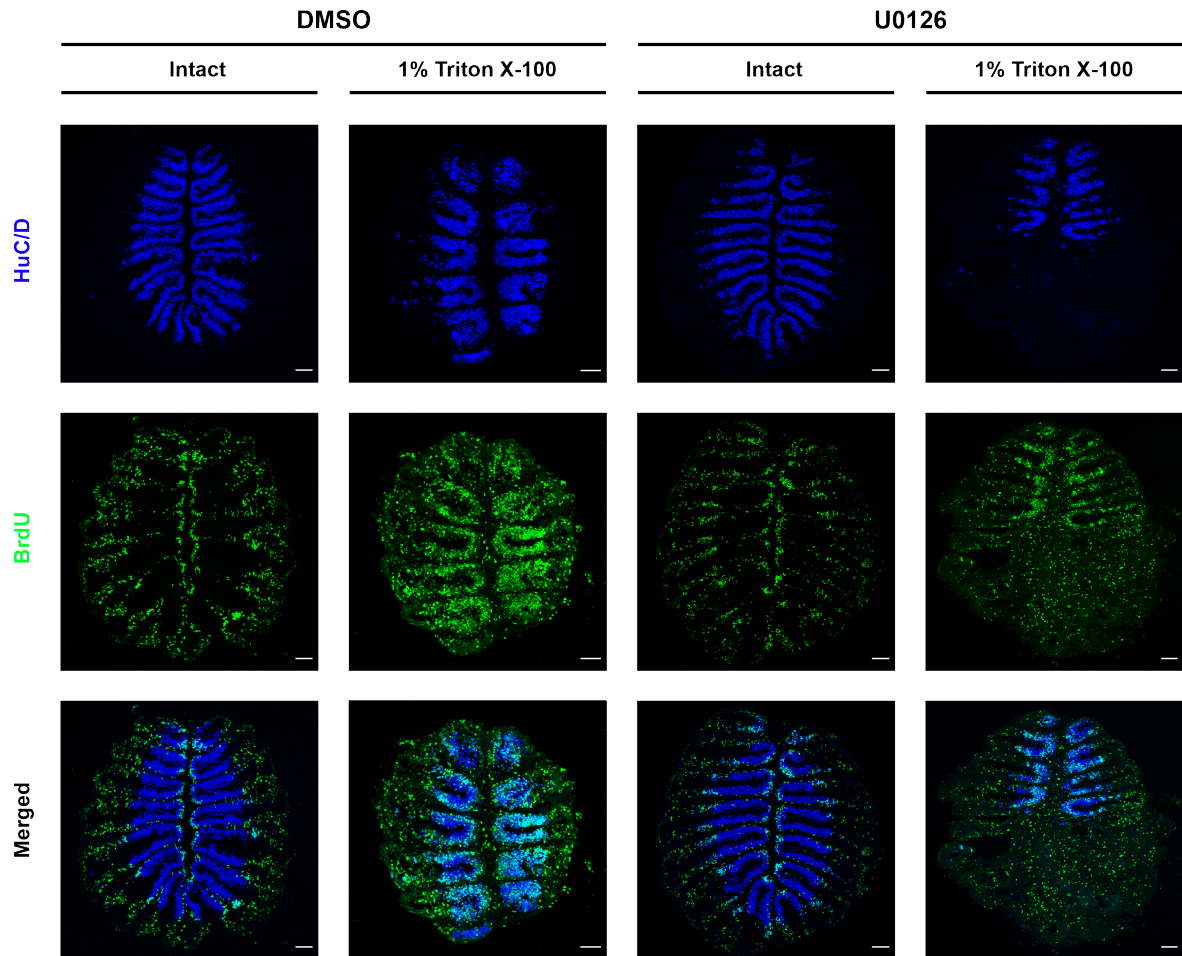


Figure 4.3. Effect of inhibition by U0126 on cell proliferation and OSN regeneration at 5 dpi. Immunohistochemistry against HuC/D (blue) and BrdU (green) in the intact and damaged OEs of DMSO- and U0126-injected groups. Scale bars are 50 μm .

In Figure 4.3, images of OEs collected from DMSO- and U0126-injected groups are shown. Starting from the left, the first and second column contains the intact and damaged OEs of the DMSO group. A homogeneous recovery of HuC/D⁺ cells (blue) can be seen in the top row when the damaged OE and intact OE are compared. However, while the OSN population has been largely restored, recovery is not complete but reaches around 80% as previously reported (Kocagöz *et al*, 2022). Consistent with the injury condition, a remarkable induction of cell proliferation can be observed in the BrdU channel (green) for the damaged OE. When the merged images are inspected, most of the BrdU⁺ cells also stain positive for HuC/D, which confirms the efficient

regeneration of OSNs in the damaged OE of the DMSO group by 5 dpi. The third and fourth column show corresponding images of the intact and damaged OEs of the U0126 group. When the HuC/D channel is examined, an apparent decrease in HuC/D signal in the damaged OE can be observed, which suggests an impairment in neuronal regeneration at 5 dpi in U0126 group. When the BrdU channel is examined, a clustering of BrdU signal similar to the damaged OE of the DMSO group can only be observed in anterior folds in the damaged OE of U0126 group in areas overlapping with HuC/D signal, while the rest of the tissue appears more similar to the random BrdU pattern that is typically observed at 1 dpi.

In Figure 4.4.a, at which the positional profiles HuC/D⁺/BrdU⁺ double-positive cells of the damaged OEs are plotted, the markedly high presence of HuC/D⁺/BrdU⁺ double-positive cells in the sensory OE and a lower number in the ILC and SNS can be interpreted as ongoing regeneration of neurons under both conditions. However, in the ILC, mean number of double-positive cells decreased from 17.9 ± 2.43 in the damaged OE of DMSO group to 7.1 ± 1.24 in the damaged OE of U0126 group, which was found to be significant (ANOVA: $F_{(3,120)} = 4.12$ p-value = 0.0005, Tukey's p-value = 0.0020). Similar to the ILC, mean number of double-positive cells decreased approximately by half in the sensory region from 148.8 ± 11.65 in the damaged OE of the DMSO group to 69.0 ± 6.54 in the damaged OE of the U0126 group (ANOVA: $F_{(3,120)} = 96.55$ p-value <0.0001, Tukey's p-value <0.0001). Consistent with the other neurogenic regions, the mean number of double-positive cells was also decreased from 9.7 ± 2.39 in the damaged OE of DMSO group to 0.8 ± 0.38 in the U0126 group in the SNS (ANOVA: $F_{(3,120)} = 7.83$ p-value = 0.0002, Tukey's p-value = 0.0002). When the sensory regions of damaged OEs are compared to their respective intact OEs, both DMSO and U0126 groups showed a significant increase in the number of HuC/D⁺/BrdU⁺-double positive cells in, which is indicative of regeneration of neurons (Tukey's p-value of intact vs damaged sensory of DMSO and intact vs damaged sensory of U0126 <0.0001).

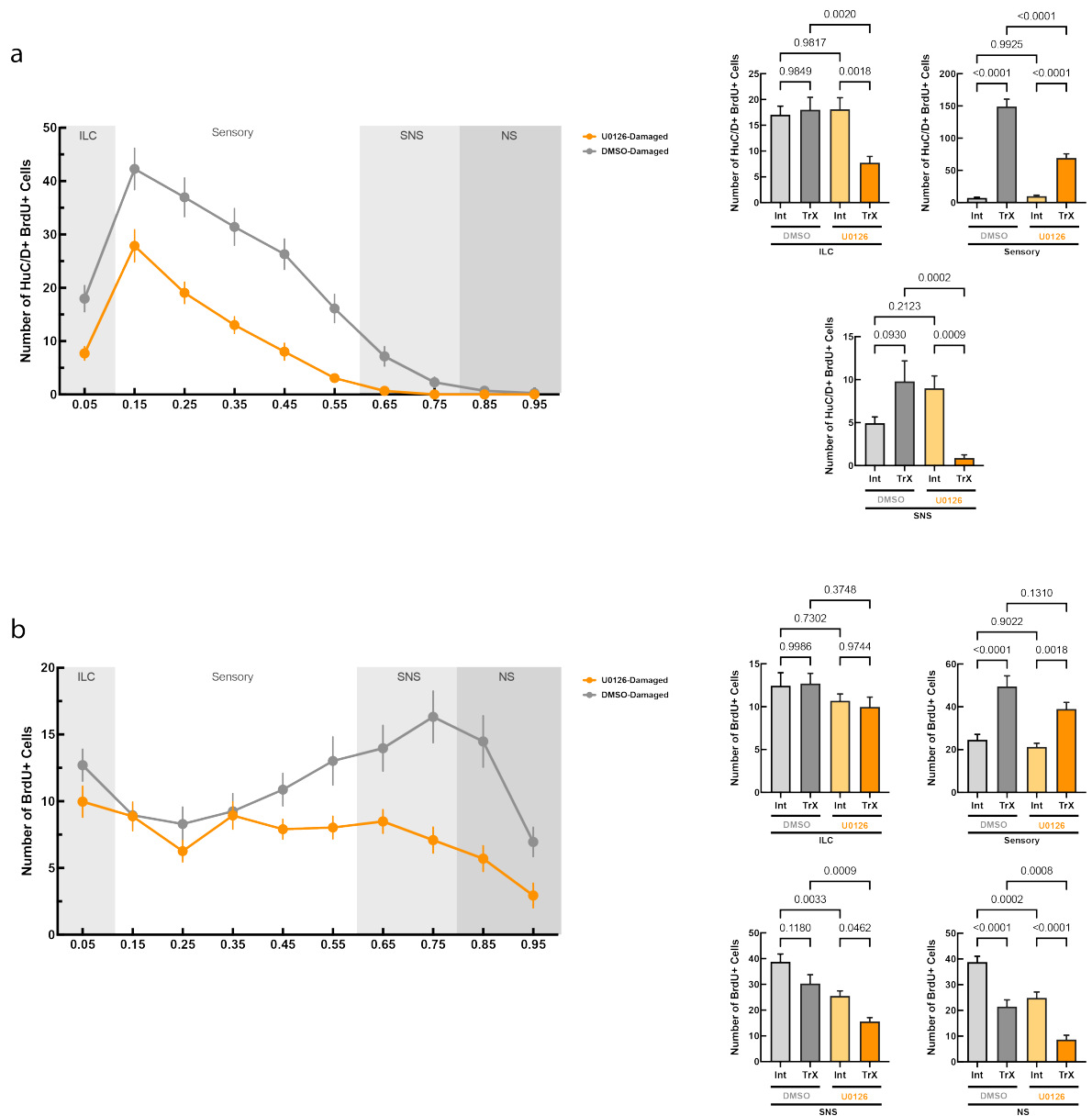


Figure 4.4. Positional profiles and quantitative comparisons of HuC/D⁺/BrdU⁺ (a) and BrdU⁺ (b) cells in the intact and damaged OEs of control and U0126 group.

A quantitative analysis of single-BrdU⁺ cells is presented in the Figure 4.4.b. According to the positional profiles BrdU⁺ cells of the damaged OEs, a mild decrease in the number of cells can be found in the ILC and sensory OE, while stronger decreases are observed in the SNS and NS in the damaged OE of the U0126 group. Among these, the approximately 50% decreases observed in the SNS (from 30.2 ± 3.47 to 15.5 ± 1.54

cells/hemi-OE) and the NS (from 21.4 ± 2.69 to 8.63 ± 1.72 cells/hemi-OE) regions of the damaged OE was found to be statistically significant (SNS: ANOVA $F_{(3,120)} = 10.36$ p-value <0.0001 , Tukey's p-value = 0.0009; NS: ANOVA $F_{(3,120)} = 21.70$ p-value <0.0001 , Tukey's p-value = 0.0008). Since there was no significant difference in cell proliferation of ILC (DMSO: 12.7 ± 1.18 cells/hemi-OE, U0126: 9.9 ± 1.15 cells/hemi-OE; Tukey's p-value = 0.90) and sensory region (DMSO: 49.4 ± 5.06 cells/hemi-OE, U0126: 38.9 ± 3.16 cells/hemi-OE; Tukey's p-value = 0.73), it can be suggested that inhibitory effects of U0126 on cell proliferation which was injected for the last time at 6 hpi has vanished until 3 dpi. However, inhibition of cell proliferation still persists in the SNS and NS. Overall, these results suggest that the generation of neurons in the injured OE is impaired but not entirely prevented in the presence of U0126, probably due to an early effect on injury-induced cell proliferation but subsequent removal of the inhibitor due to its relatively short half-life.

A final analysis, which was performed to understand the impact of inhibition by U0126 on OE regeneration, was the quantitative analysis of the area covered by HuC/D⁺ cells at 5 dpi. This analysis reveals the efficiency of regeneration in the injured OEs by evaluating how many new OSNs have been generated over the 5 d recovery period. For this analysis, 5 sections were collected for each condition and the area covered by HuC/D⁺ cells relative to the total section area was determined according to section 3.2.10. The results of the quantitative area analysis are plotted in Figure 4.5. To compare each group statistically, one-way ANOVA with Tukey HSD test was performed. Since the intact OE of the DMSO group was used for normalization, the mean value of the HuC/D area corresponds to 1.0 ± 0.07 in percent area. The mean values of the HuC/D area could be calculated to 0.82 ± 0.06 for the damaged OEs collected from DMSO group. Thus, the damaged OE recovered approximately 80% of its sensory neurons by 5 dpi, similar to previous observations (Kocagöz *et al*, 2022). When compared to the intact OE, this difference was not significant (ANOVA: $F_{(3,56)} = 20.88$ p-value <0.001 , Tukey's p-value = 0.14) and suggests that regeneration is almost complete under these conditions. In contrast, the mean value of the HuCD area of the damaged OE from the U0126 group only reached to 0.38 ± 0.03 .

Interestingly, the mean value of HuCD-covered area of the intact OE of U0126-treated animals was also decreased compared to the intact OEs of DMSO group (0.70 ± 0.02). When statistically compared to the intact OE of the DMSO group, both the intact and the damaged OEs of U0126 had significantly less coverage with HuC/D⁺ cells (Tukey's p-values are 0.0027 and <0.0001 respectively for intact and damaged OE of U0126). When the regeneration efficiency between the damaged OEs of DMSO and U0126 was compared statistically, the approximately 50% decrease from 38% in the U0126 group relative to the 82% in controls was found to be significant (Tukey's p-value <0.001). Thus, despite the observation that OSN neurogenesis is elevated in injured OEs of the U0126 group with respect to their intact OEs at this time point, the process of regeneration is diminished or delayed when compared to the damaged OEs of DMSO group.

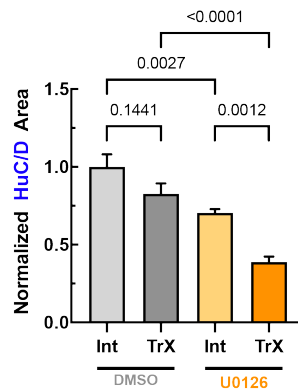


Figure 4.5. Analysis of HuC/D covered area in the OEs of DMSO and U0126 groups by 5 dpi.

Unexpectedly, however, the intact OE of the U0126 group also showed a significant decrease in the area covered by HuC/D⁺ cells. The reasons for this observation are not clear but it can be speculated that because U0126 does not affect cell proliferation in the intact OE, the decrease might be arising from an interference with the survival of existing neurons.

4.1.3. Activation Pattern of ERK Signaling During OE Regeneration

Inhibition of ERK signaling by the MEK1/2 inhibitor U0126 during the early phase of regeneration strongly reduced injury-induced cell proliferations in the sensory region and led to a reduction in the generation of neurons, which markedly decreased regeneration of the OE at 5 dpi. This suggests that ERK signaling should be activated during the early time points of regeneration. To substantiate this hypothesis, OE sections were collected from 1 dpi, 3 dpi, and 5 dpi and were stained against the phosphorylated active form of ERK (pERK), the proliferation marker EdU, and the nuclear stain DAPI. EdU was used instead of BrdU in these experiments because BrdU was not compatible with the staining protocol for pERK, which required an antigen retrieval protocol. Simultaneously staining for DAPI enabled the visualization of all cells, including the ones that are not EdU⁺ and allows for a better discrimination of pERK⁺ cells based on the presence of nuclei that are associated with stained profiles.

Representative confocal images of the intact and injured OE at 1 dpi are presented in Figure 4.6. pERK⁺ cells can be seen in red, while EdU⁺ cells are shown in green and DAPI staining in gray. In the intact OE at the left column, occasional cells in the apical side of the sensory region can be found to be pERK⁺. These cells are most likely neurons and the use of pERK staining has been established to visualize neuronally active nerve cells in the OE (Mirich *et al*, 2004). In images of the damaged OE in the right column, a widespread induction of pERK activity can be observed. The stained cells appear to be larger than the cells observed in the apical sensory region of the intact OE. More importantly, the pERK signal is most intense in the cells that are localized towards the most basal parts of the epithelial folds, where HBCs reside and which are activated upon injury. This observation further confirms that MAPK/ERK signaling is activated in the injured OE at 1 dpi, which correlates with the time at which HBCs are activated upon injury (Kocagöz *et al*, 2022). Localization of cells with the strongest pERK signal to basal layers with injury further supports the hypothesis that ERK signaling is activated in HBCs. Intriguingly, these basal pERK⁺ cells appear to be rarely positive for EdU, which suggests that they are either not di-

viding at all, or in an earlier phase of the cell cycle at which they have not yet completed DNA replication, which is necessary for EdU incorporation.

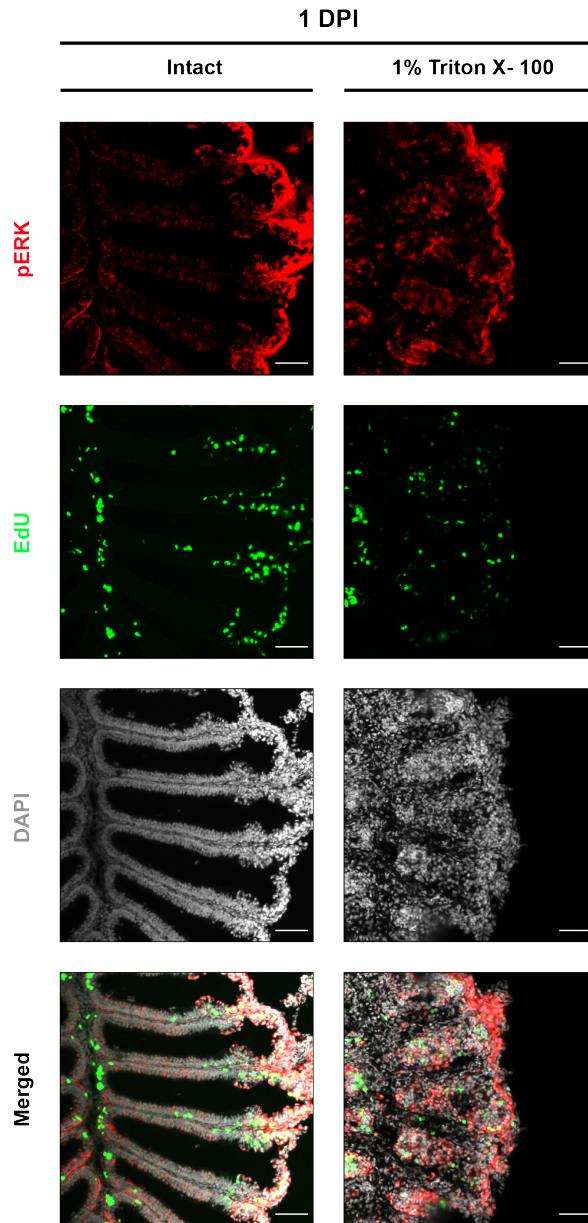


Figure 4.6. Immunohistochemistry against pERK (red) EdU (green) and DAPI (grey) in the intact (left) and injured OE (right) at 1 dpi. Scale bars are 50 μm .

Images of the intact and injured OE at 3 dpi are presented in Figure 4.7. The time point at 3 dpi represents the middle phase of the regeneration at which the division of HBCs and other progenitors peak during regeneration (Kocagöz *et al.*, 2022). Fish received EdU between 48 and 72 hpi to cover the peak phase. Images of intact and damaged OE sections are present at left and right, respectively. When the intact OE is examined, occasional pERK⁺ cells can again be found towards the apical regions of the sensory OE, similar to the observation at 1 dpi. Intriguingly, in the damaged OE at 3 dpi, an even greater and more uniform induction of pERK signal and pERK⁺ cells can be observed within each epithelial fold. This was the case for all folds of the damaged OE at 3dpi, with the exception of the fold on the top. When this fold is examined closely, a cluster of EdU⁺ cells that resembles the HuC/D⁺/BrdU⁺ double-positive cell clusters observed in the regenerated OE of DMSO group in Figure 4.3 can be seen. Interestingly, these cells are found to be negative for pERK. This suggests that ERK is activated upon injury and persists only during early phases that require progenitor expansion but is not active once generation of OSNs by other progenitor cells is established. Importantly, however, in other epithelial folds with no apparent clustering of EdU⁺ cells, pERK⁺/EdU⁺ cells can be found abundantly. These cells are most likely progenitors which divided once and became positive for EdU but keep proliferating, which may explain why they are also positive for pERK. When this information is combined with the observation of pERK-positive/EdU-negative basal cells in Figure 4.6, it can suggest that ERK is active before and during mitosis but deactivated in post-mitotic cells.

To further observe ERK activity during the late phase of the regeneration at 5 dpi, fish received EdU between 96 and 120 hpi and were stained against pERK (red), EdU (green), DAPI (gray), and HuC/D (blue). Although the antibody for HuC/D does not perform well with the staining protocol for pERK, the presence of neurons can still be observed to judge the overall regeneration by 5 dpi, which is also an established timepoint for HBCs to revert back to dormancy (Kocagöz *et al.*, 2022).

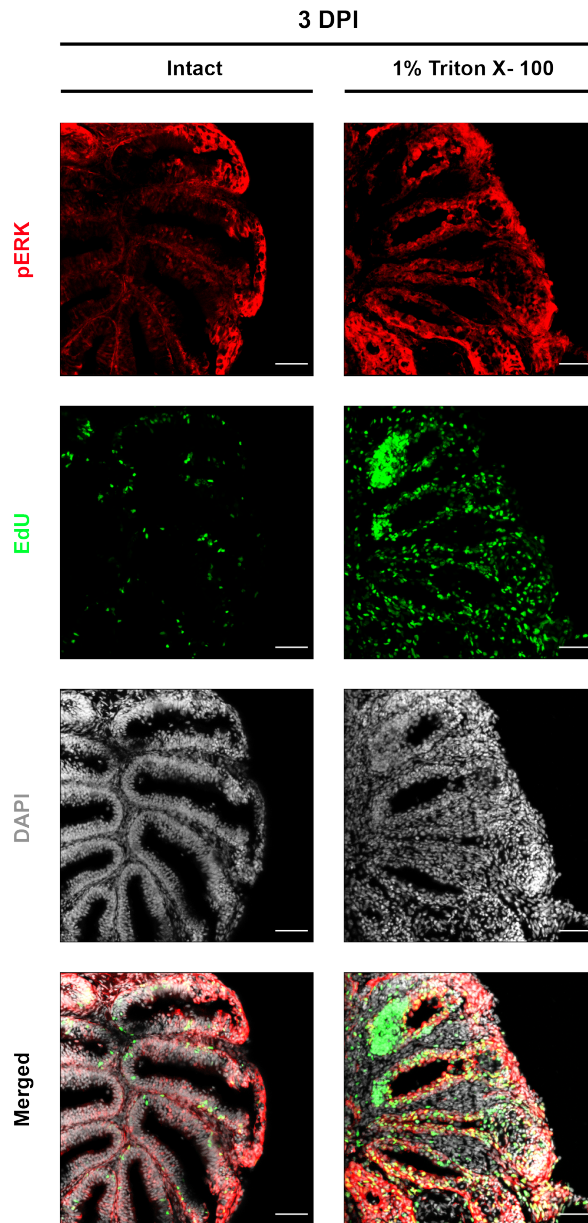


Figure 4.7. Immunohistochemistry against pERK (red) EdU (green) and DAPI (grey) in the intact (left) and injured OE (right) at 3 dpi. Scale bars are 50 μm .

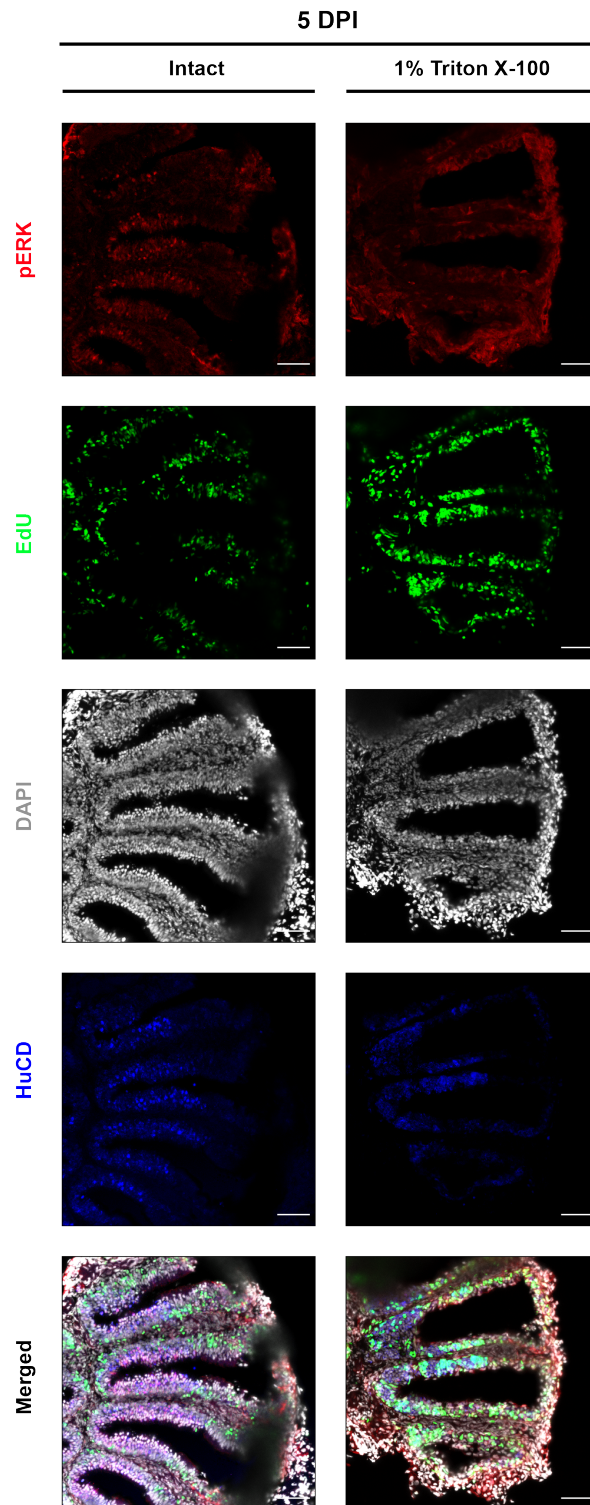


Figure 4.8. Immunohistochemistry against pERK (red) EdU (green) and DAPI (grey) in the intact (left) and injured OE (right) at 5 dpi. Scale bars are 50 μ m.

Images for this experiment can be seen in Figure 4.8. When pERK staining in the intact and damaged OEs at 5 dpi is examined carefully, the pERK pattern in the damaged OE does not seem to differ much from what is observed in this intact OE or what was observed in other intact OEs shown in Figures 4.6 and 4.7. When considered together, these results demonstrates a valid correlation between HBC activity and ERK activity both of which shows inductions with injury at 1 dpi that peaks at 3 dpi and reverts back to its basal state by 5 dpi.

4.1.4. Activation of ERK in Dividing Cells During Regeneration

Although ERK is most likely activated before or during cell division, colocalization of pERK with EdU-positive cells was not commonly observed at 1 dpi. This is most likely due to the labeling approach by EdU, which reveals both actively dividing cells at the end of the S-phase and post-mitotic cells. To better correlate ERK activation with cell division, damaged and intact OE collected 1 dpi were stained for the alternative cell cycle marker PCNA to observe only actively dividing cells at the time point of analysis. EdU staining was still performed in this experimental setup for comparison and conformation of previous observations. As a negative control for the comparison, the damaged OE of U0126 inhibited fish was used and inhibition of ERK phosphorylation by U0126 was also confirmed through pERK staining and are shown in Figure 4.9, while in Figure 4.10, individual epithelial folds representative of the qualitative analysis performed later are presented.

When the arrowheads in the folds are followed, a high number of PCNA-positive cells can be seen to be also positive for pERK. Although not marked with arrowheads, a good portion of PCNA-positive cells were also positive for EdU, which shows that the PCNA antibody works effectively with the pERK staining protocol. When pERK cells are followed carefully within epithelial folds, it can be seen that they are rarely EdU⁺, which confirms that ERK activation is probably an earlier event than EdU incorporation into cells and actually overlaps more with the activity of PCNA at the beginning of S-phase in the cells of the damaged OE. The observations on Figure 4.10

are supported by qualitative analysis of positional profiling of PCNA⁺/pERK⁺ double-positive cells and single PCNA⁺ cells with their statistical analysis by one-way ANOVA followed by Tukey HSD for multiple comparisons, which is presented in Figure 4.11.

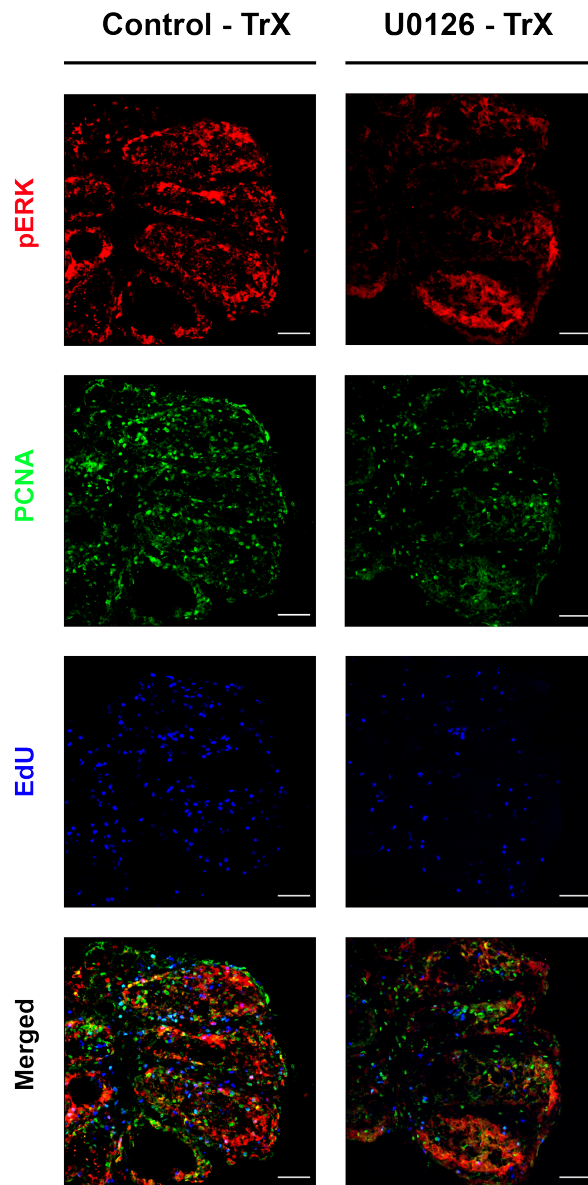


Figure 4.9. Immunohistochemistry against pERK (red) and PCNA (green) with simultaneous detection of EdU (blue) at 1dpi. Scale bars are 50 μm .

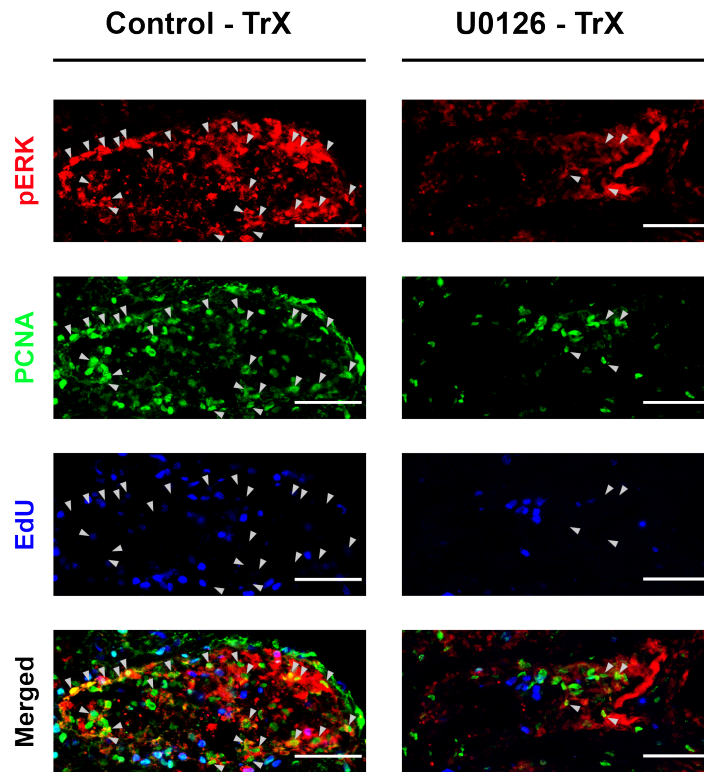


Figure 4.10. Immunohistochemistry against pERK (red) and PCNA (green) with simultaneous detection of EdU (blue) at 1dpi. Scale bars are 50 μm .

Manual counting in the FIJI software was performed on cropped epithelial folds. As usual, 5 sections of damaged OEs of control and U0126-treated fish were imaged and 4 folds were cropped from each of section for quantitative analysis, thus 20 samples for each group. According to the positional profile of PCNA⁺/pERK⁺ double-positive cells in the Figure 4.11.a, a strong decrease in the number of pERK⁺/PCNA⁺ cells can be observed in U0126-treated fish. When the mean numbers of PCNA⁺/pERK⁺ double-positive cells are calculated, control folds were found to have 43.6 ± 6.53 cells/epithelial fold, while an approximately only half as many cells were seen in U0126-treated animals with only 20.3 ± 4.08 PCNA⁺/pERK⁺ double-positive cells per epithelial fold. When the occurrence of cells was analyzed according to individual OE regions a reduction to approximately 30% could be observed in the sensory region between the folds of control and U0126-injected fish (ctr: 23.3 ± 2.26 , U0126: 7.5 ± 0.99 cells/epithelial fold), which was found to be statistically significant (ANOVA: $F_{(7,152)} = 35.31$ p-value < 0.0001 ,

Tukey's p -value <0.0001). Differences in the ILC, SNS and NS were not significant. A similar scenario was observed in the Figure 4.11.b when the total number of PCNA-positive cells were analyzed to understand whether proliferative changes that were previously seen in the early experiment with the EdU marker can be reproduced with the PCNA marker as well. While the epithelial folds of U0126-treated animals demonstrated an approximately 50% in the ILC and an almost 70% decrease in the sensory region, a change in proliferating PCNA⁺ cells was not observed in the SNS and NS. The decrease observed in the PCNA⁺ cells was found to be significant (ANOVA $F_{(7,152)} = 40.74$ p -value <0.0001 , Tukey's p -value <0.0001), while changes observed in other regions was not significant.

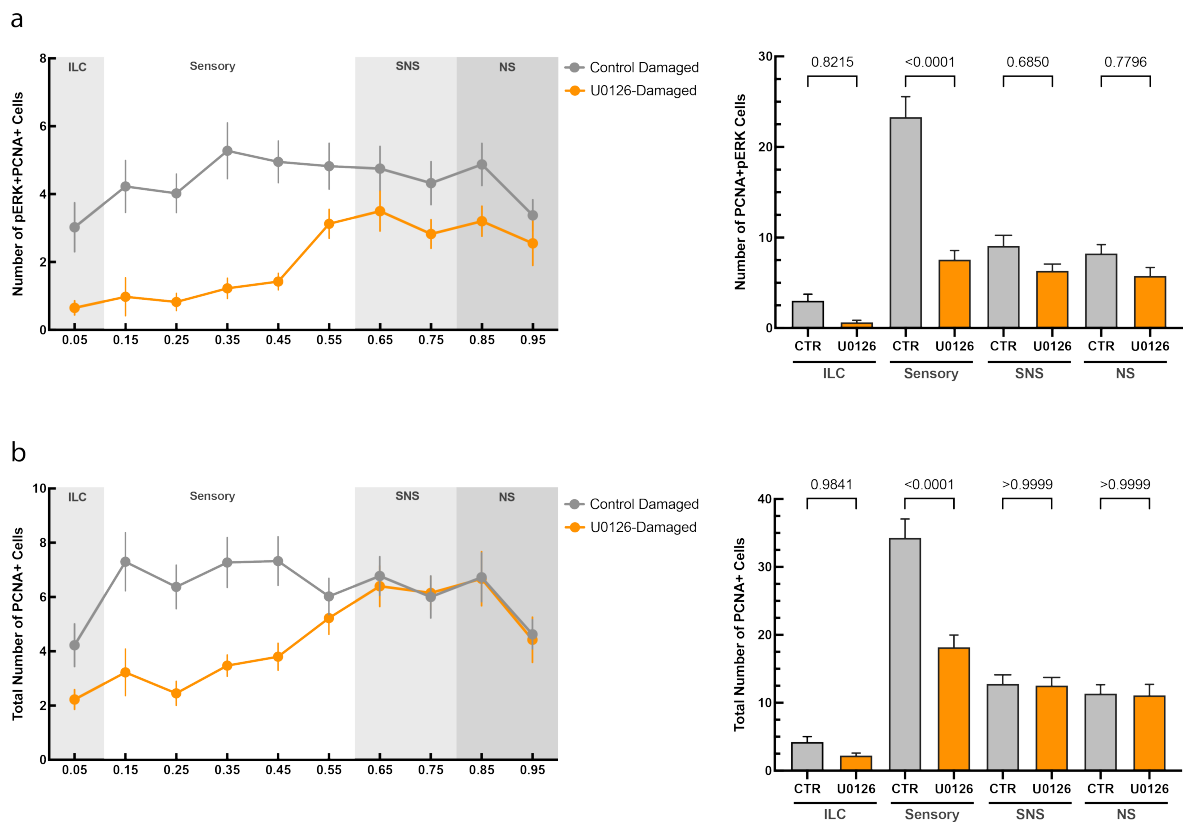


Figure 4.11. Positional profiles and quantitative analysis of pERK⁺/PCNA⁺ (a) and PCNA⁺ (b) in the damaged OEs of control and U0126 groups.

4.2. Upstream Regulators of ERK

In addition to understanding the contributions of MAPK/ERK signaling to OE regeneration, another purpose of the study was to see whether MAPK/ERK is activated by the HB-EGF and EGFR interaction. A significant prevention of regeneration at 5 dpi by HB-EGF inhibitor CRM-197 and by EGFR inhibitor PD153035 was observed in previous studies from our lab (Şireci, unpublished; Alkiraz, 2022). To check whether HB-EGF and EGFR are upstream transducers of MAPK/ERK signaling in the regenerating OE, an experimental setup containing a fish which did not receive any inhibitor and serving as a positive control, another fish which was injected with U0126 with the usual timeline and serving as a negative control was established. Experiment groups in this setup was a fish that was injected with 1 μg of CRM-197 6 h prior to injury and during the injury, and another fish which was injected with PD153035 6 h prior to, during and 6 h after the injury in addition to a final shot 6 h prior to dissection with each shot containing 27 μg of PD153035. All fish were dissected at 1 dpi and EdU was provided until dissection to mark dividing cells. The fourth shot 6 hours prior to dissection was done only for the EGFR group to make sure that inhibition still persists during the analysis at 1 dpi, while inhibition of CRM-197 and U0126 were known to be still effective by 1 dpi. Total number of fishes in this experiment was one for control, U0126, CRM-196 groups and three for the PD153035 group.

4.2.1. Activation of ERK Under MEK1/2 Inhibition

In Figure 4.12, pERK⁺ cells (red), EdU⁺ cells (green), and DAPI staining (grey) are presented. When images are observed horizontally from left, first and second columns are representative images of the intact and damaged OEs of the control group, which did not receive any inhibitor and allowed to proliferate after damage. The third and fourth columns contain representative images for OEs collected from one U0126 fish, at which a visible reduction in the pERK signal along with a decrease in the number of EdU⁺ cells can be observed when compared with the damaged OE of the control group, consistent with previous findings presented in Figure 4.9. Different from

the experiment in section 4.1.4 where the PCNA marker was used, each pERK⁺ cell is counted with the guidance of DAPI signal for quantitative analysis, to uncover all pERK⁺ cells regardless of their stage in cell cycle. When the positional profiles of pERK⁺ cells are followed in of Figure 4.13, a reduction of pERK⁺ cells becomes apparent in sensory region of U0126-treated fish. According to statistical analysis done with ANOVA and Tukey HSD tests, a 50% decrease in the number of pERK⁺ cells from 63.3 ± 4.29 to 29.7 ± 1.77 in the sensory region of damaged folds was significant (ANOVA: $F_{(3,116)} = 48.18$ p-value <0.0001 , Tukey's p-value <0.0001). This further confirms the inhibition of ERK phosphorylation with injury in the damaged OE of fish injected with the U0126 inhibitor. A similar reduction should be observed in the HB-EGF inhibited group by CRM-197 and EGFR inhibited group by PD153035, if HB-EGF and EGFR regulate the activation of ERK upon injury.

4.2.2. Activation of ERK under HB-EGF Inhibition

In Figure 4.12, fifth and sixth columns are representative images of intact and damaged OEs collected from a fish in which the soluble cleaved ectodomain of HB-EGF was sequestered by CRM-197. Again, CRM-197 treatment resulted in a severe reduction in the number of pERK⁺ cells in the damaged OE. The number and distribution of EdU⁺ cells in the damaged OEs also follows a similar pattern to U0126 inhibition in which a decrease in number and randomization of positions can be observed. A positional profile of pERK⁺ cells based on 20 folds cropped from the damaged OE of CRM-197 fish is presented in Figure 4.13 and corresponds to the yellow line. An obvious reduction is observed in the sensory region, in addition to the SNS region of the epithelial fold, which was not observed when U0126 and control was compared. When the average numbers of pERK⁺ cells are compared in the sensory region a decrease from 63.3 ± 4.29 to 22.7 ± 2.35 can be detected for CRM-197, which is even slightly lower than for the U0126 group. When the pERK⁺ cells of CRM-197 was compared with control and U0126 groups, a significant difference was observed with respect to control (Tukey's p-value <0.0001) while no statistically meaningful change detected with respect to U0126 (Tukey's p-value = 0.29).

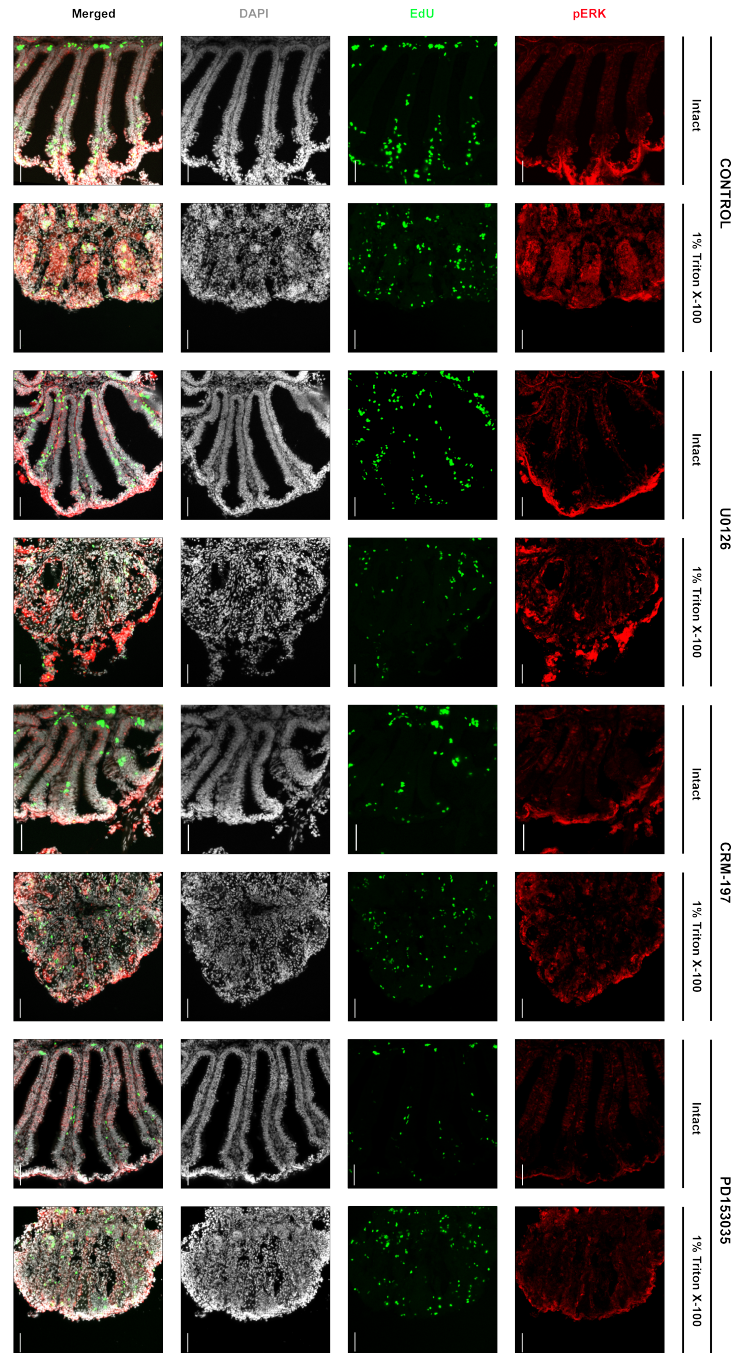


Figure 4.12. pERK⁺ cells in control, and U0126, CRM-197, PD153035 received OEs at 1 dpi. Immunohistochemistry for pERK (red), EdU (green) and DAPI (gray).

Scale bars are 50 μ m.

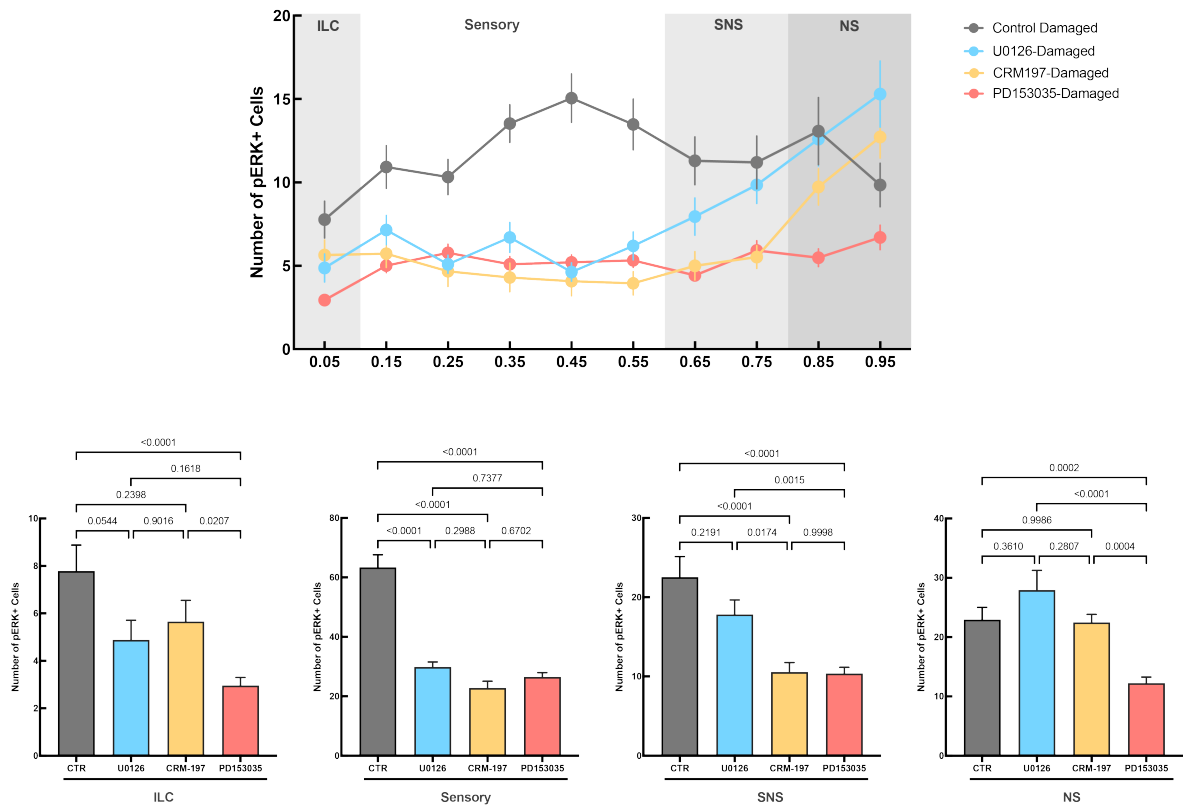


Figure 4.13. Positional profile and quantitative comparisons of pERK⁺ cells in the damaged OEs collected from control and U0126-, CRM-197-, and PD153035-injected groups.

This indicates that HB-EGF inhibition is as effective as MEK1/2 inhibition, if not more effective, in preventing the activation of ERK during injury. This strongly suggests that HB-EGF is an upstream transducer of MAPK/ERK signaling.

4.2.3. Activation of ERK under EGFR Inhibition

The seventh and eighth columns of Figure 4.12 show representative images of intact and damaged OEs collected from three fish that were treated with the EGFR inhibitor PD153035. When pERK⁺ signal is compared with the damaged OE of control fish a reduction in pERK activation can be seen similar to the effect of U0126 and CRM-197. PD153035 also resulted in a randomization of the EdU staining pattern as

previously reported (Alkiraz, 2022). Positional profiles of pERK⁺ cells based on 60 folds cropped from the damaged OE of three animals that were injected with PD153035 corresponds to red line in the positional profile presented in Figure 4.13. A strong reduction is again observed in the sensory region, in addition to the ILC, SNS and NS region of the epithelial fold, which was not observed when U0126 and CRM-197 were used. When the average numbers of cells are compared in the sensory OE, a decrease from 63.3 ± 4.29 to 26.4 ± 1.53 can be seen with respect to the control group, which is again slightly lower than what was previously calculated for the U0126 group and at a similar level with CRM-197. When the pERK⁺ cells of PD153035 was compared with control, U0126, CRM-197 groups in the sensory region of damaged folds, a significant difference was observed with respect to control (Tukey's p-value <0.0001) while no statistically meaningful change detected with respect to U0126 and CRM-197 (Tukey's p-value = 0.73 and 0.67). This indicates that inhibition of EGFR activation by PD153035 is as effective as MEK1/2 inhibition and HB-EGF inhibition for preventing the activation of ERK during injury. Distinctly from the U0126 and CRM-197, PD153035 inhibition was able to significantly decrease the pERK⁺ cells also in the ILC, a region of the OE that is occupied by GBC-like cells in zebrafish (Demirler *et al*, 2020; ANOVA: $F_{(3,116)} = 10.18$ p-value <0.0001, Tukey's p-value <0.0001). Moreover, differing from the effects of U0126 and CRM-197 in NS, PD153035 inhibition was also able to significantly decrease the pERK⁺ cells in the NS region (ANOVA: $F_{(3,116)} = 17.54$ p-value <0.0001, Tukey's p-value = 0.0002). This might indicate an induction of ERK pathway through EGFR receptor but upon binding of another ligand for ILC and NS regions, since HB-EGF inhibition in the ILC did not led to a significant reduction in pERK⁺ cells (Tukey's p-value = 0.99). Overall, these results establish a framework for signaling mechanisms of the dividing cells within the fold. In the sensory region occupied with neurons and HBCs that are activated at 1dpi, HB-EGF: EGFR interaction transduces the MAPK/ERK signaling. When taken into consideration together with the results of PCNA/pERK experiment, MAPK/ERK signaling is required for mediating the regenerative effects of HB-EGF and EGFR interaction that was previously established (Kocagöz and Şireci, unpublished) by triggering division in the cells of the OE. A similar activation of EGFR receptor to generate a regenerative response in the

ILC occupied with constitutively active GBC-like progenitors and within the NS, an epithelial structure devoid of neurons, is probably the result of other receptor/ligand interactions to activate the MAPK/ERK signaling.

4.2.4. Activation of ERK under EGFR Inhibition

The seventh and eighth columns of Figure 4.12 show representative images of intact and damaged OEs collected from three fish that were treated with the EGFR inhibitor PD153035. When pERK⁺ signal is compared with the damaged OE of control fish a reduction in pERK activation can be seen similar to the effect of U0126 and CRM-197. PD153035 also resulted in a randomization of the EdU staining pattern as previously reported (Alkiraz, 2022). Positional profiles of pERK⁺ cells based on 60 folds cropped from the damaged OE of three animals that were injected with PD153035 corresponds to red line in the positional profile presented in Figure 4.13. A strong reduction is again observed in the sensory region, in addition to the ILC, SNS and NS region of the epithelial fold, which was not observed when U0126 and CRM-197 were used. When the average numbers of cells are compared in the sensory OE, a decrease from 63.3 ± 4.29 to 26.4 ± 1.53 can be seen with respect to the control group, which is again slightly lower than what was previously calculated for the U0126 group and at a similar level with CRM-197. When the pERK⁺ cells of PD153035 was compared with control, U0126, CRM-197 groups in the sensory region of damaged folds, a significant difference was observed with respect to control (Tukey's p-value <0.0001) while no statistically meaningful change detected with respect to U0126 and CRM-197 (Tukey's p-value = 0.73 and 0.67). This indicates that inhibition of EGFR activation by PD153035 is as effective as MEK1/2 inhibition and HB-EGF inhibition for preventing the activation of ERK during injury. Distinctly from the U0126 and CRM-197, PD153035 inhibition was able to significantly decrease the pERK⁺ cells also in the ILC, a region of the OE that is occupied by GBC-like cells in zebrafish (Demirler *et al*, 2020; ANOVA: $F_{(3,116)} = 10.18$ p-value <0.0001, Tukey's p-value <0.0001). Moreover, differing from the effects of U0126 and CRM-197 in NS, PD153035 inhibition was also able to significantly decrease the pERK⁺ cells in the NS region (ANOVA: $F_{(3,116)} =$

17.54 p-value <0.0001, Tukey's p-value = 0.0002). This might indicate an induction of ERK pathway through EGFR receptor but upon binding of another ligand for ILC and NS regions, since HB-EGF inhibition in the ILC did not lead to a significant reduction in pERK⁺ cells (Tukey's p-value = 0.99). Overall, these results establish a framework for signaling mechanisms of the dividing cells within the fold. In the sensory region occupied with neurons and HBCs that are activated at 1dpi, HB-EGF: EGFR interaction transduces the MAPK/ERK signaling. When taken into consideration together with the results of PCNA/pERK experiment, MAPK/ERK signaling is required for mediating the regenerative effects of HB-EGF and EGFR interaction that was previously established (Kocagöz and Şireci, unpublished) by triggering division in the cells of the OE. A similar activation of EGFR receptor to generate a regenerative response in the ILC occupied with constitutively active GBC-like progenitors and within the NS, an epithelial structure devoid of neurons, is probably the result of other receptor/ligand interactions to activate the MAPK/ERK signaling.

4.3. The Effect of Inhibition of PI3K/AKT Signaling on OE Regeneration

Signaling downstream of EGFR is complex and a multitude of different signaling pathways have been demonstrated (Schlessinger, 2000). A second major signaling pathway, however, is the PI3K/AKT pathway. A similar approach to the examination of MAP/ERK signaling was followed to investigate whether PI3K/AKT signaling also plays a role for regeneration in the injured OE. Ly294002 is an inhibitor of kinase activity of class I PI3K family and was used in experiments presented below. The kinase phosphorylates and activates AKT and inhibition of PI3K effectively shut down the AKT signaling (Vlahos *et al*, 1994). Intact and injured OEs of fish injected with Ly294002 were collected at 1 and 5 dpi and compared to the same control group that was injected with the DMSO for the MAPK/ERK experiments. The OEs were stained for proliferation markers and HuC/D to analyze mitotic cells during 1 dpi and 3 dpi in addition to the overall efficiency of regeneration by 5 dpi. Activation of AKT upon injury was further investigated by staining intact and damaged OEs with a pAKT antibody at 1 dpi along with the proliferation marker PCNA to understand

if PI3K/AKT signaling has a similar mitotic effect as MAPK/ERK signaling.

4.3.1. Early Phase of OE Regeneration with AKT Inhibition

To check the impact of Akt inhibition during the early phase of regeneration, injections of the Ly294002 were given 4 h prior to, during, and 4 h post injury. Each injection contained 25 μg of Ly294002 in 2.5 μl of DMSO which was further dissolved in 30 μl of PBS for injection purposes. A total of 3 fish were injected with Ly294002 and incubated in tank water containing 30 mg/L BrdU until 1 dpi.

Representative images for this experiment are shown in Figure 4.14, in which HuC/D channel is shown in blue and the BrdU channel is shown in green. Starting from the left, the first and second column contain images of the intact and damaged OE of the DMSO group, while the third and fourth column contain images of intact and damaged OE of the Ly294002 group at 1 dpi. Observations for the DMSO group at 1 dpi were presented previously in section 4.1.1 and can be summarized as a change in the pattern of BrdU⁺ cells in the damaged OE upon successful injury. When the intact and damaged OE of Ly294002 group was examined carefully, BrdU⁺ cells can also be seen to be randomly distributed compared to the intact OE of Ly294002 but with a reduced number in comparison to the damaged OE of the DMSO control group. Distinctly from the U0126 experiment, however, the presence of BrdU⁺ cells also decrease in the intact OE of Ly294002-treated animal when compared to the intact OE of the DMSO group. These observations suggest an overall decrease in the cell proliferations by AKT inhibition, independent of tissue conditions.

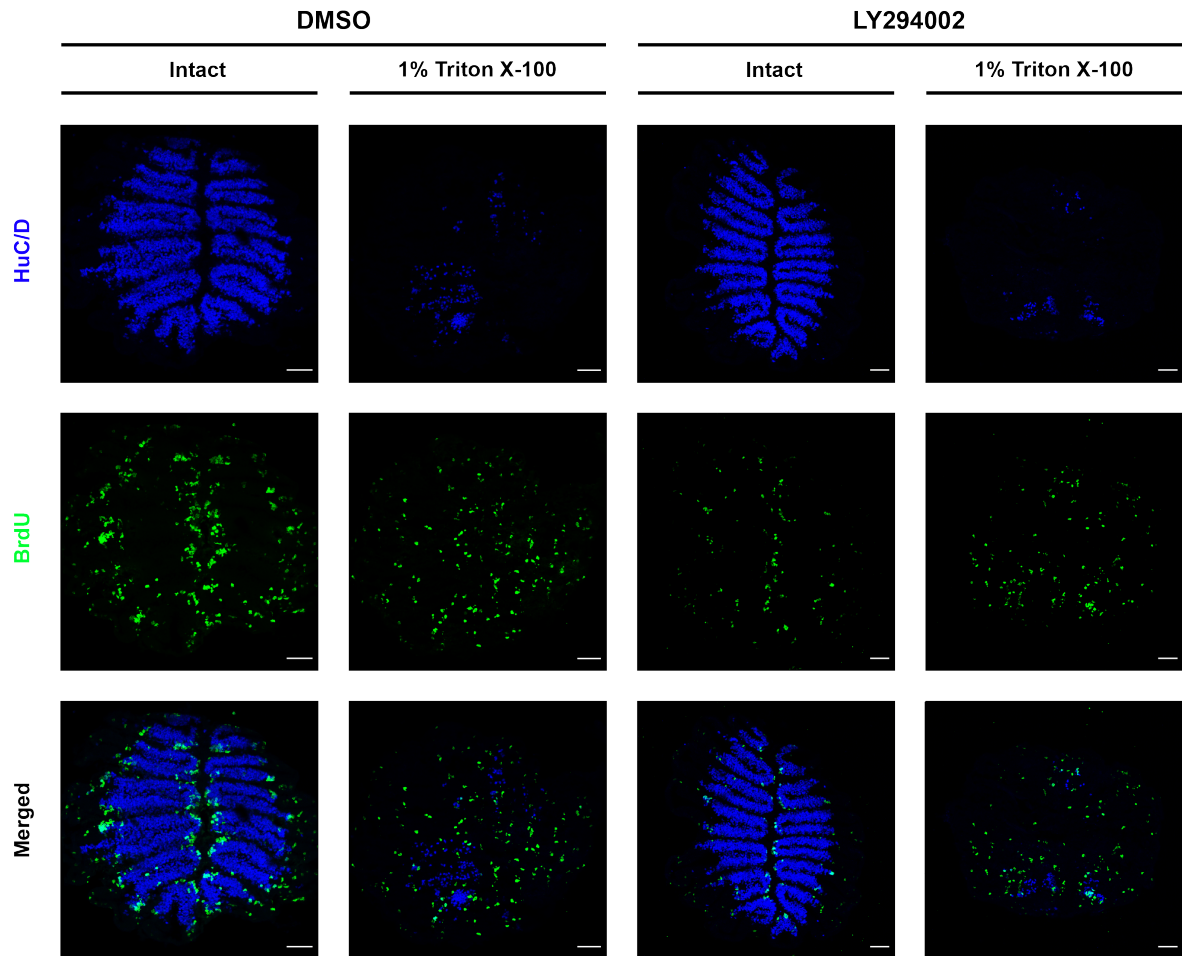


Figure 4.14. Effect of inhibition by Ly294002 on cell proliferation observed at 1 dpi. Immunohistochemistry against BrdU (green) and HuC/D (blue) in the intact and damaged OE of DMSO and Ly294002 groups. Scale bars are 50 μm .

Quantitative analysis and their statistically relevant comparisons for the intact OE are presented in Figure 4.15. In the Figure 4.15.a, positional profiles of BrdU⁺ cells were generated based on intact OEs of 30 data points for DMSO and 20 data points for Ly294002 due to technical issues. However, the apparent decrease in the intact OE of Ly294002 is confirmed with a decrease in the average number of BrdU⁺ cells in the ILC, SNS and NS. When compared with ANOVA with Tukey's HSD test, an almost 80% decrease in the ILC region of the epithelial fold from 19.0 ± 1.71 in the intact OE of DMSO fish to 3.6 ± 0.55 in the intact OE of Ly294002-treated animals was found to be statistically significant (ANOVA: $F_{(3,106)} = 44.20$ p-value < 0.0001 , Tukey's p-value

<0.001). Additionally, approximately 45% decreases could be observed in the SNS (from 18.8 ± 1.53 to 10.43 ± 1.88 ; ANOVA: $F_{(3,106)} = 28.12$, p-value <0.0001, Tukey's p-value = 0.0002) and in the NS regions (from 15.5 ± 1.61 to 7.4 ± 1.56 ; ANOVA: $F_{(3,106)} = 24.31$, p-value <0.0001, Tukey's p-value <0.0001) was also found to be statistically significant. These quantitative and statistical results confirm the hypothesis that inhibition of AKT decreases the cell proliferation overall, regardless of whether they are contributing to the neurogenesis or not, since NS region of the fold which is devoid of neurons also found to have significant decreases in cell proliferation.

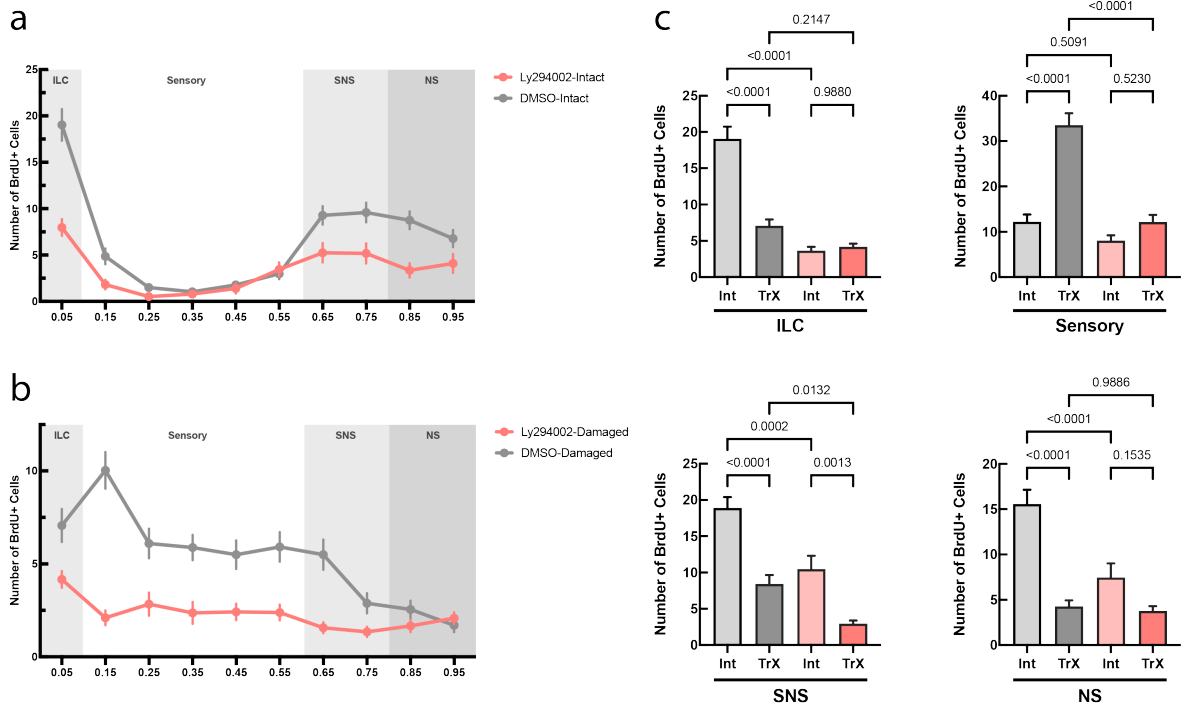


Figure 4.15. Positional profiles and statistical comparisons of BrdU⁺ cells in the intact (a) and damaged (b) OEs of control and Ly294002 group.

The positional profile of BrdU⁺ cells in the damaged OE shown in the Figure 4.15.b was generated based on 30 data points from the damaged OEs of both the DMSO and Ly294002 group. A decrease in the ILC, sensory, and SNS region similar to what was observed for U0126 in the early phase of regeneration, can be seen. When statistically checked the change in ILC was not found to be significant (Tukey's p-value

= 0.21), however, the strong 65% decreases in the mean number of BrdU⁺ cells in the sensory region (from 33.4 ± 2.67 to 12.10 ± 1.64 ; Tukey's p-value < 0.0001) and SNS (from 8.3 ± 1.26 to 2.9 ± 0.45 ; Tukey's p-value = 0.0132) was found to be statistically significant. This indicates that inhibition of PI3K/AKT signaling is sufficient to halt the induction of cell proliferation in the sensory that is occupied by injury-responsive HBCs.

4.3.2. Late Phase of OE Regeneration with AKT Inhibition

Next, possible contributions of PI3K/AKT signaling to OE regeneration was examined by analyzing the overall regeneration efficiency at 5 dpi in addition to observing new-born neurons which are progeny of cells divided during the labeling period between 48 and 72 hpi. Again, same control fish injected with DMSO that were used to analyze the impact of U0126 on the late-phase of regeneration at section 4.1.2 was utilized for comparing the effect of PI3K/AKT signaling by Ly294002 inhibition. Because of technical issues with the BrdU antibody and time constraints, BrdU was swapped to EdU for this experiment. Fish received EdU injection at 48 hpi to mark dividing cells during third day of the injury. In Figure 4.16, the first-two columns contain representative images of the DMSO control group while the last-two columns consist of representative images from the Ly294002 group both collected 5 dpi. When the HuC/D channel is observed, the damaged OEs of both groups are uniformly filled with HuC/D⁺ cells. When the HuC/D signal is considered together with EdU activity, HuC/D⁺ cells observed in the damaged OEs can often be seen to be positive for EdU, suggesting that these neurons are newborn and regenerated after the injury. The decrease in the BrdU⁺ cells observed in the early-phase experiment with Ly294002 could not be reproduced in the intact OE of Ly294002 group at Figure 4.16, suggesting that inhibitory effects of Ly294002 have vanished. Nevertheless, to understand the impact, if any, of early-inhibition by Ly294002 on the overall production of neurons, positional profiles of HuC/D⁺/BrdU⁺ double-positive cells were generated and compared with ANOVA followed by Tukey's test to compare the effects at neurogenic region of the fold. Both of these are presented in the Figure 4.17.

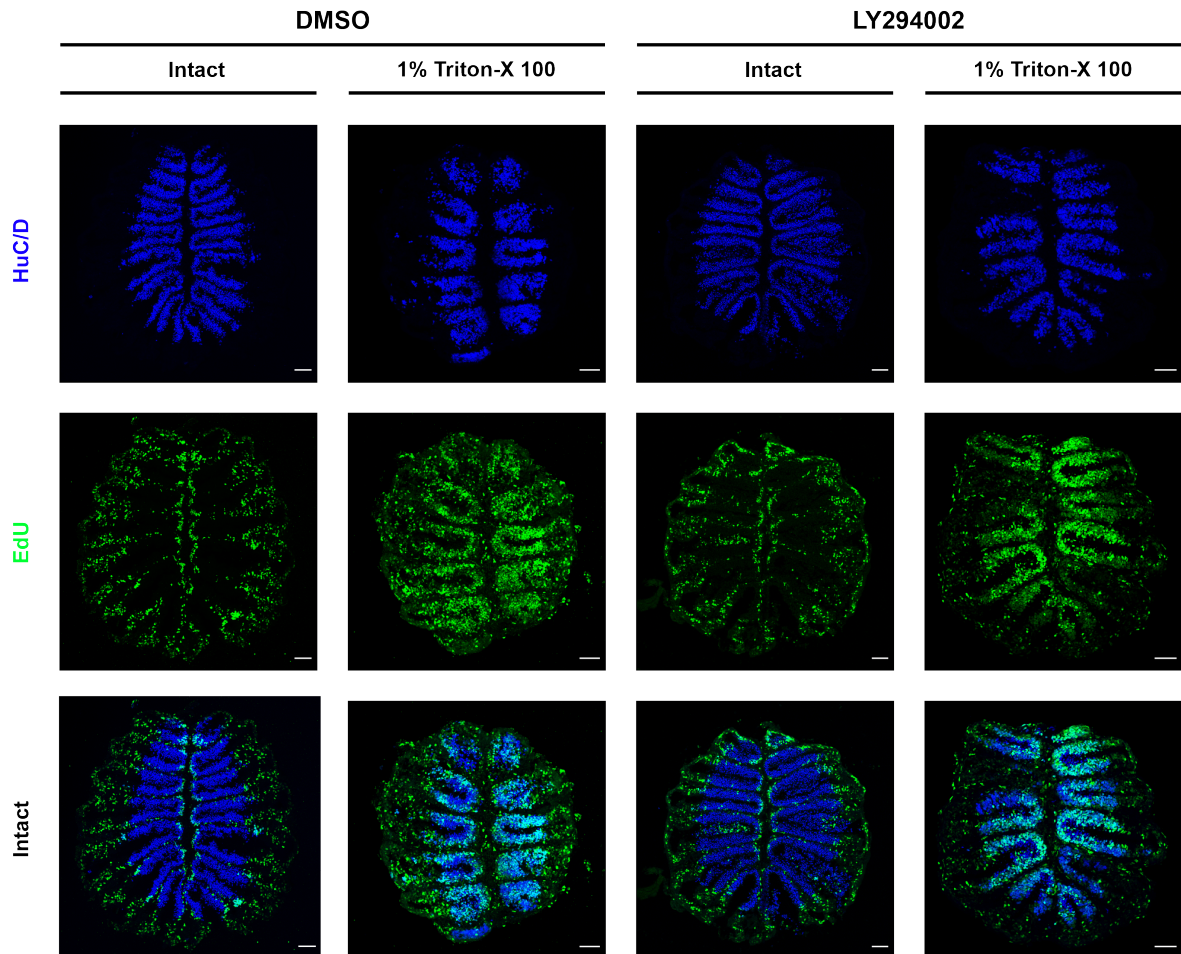


Figure 4.16. Effect of Ly294002 on cell proliferation and OSN regeneration at 5 dpi. Immunohistochemistry against HuC/D (blue) and BrdU (green) in the intact and damaged OEs of DMSO- and Ly294002-injected groups. Scale bars are 50 μm .

In the left part of the Figure 4.17 the positional profile of $\text{HuC/D}^+/\text{BrdU}^+$ double-positive cells in the DMSO and Ly294002 groups are shown. In this graph, only a mild decrease in the sensory OE and SNS regions can be observed, while $\text{HuC/D}^+/\text{BrdU}^+$ cells in the ILC are slightly increased. This effect could be explained by superior performance of labelling of these cells with the EdU detection cocktail compared to antibody staining with BrdU. These slight changes were not statistically significant except for the sensory region (ANOVA: $(5,174) = 112.9$, p-value < 0.0001 , ILC: Tukey's p-value = 0.93; Sensory: Tukey's p-value = 0.03; SNS: Tukey's p-value = 0.99). Thus, the dam-

aged OE, even in the presence of Ly294002 at an early time point during the injury, is able to produce a high number of neurons in the sensory region which is similar to the rate of OSN generation observed in the DMSO control group.

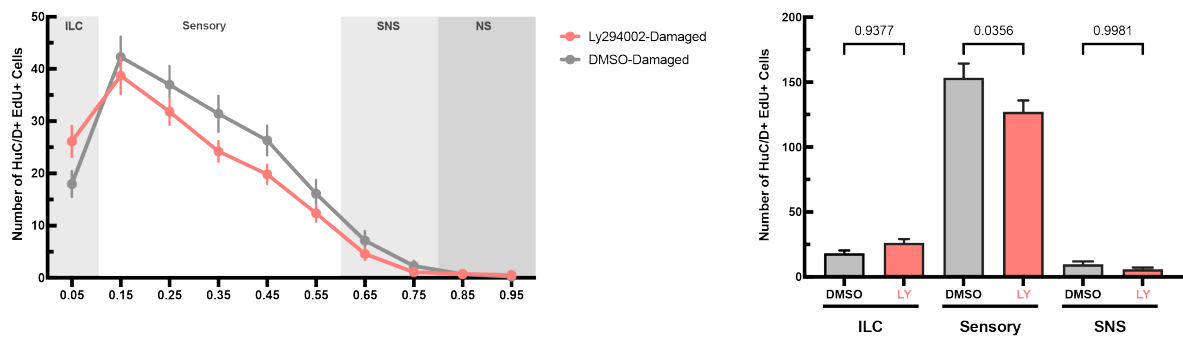


Figure 4.17. Positional profiles and quantitative comparisons of HuC/D⁺/BrdU⁺ cells in the damaged OEs of control and Ly294002 group

Finally, to analyze the impact of inhibition by Ly294002 on the late-phase of regeneration, an area analysis for HuC/D-coverage of the OE was performed and is shown in Figure 4.18. Same control group presented in Figure 4.5 for normalizing of the effect of ERK inhibition on regeneration efficiency by 5 dpi is also present in this figure and was used for normalization of the effect of AKT inhibition. While the mean of the normalized HuC/D area could be calculated as 0.82 ± 0.06 for the damaged OE of the DMSO group, it only reached 0.68 ± 0.04 , in Ly294002-injected animals. Thus, a mild decrease in the recovery efficiency occurs in the damaged OEs of Ly294002 group. To check whether this reduction is statistically meaningful, ANOVA was followed with Tukey's HSD to compare each condition. According to the statistical test, the mild decrease observed in the damaged OEs of Ly294002 group was not significant (ANOVA: $F_{(3,56)} = 5.285$, p-value = 0.0028; Tukey's p-value = 0.35). This observation is consisted with the high abundance of HuC/D⁺/EdU⁺ cells in the damaged OE of the Ly294002 group at 3 dpi. Overall, these results indicate that PI3K/AKT inhibition might be causing arrests in the cell cycle in the early phase of regeneration, and this can be overcome and compensated for with signals for growth

and proliferation that are still present once the effect of the inhibitor ceases. Thus, early PI3K/AKT inhibition is not sufficient to impair regeneration and probably contributes indirectly by promoting growth of the cells during regeneration.

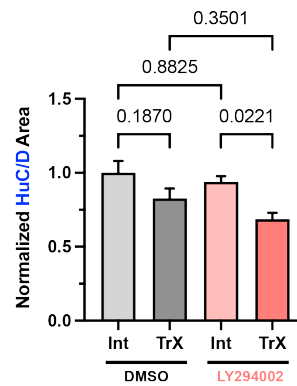


Figure 4.18. Analysis of HuC/D covered area in the OEs of DMSO and Ly294002 groups by 5 dpi.

4.3.3. Activation of AKT During OE Regeneration

To examine the activation of AKT at 1 dpi, during which inhibition resulted in reduced proliferation of cells, the same protocol that was previously used for the pERK staining was utilized with an antibody against the phosphorylated form of AKT (pAKT). As before, the sections were counterstained with PCNA and DAPI. Images from this experiment are presented in Figure 4.19. pAKT staining can be observed in the red channel, while, PCNA and DAPI can be seen in green and gray channel, respectively. When the intact OE in the first column of the figure is closely examined, pAKT signal can be observed in the apical, water-facing part of the fold, in which cilia of OSNs are present. pAKT signal can also be seen spanning the baso-apical axis of the intact OE, which might suggest that sustentacular cells or OSNs can occasionally be found positive for pAKT. The PCNA cells observed in the ILC of intact OE with globular nuclear shapes are most likely transit-amplifying GBCs and do not colocalize with pAKT signal. When the damaged OE is examined, most-basal become positive

for pAKT, however, these cells are only occasionally positive for PCNA. This suggests that activation of AKT is probably occurring in the folds and required for cell division but do not trigger mitosis directly and contribute through other mechanisms that ensure progression of cell cycle.

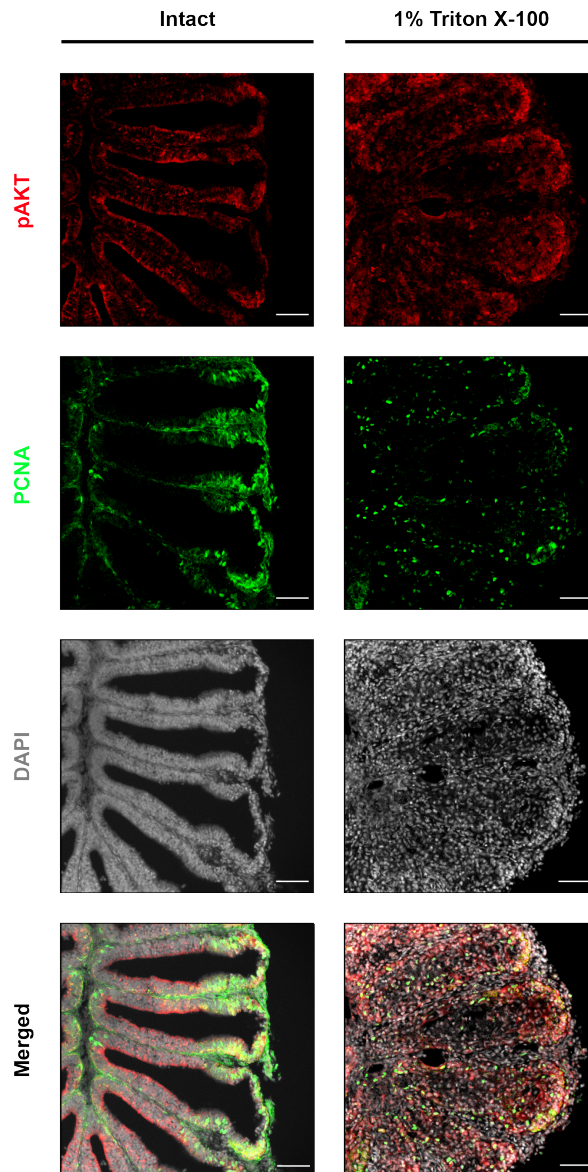


Figure 4.19. pAKT⁺ and proliferating cells at 1 dpi. Immunohistochemistry against pAKT (red), and PCNA (green) and simultaneous detection of nuclei by DAPI (gray) in the intact and damaged OE. Scale bars are 50 μm .

5. DISCUSSION

The OE is a unique organ that has both a nervous and epithelial architecture. While most nervous tissues have an epithelial origin, the OE has maintained an ability to regenerate OSNs both in the intact and injured tissue that resembles other epithelial stem cell niches, such as the skin and intestine (Schwob, 2002; Li & Clevers, 2010). Remarkably, this regeneration is not only restricted to axonal re-growth or re-establishment of lost synapses, as can also be seen in other regions of the nervous system (Varadajaran *et al*, 2022), but includes the process of adult neurogenesis, which, with a few exceptions, is uncommon across the central and peripheral nervous system (Arzate & Covarrubias, 2020) Unlike other neural tissues which are well protected by bone and supportive structures, the OE directly faces the external environment to detect odorants and, hence, evolved to be equipped with progenitor cells that could replace neurons that might die from exposure to toxins or infections (Schwob, 2017). The goal of this study is to understand the signaling mechanisms that contribute to the generation of the regenerative response of the OE to severe damage. In this context, the contributions of MAPK/ERK and PI3K/AKT signaling, which are both well-known to regulate cell fate and division (Lavoie *et al*, 2020; Engelman *et al*, 2006), to the regeneration of the zebrafish OE were investigated in detail. Loss of function experiments with pharmacological inhibitors for these pathways revealed that both the MAPK/ERK and PI3K/AKT pathways are necessary for efficient regeneration but to different degree. A major hypothesis for the context of activation of these pathways is that they are induced through the HB-EGF/RGFR axis (Kocagöz and Şireci, unpublished). The relationship of the MAPK/ERK signaling pathway could be confirmed in the context of HB-EGF:EGFR interaction. Finally, evidence could be gathered that HBCs are the main cell type in which these pathways are activated during regeneration.

5.1. An Overview of Regeneration

Based on their plasticity and ability to regenerate from trauma or degeneration, neural and other epithelial tissues can be accepted to be at the opposite ends of the regenerative spectrum. While regeneration of epithelial tissues such as skin, intestine and respiratory epithelium is common in mammals (Dekoning & Blanpain, 2019; Hageman *et al*, 2020; Lee & Rawlins, 2018) to ensure the stability and continuity of function of the respective organ, regeneration of dying or lost neurons is not a phenomenon commonly observed in mammals (Arzate & Covarrubias, 2020). However, efficient nervous system regeneration can be seen in lower vertebrates such as zebrafish (Ganz & Brand, 2013), axolotl (Amamoto *et al*, 2016), and newt (Lust & Tanaka, 2019). Generation of new neurons is highly restricted in nervous tissues of mammals and at high rate only occurs in the hippocampus and V-SVZ (Eriksson *et al*, 1998; Bedard & Parent, 2004). However, the purpose of this ongoing neurogenesis is not primarily to replace dying neurons but to support functional plasticity (Kempermann, 2022). It is still being investigated whether intrinsic neurogenesis in the mammalian brain can be manipulated to regenerate dying neurons as is commonly observed in neurodegenerative diseases, such as Alzheimer's disease (Cosacak *et al*, 2020). A prominent principle in the regeneration of tissue in general is the presence of competent and injury-responsive progenitor cell that can generate resident cell types of the tissues if they are lost (Dekoning & Blanpain, 2019; Hageman *et al*, 2020; Lee & Rawlins, 2018, Ganz & Brand, 2013). Some of the examples of these progenitors are RGCs of zebrafish giving rise to neurons in telencephalon after stab injuries (Kızıl *et al*, 2012), HFSCs in skin epithelium that can generate epidermis after wound and even burn injuries (Dekoning & Blanpain, 2019), CBCs and clusterin-positive cells that can regenerate an absorptive intestine epithelium (Hageman *et al*, 2020), BSCs in respiratory epithelium that generate ciliated cells upon SO₂ inhalation (Basil *et al*, 2020) and HBCs that can regenerate all cell types in the OE upon injury (Herrick *et al*, 2017). Another common principle observed during episodes of regeneration is the emergence of an immune response that promotes recovery (Hannis & Kettenman, 2007; Hewitt & Lloyd, 2021; Monavarian *et al*, 2019).

This, however, requires a delicate balance since prolonged immune signaling has been shown to prevent regeneration and result in scar formation both in neural and epithelial tissues (Kyritsis *et al.*, 2014; Wang & Higgins, 2020; Hageman *et al.*, 2020). In the skin epithelium, immune cells arriving to the injured area are known to secrete growth factors that stimulate cell proliferation in progenitors (Sun *et al.*, 2014). Despite the fact that these growth factors vary based on the tissue, they all converge on the regulation of a set of common signaling pathways in progenitors that includes a combination of Wnt, Notch, BMP, Hippo, MAPK/ERK and PI3K/AKT signaling (Wen *et al.*, 2022; Blanpain *et al.*, 2007; Li & Clevers, 2010; Beumer & Clevers, 2016; Wan *et al.*, 2012). These pathways can also interact with each other for regulation of relevant transcription products that are required for the differentiation of mitotic cells into mature cell types (Wen *et al.*, 2022; Beumer & Clevers, 2021), or to maintain stemness in a fraction of progenitors (Gehart & Clevers, 2021; Blanpain & Fuchs, 2006; Wen *et al.*, 2022; Zepp & Morissey, 2019). Among these pathways, ERK and AKT were mostly studied in cancer studies in which these processes are dysregulated and they were found to be promoting malignant tumors by changing the metabolism of cells and stimulating their division if overactivated (Asati *et al.*, 2016). However, more studies that focus on ERK and AKT pathways during neural development, activation and quiescence of NSCs, and regeneration are emerging each day.

5.2. MAPK/ERK Signaling Is Active in Proliferating Progenitor Cells of the OE

In this study, the effect of MAPK/ERK signaling on both regeneration and maintenance of the OE was observed with a primary focus on regeneration. At 1 dpi, inhibition of MAPK/ERK signaling by U0126 was found to strongly prevent the pattern of cell proliferation that is normally seen in regenerating OEs. Interestingly, inhibition of ERK signaling did not interfere with cell proliferation in the intact OE, which ensures a steady and regular turnover of dying neurons from the ILC and SNS (Bayramli *et al.*, 2017). This suggested that ERK signaling is not active under normal conditions but gets activated with injury. This is further confirmed by analysis of tissue distribution

of the activated phosphorylated form of pERK, which is restricted to a few neurons in middle to apical layers of the OE. The pERK signal has often been used to label active OSNs that respond to specific odorants (Mirich *et al*, 2004). Thus, these cells most likely represent OSNs that have encountered ligands from the supplied food or other water contaminants. To further confirm the hypothesis that ERK activation upon injury is not only necessary for activation of cell divisions but ultimately contributes to tissue regeneration, fish inhibited for ERK signaling during the early phase of regeneration were allowed to regenerate for 5 days, which is a timepoint at which regeneration is almost complete and at which the proliferation pattern reverts back to confined zones of ILC and SNS (Kocagöz *et al*, 2022). The importance of early ERK activation could be confirmed by impaired regeneration in the damaged OE upon ERK inhibition. This impairment was consistent with a lower abundance of newborn neurons and a lower expansion of progenitors during the third day of regeneration. The reduced emergence of neurons was uniform for all regions of epithelial fold. However, because the inhibition regime was transient, early ERK inhibition did not completely prevent neurogenesis. Therefore, it could be suggested that ERK inhibition does not interfere with the differentiation of progenitors to OSNs but impairs the expansion of progenitors to sufficient numbers to support complete regeneration. To further test this hypothesis, instead of inhibiting ERK signaling only during the first day, ERK should be inhibited also at later time points regeneration, such as 3 and 5 dpi, which are timepoints that are largely dominated by differentiation of progenitors and transiently dividing precursors into neurons (Kocagöz *et al*, 2022). If, under continued inhibition, a significant impairment reforming the HuC/D area is not seen by 5 dpi, it can be concluded that ERK is involved only in activation of progenitor expansion only but not involved in the differentiation of progenitors. To confirm the cellular identity of pERK-positive proliferating cells, an ideal experiment would be counterstaining of the OE with cellular identity markers for progenitors such as K5 or Tp63 for HBCs and Ascl1 for GBCs. Unfortunately, all these antibodies were derived from the same host species as the pERK antibody and could not be used in this study. However, inhibitory effects of ERK on proliferation was observed in the sensory region of the epithelial fold, which is occupied by HBCs but not GBCs, and significant decreases could not be found

in the ILC and SNS at which GBCs are present. Therefore, since the inhibition of ERK effected cell proliferations profoundly in the sensory region and not the ILC/SNS, it can be speculated that pERK-positive cells induced upon injury at 1 dpi most likely comprise HBCs. This idea is further supported by correlating temporal profiles of ERK phosphorylation observed in section 4.1.3, and HBC activation (Kocagöz *et al*, 2022). Although inhibition of ERK was successful to prevent cell proliferation and thereby found to be necessary for mitosis at 1 dpi, colocalization with the EdU proliferation marker was poor, which raised the questions whether ERK activation promotes mitotic activity. This question was addressed with use of an additional marker of proliferation. PCNA is also known as the sliding clamp of the DNA replication complex, which is assembled with prior to replication to make sure that each daughter cell receives the genomic information (Boehm *et al*, 2016). On the other hand, EdU is a thymidine analog that will be present in the nucleus of the cell only if that cell divided at least once during the EdU pulse or if a labeled cells continued to divide. Since our hypothesis is that ERK signaling is required for cell proliferation, searching for pERK signals in an EdU-positive cell that divided earlier was not meaningful. Consequently, colocalization of pERK-positive cells with PCNA that marks cells from the S-phase of the cell cycle and in the process of mitosis, it could be shown that ERK contributes OE regeneration by triggering mitosis in otherwise dormant HBCs upon injury. This effect could further be blocked by application of the ERK inhibitor U0126. Further experiments were performed to understand the upstream transducer of ERK signaling. In this study ERK signaling is found to be necessary for OE regeneration most probably through activation of the HB-EGF/EGFR axis in HBCs. It would be interesting to see whether it is also sufficient to wake up HBCs from dormancy with the use of alternative ERK agonists in the intact OE that bypass EGFR signaling, which can add another layer to current understanding about the NSCs activation for regenerative purposes.

5.3. Survival of Neurons and MAPK/ERK Signaling

When the intact OE of ERK-inhibited fish was compared to the intact OE of a control group at 5 dpi, a significant decrease in the area covered with HuC/D-positive cells was observed. Since ERK inhibition did not significantly interfere with proliferation in the intact OE at 1 dpi, it can be concluded that this effect was not due to decrease birth of neurons for during normal OSN turnover. However, this decrease could be explained by an increased death rate of neurons that could not be compensated with the usual rate of proliferations in the intact OE. It would be interesting to see whether a one-day ERK inhibition could led to a 30% decrease in the HuC/D-covered area. When intact OEs of pERK stainings were examined closely, cells who are most likely to be neurons based on their nuclear shape and position towards the apical side of the stratified epithelium were occasionally seen to be positive for pERK, and thereby, have an active ERK signaling. Taken into consideration that those cells were not positive for EdU, the presence of a distinct role of ERK signaling in mature neurons can be proposed. Since ERK-inhibition led to a decrease in the HuC/D-positive cell population in the intact OE, this role of ERK could be related to survival of neurons, since ERK is also known to be regulate the apoptotic decisions in cells and promote cell survival (Lavoie *et al*, 2020). In post-mitotic neurons challenged with the toxin araC, inhibition of ERK with PD98059 has been shown to increase the rate of the apoptosis (Anderson & Tolkovsky, 1999). This might also be the case for the OE, at which mature neurons are constantly exposed to toxins, and a neuroprotective effect of ERK by promoting survival of these neurons could be required for their daily maintenance. To confirm this, ERK can be inhibited for longer periods and checked to see further decreases in the HuC/D area. Alternatively, these neurons can be simply activated by odorant, since pERK is also a marker of presence of action-potential in OSNs which can be induced upon activation of odorant receptor by an odor in OSNs (Mirich *et al*, 2004).

5.4. MAPK/ERK Signaling Is The Downstream Mediator of HB-EGF:EGFR

In the damaged OE, *hbegfa* was found to upregulated transiently at 4 hpi. Exogenous administration of human recombinant HB-EGF was shown to increase the mitotic activity in the intact OE with a neurogenic bias, while inhibition of soluble HB-EGF binding to EGFR led to impaired regeneration at day 5 (Şireci, unpublished). As for the inhibition of HB-EGF, inhibition of EGFR was also shown to impair regeneration of OE (Alkiraz, 2022). Hence, HB-EGF signaling through EGFR is found to be pivotal to the OE regeneration. Downstream pathways frequently associated with EGFR activation are MAPK/ERK, PI3K/AKT, and JAK/STAT. Among these pathways a link between JAK/STAT and HB:EGFR has been ruled out in previous studies (Alkiraz, 2022) One aim of this study was to understand whether MAPK/ERK activation observed upon OE injury and its contribution to progenitor expansion is activated by binding of soluble HB-EGF to EGFR. Epistasis experiments with inhibitors of HB-EGF and EGFR revealed that both EGFR activation and availability of the HB-EGF ligand are necessary for induction of ERK signaling following injury. These pathways were previously found to be involved in the regeneration of OE, however, the downstream effector of this pathways in OE progenitors was not established. When results of positional profiles were analyzed for each region of the epithelial fold, it can be seen that impact of HB-EGF, EGFR and MEK1/2 inhibition on ERK activation previously shown to induce cell proliferations is indistinguishable in neurogenic parts of the fold such as ILC, sensory OE and SNS. However, there is significant variance within the NS region, at which EGFR inhibition appeared to suppress ERK activation but HBEGF inhibition did not. This points to the presence of another growth factor such as EGF or FGF that might be binding to EGFR to induce cell proliferation through ERK signaling for the non-sensory part of the OE. As a hybrid organ with both neural and epithelial components, it would be interesting to see how distinct ligands are able to activate regeneration in a relatively small area and how the source of these ligands is localized within the stem cell niche.

5.5. AKT Regulates Mitosis but Not Regeneration in the OE

The impact of PI3K/AKT signaling was analyzed with a similar set of experiments that was used to investigate the contribution of MAPK/ERK, including the same control animals since the vehicle load was identical in both sets of experiments, and thereby allowed comparisons of their roles in OSN neurogenesis in the intact and injured OE. Distinctively from MAPK/ERK, PI3K/AKT pathway lead to general decrease in mitotic activity both in the intact and damaged OEs at 1 dpi. Their impact on cell proliferation upon injury was almost identical in terms of the positional profiles of BrdU-positive cells. Interestingly, this similarity in the strong effect during the early phase of regeneration was not seen at later time points. In the presence of the PI3K/AKT inhibitor Ly294002, the OEs was almost as successful as the control OEs to regenerate by 5 dpi and only minor, statistically not significant differences were seen in terms of production of new neurons that are the progeny of proliferating cells marked at 3 dpi. This could be due to a faster degradation rate of the AKT inhibitor with respect to ERK inhibitor or AKT inhibition could be causing a transient decrease in protein synthesis, which is required for the progression of cell cycle, and, thereby, prevent mitosis independently from being a regulator of regeneration. Once this arrest is over, progenitors might be starting again to proliferate to sufficient extents for functional OE regeneration. Signaling cues that direct OE progenitors may be persisting and exert their pro-mitotic effect through other signaling pathways that are independent of a general role of PI3K/AKT. Since, Ly294002 was a PI3K inhibitor that phosphorylates other important cellular regulators along with AKT (Cheng *et al*, 2005), experiments utilizing an pAKT antibody at 1 dpi was performed to confirm the involvement of AKT in mitosis. A colocalization of pAKT to PCNA cells of the intact OE could not be observed but in the injured OE, pAKT was found abundantly in the cytoplasm of cells present at the basal OE that are again most likely to be HBCs. However, pAKT-positive cells in the damaged OE were not observed to be PCNA-positive as frequent as pERK-positive cells. Despite this observation, pAKT-positive cells were still induced in the damaged OE with respect to intact OE and they were visible in

the basal of the epithelial fold, with cytosolic localization in cells with spiky morphologies. Upon activation by PI3K, AKT is well-known to promote cellular growth through mTOR and other metabolic pathways (Engelman *et al*, 2016). Metabolism is also known to correlate with the quiescence or activation of NSCs (Adusumilli *et al*, 2021) and through regulation of metabolism with mTOR pathway, it might be involved in pushing HBCs to leave the dormancy to regenerate OE without directly triggering mitosis. This could be investigated by combination of staining against the HBC marker Tp63 and PI3K/AKT inhibition in damaged OE to see whether HBCs that normally downregulate Tp63 expression (Packard *et al*, 2011) under injury still do so if AKT is inhibited. If Tp63 was found to be lesser in the damaged OE of vehicle controls with respect to PI3K-inhibited fish, it would suggest that PI3K regulate the dormancy of HBCs through Tp63 which is also known as the master regulator for activation of these dormant stem cells (Schnittke *et al*, 2015). In addition to the mechanism of AKT for regulating mitosis, it would be interesting to see whether pERK and pAKT are active in same cells and work synergistically in the injured OE and further experiments are needed to explore whether HBEGF and EGFR are also the upstream activators of AKT pathway.

5.6. Updated Model of OE Regeneration

Based on the experiments conducted in this thesis, new signaling aspects are added onto our current proposed model of zebrafish OE regeneration. This model starts with binding of soluble HB-EGF to the EGFR expressed by HBCs. This binding induces the activation of MAPK/ERK signaling to trigger mitosis of HBCs in order to expand sufficiently for regeneration of the whole OE with neurons. In HBCs, PI3K/AKT/mTOR pathway is also active to provide cellular growth that can fuel multiple rounds of mitosis. Once the differentiation stage is reached within regeneration, ERK is deactivated in progenitors to allow differentiation. This model is schematically presented in Figure 5.1.

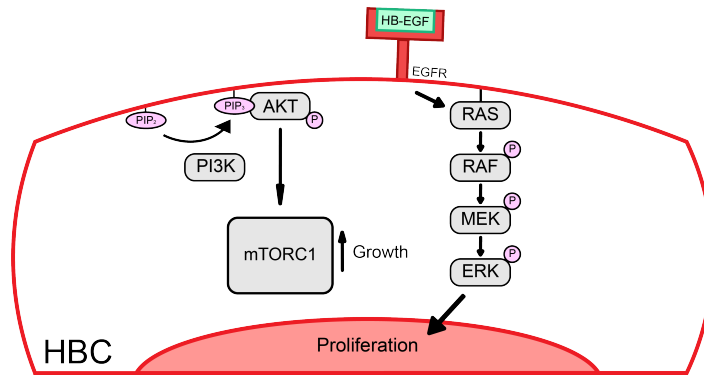


Figure 5.1. A proposed model of MAPK/ERK activation by HBE-GF:EGFR along with PI3K/AKT/mTOR activity during OE regeneration.

REFERENCES

- Adusumilli, V. S., T. L. Walker, R. W. Overall, G. M. Klatt, S. A. Zeidan, S. Zocher, D. G. Kirova, K. Ntitsias, T. J. Fischer, A. M. Sykes, S. Reinhardt, A. Dahl, J. Mansfeld, A. E. Rünker and G. Kempermann, 2021, “ROS Dynamics Delineate Functional States of Hippocampal Neural Stem Cells and Link to Their Activity-Dependent Exit from Quiescence.”, *Cell Stem Cell*, Vol. 28, No. 2, pp. 300–314.
- Aguirre, A., M. E. Rubio, and V. Gallo, 2010, “Notch and EGFR Pathway Interaction Regulates Neural Stem Cell Number and Self-Renewal.”, *Nature*, Vol. 467, No. 7313, pp. 323–327.
- Aimone, J. B., J. Wiles, and F. H. Gage, 2006, “Potential Role for Adult Neurogenesis in the Encoding of Time in New Memories.”, *Nature Neuroscience*, Vol. 9, No. 6, pp. 723–727.
- Alkiraz, A., 2022, *The Role of EGFR and JAK/STAT Signaling During Regenerative Neurogenesis in the Zebrafish Olfactory Epithelium*, M.S. Thesis, Bogaziçi University.
- Alonso, L., and E. Fuchs, 2003, “Stem Cells of the Skin Epithelium.”, *Proceedings of the National Academy of Sciences of the United States of America*, Vol. 1, pp. 11830–11835.

- Amamoto, R., V. G. Huerta, E. Takahashi, G. Dai, A. K. Grant, Z. Fu, and P. Arlotta, 2016, "Adult Axolotls Can Regenerate Original Neuronal Diversity in Response to Brain Injury.", *E-life*, Vol. 5, p. 13998.
- Anderson, C. N., and A. M. Tolkovsky, 1999, "A Role For MAPK/ERK in Sympathetic Neuron Survival: Protection Against a p53-Dependent, JNK-Independent Induction of Apoptosis by Cytosine Arabinoside.", *The Journal of Neuroscience*, Vol. 19, No. 2, pp. 664–673.
- Asati, V., D. K. Mahapatra, and S. K. Bharti, 2016, "PI3K/Akt/mTOR and Ras/Raf/MEK/ERK Signaling Pathways Inhibitors as Anticancer Agents: Structural and Pharmacological Perspectives.", *European Journal of Medicinal Chemistry*, Vol. 109, pp. 314–341.
- Ayyaz, A., S. Kumar, B. Sangiorgi, B. Ghoshal, J. Gosio, S. Ouladan, M. Fink, S. Barutcu, D. Trcka, J. Shen, K. Chan, J. L. Wrana, and A. Gregorieff, 2019, "Single-Cell Transcriptomes of The Regenerating Intestine Reveal a Revival Stem Cell.", *Nature*, Vol. 569, No. 7754, pp. 121–125.
- Babcock, K. R., J. S. Page, J. R. Fallon, and A. E. Webb, 2021, "Adult Hippocampal Neurogenesis in Aging and Alzheimer's Disease.", *Stem Cell Reports*, Vol. 16, No. 4, pp. 681–693.
- Bachmann, C., H. Nguyen, J. Rosenbusch, L. Pham, T. Rabe, M. Patwa, G. Sokpor, R. H. Seong, R. Ashery-Padan, A. Mansouri, A. Stoykova, J. F. Staiger, and T. Tuoc, 2016, "mSWI/SNF (BAF) Complexes Are Indispensable

for the Neurogenesis and Development of Embryonic Olfactory Epithelium.”, *PLoS Genetics*, Vol. 12, No. 9, p. 1006274.

Bayramli, X., Y. Kocagoz, U. Sakizli, and S. H. Fuss, 2017, “Patterned Arrangements of Olfactory Receptor Gene Expression in Zebrafish are Established by Radial Movement of Specified Olfactory Sensory Neurons.”, *Scientific Reports*, Vol. 7, No. 1, p. 5572.

Beumer, J., and H. Clevers, 2016, “Regulation and Plasticity of Intestinal Stem Cells During Homeostasis and Regeneration.”, *Development*, Vol. 143, No. 20, pp. 3639–3649.

Beumer, J., and H. Clevers., 2021, “Cell Fate Specification and Differentiation in the Adult Mammalian Intestine.”, *Nature Reviews: Molecular Cell Biology*, Vol. 22, No. 1, pp. 39–53.

Blanpain, C., and E. Fuchs, 2006, “Epidermal Stem Cells of the Skin.”, *Annual Review of Cell and Developmental Biology*, Vol. 22, pp. 339–373.

Blanpain, C., and E. Fuchs, 2009, “Epidermal Homeostasis: A Balancing Act of Stem Cells In The Skin.”, *Nature Reviews: Molecular Cell Biology*, Vol. 10, No. 3, pp. 207–217.

Boehm, E. M., M. S. Gildenberg, and M. T. Washington, 2016, “The Many Roles of PCNA in Eukaryotic DNA Replication.”, *The Enzymes*, Vol. 39, pp. 231–254.

- Bonaguidi, M. A., M. A. Wheeler, J. S. Shapiro, R. P. Stadel, G. J. Sun, G. L. Ming, and H. Song, 2011, “In Vivo Clonal Analysis Reveals Self-Renewing and Multipotent Adult Neural Stem Cell Characteristics.”, *Cell*, Vol. 145, No. 7, pp. 1142–1155.
- Brann, J. H., and S. J. Firestein, 2014, “A Lifetime of Neurogenesis in The Olfactory System.”, *Frontiers in Neuroscience*, Vol. 8, p. 182.
- Cau, E., G. Gradwohl, S. Casarosa, R. Kageyama, and F. Guillemot, 2000, “Hes Genes Regulate Sequential Stages of Neurogenesis in The Olfactory Epithelium.”, *Development*, Vol. 127, No. 11, pp. 2323–2332.
- Chang, L., and M. Karin, 2001, “Mammalian MAP Kinase Signalling Cascades.”, *Nature*, Vol. 410, No. 6824, pp. 37–40.
- Chen, C. R., C. Kachramanoglou, D. Li, P. Andrews, and D. Choi, 2014, “Anatomy and Cellular Constituents of The Human Olfactory Mucosa: A Review.”, *Journal of Neurological Surgery*, Vol. 75, No. 5, pp. 293–300.
- Chen, X., H. Fang, and J. E. Schwob, 2004, “Multipotency of Purified, Transplanted Globose Basal Cells in Olfactory Epithelium.”, *The Journal of Comparative Neurology*, Vol. 469, No. 4, pp. 457–474.
- Chen, Z. H., X. C. Luo, C. R. Yu, and L. Huang, 2020, “Matrix Metalloprotease-Mediated Cleavage of Neural Glial-Related Cell Adhesion Molecules Activates Quiescent Olfactory Stem Cells via EGFR.”, *Molecular and Cellular Neurosciences*, Vol. 108, p. 103552.

- Cheng, Y. C., F. Y. Hsieh, M. C. Chiang, P. J. Scotting, H. Y. Shih, S. J. Lin, H. L. Wu, and H. T. Lee, 2013, “Akt1 Mediates Neuronal Differentiation in Zebrafish via A Reciprocal Interaction With Notch Signaling.”, *PloS One*, Vol. 8, No.1, p. 54262.
- Choi, P. S., L. Zakhary, W. Y. Choi, S. Caron, E. Alvarez-Saavedra, E. A. Miska, M. McManus, B. Harfe, A. J. Giraldez, H. R. Horvitz, A. F. Schier, and C. Dulac, 2008, “Members of the miRNA-200 Family Regulate Olfactory Neurogenesis.”, *Neuron*, Vol. 57, No. 1, pp. 41–55.
- Cosacak, M. I., P. Bhattarai, and C. Kizil, 2020, “Alzheimer’s Disease, Neural Stem Cells and Neurogenesis: Cellular Phase at Single-Cell Level.”, *Neural Regeneration Research*, Vol. 15, No. 5, pp. 824–827.
- Cuschieri, A., and L. H. Bannister, 1975, “The Development of The Olfactory Mucosa in The Mouse: Light Microscopy.”, *Journal of Anatomy*, Vol. 119, pp. 277–286.
- Dao, D. T., L. Anez-Bustillos, R. M. Adam, M. Puder, and D. R. Bielenberg, 2018, “Heparin-Binding Epidermal Growth Factor-Like Growth Factor as a Critical Mediator of Tissue Repair and Regeneration.”, *The American Journal of Pathology*, Vol. 188, No. 11, pp. 2446–2456.
- DasGupta, R., and E. Fuchs, 1999, “Multiple Roles For Activated LEF/TCF Transcription Complexes During Hair Follicle Development and Differentiation.”, *Development*, Vol. 126, No. 20, pp. 4557–4568.

- De Simone, A., M. N. Evanitsky, L. Hayden, B. D. Cox, J. Wang, V. A. Tornini, J. Ou, A. Chao, K. D. Poss, and S. Di Talia, 2021, “Control of Osteoblast Regeneration by a Train of Erk Activity Waves.”, *Nature*, Vol. 590, No. 7844, pp. 129–133.
- Dekoninck, S., and C. Blanpain, 2019, “Stem Cell Dynamics, Migration and Plasticity During Wound Healing.”, *Nature Cell Biology*, Vol. 21, No. 1, pp. 18–24.
- Diotel, N., L. Lübke, U. Strahle, and S. Rastegar, 2020, “Common and Distinct Features of Adult Neurogenesis and Regeneration in the Telencephalon of Zebrafish and Mammals.”, *Frontiers in Neuroscience*, Vol. 14, p. 568930.
- Doyle, K. L., T. Karl, Y. Hort, L. Duffy, J. Shine, J., and H. Herzog, 2008, “Y1 Receptors Are Critical for the Proliferation of Adult Mouse Precursor Cells in the Olfactory Neuroepithelium.”, *Journal of Neurochemistry*, Vol. 105, No. 3, pp. 641–652.
- Duncia, J. V., J. B. Santella, C. A. Higley, W. J. Pitts, J. Wityak, W. E. Fietze, F. W. Rankin, J. H. Sun, R. A. Earl, A. C. Tabaka, C. A. Teleha, K. F. Blom, M. F. Favata, E. J. Manos, A. Daulerio, D. A. Stradley, K. Horiuchi, R. A. Copeland, P. A. Scherle, J. M. Trzaskos, ... R. E. Olson, 1998, “MEK Inhibitors: The Chemistry and Biological Activity of U0126, Its Analogs, and Cyclization Products.”, *Bioorganic & Medicinal Chemistry Letters*, Vol. 8, No. 20, pp. 2839–2844.
- Duprey-Diaz, M. V., J. M. Blagburn, and R. E. Blanco, 2016, “Exogenous Modulation of Retinoic Acid Signaling Affects Adult RGC Survival in The

Frog Visual System After Optic Nerve Injury.”, *PloS One*, Vol. 11, No. 9, p. 162626.

Ehm, O., C. Goritz, M. Covic, I. Schaffner, T. J. Schwarz, E. Karaca, B. Kempkes, E. Kremmer, F. W. Pfrieder, L. Espinosa, A. Bigas, C. Giachino, V. Taylor, J. Frisen, and D. C. Lie, 2010, “RBP-J-Kappa-Dependent Signaling Is Essential for Long-Term Maintenance of Neural Stem Cells in the Adult Hippocampus.”, *The Journal of Neuroscience*, Vol. 30, No. 41, pp. 13794–13807.

El-Assal, O. N., and G. E. Besner, 2005, “HB-EGF Enhances Restitution After Intestinal Ischemia/Reperfusion via PI3K/Akt and MEK/ERK1/2 Activation.”, *Gastroenterology*, Vol. 129, No. 2, pp. 609–625.

Farbman, A. I., and F. L. Margolis, 1980, “Olfactory Marker Protein During Ontogeny: Immunohistochemical Localization.”, *Developmental biology*, Vol. 74, No. 1, pp. 205–215.

Gantwerker, E. A., and D. B. Hom, 2011, “Skin: Histology and Physiology of Wound Healing.”, *Facial Plastic Surgery Clinics of North America*, Vol. 19, No. 3, pp. 441–453.

Garthe, A., Behr, J., and G. Kempermann, 2009, “Adult-Generated Hippocampal Neurons Allow The Flexible Use of Spatially Precise Learning Strategies.”, *PloS One*, Vol. 4, No. 5, p. 5464.

Gechtman, Z., J. L. Alonso, G. Raab, D. E. Ingber, and M. Klagsbrun, 1999, “The Shedding of Membrane-Anchored Heparin-Binding Epidermal-Like Growth Factor Is Regulated by The Raf/Mitogen-Activated Protein Kinase Cascade

and by Cell Adhesion and Spreading.”, *The Journal of Biological Chemistry*, Vol. 274, No. 40, pp. 28828–28835.

Gehart, H., and H. Clevers, 2019, “Tales From The Crypt: New Insights Into Intestinal Stem Cells.”, *Nature Reviews: Gastroenterology & Hepatology*, Vol. 16, No. 1, pp. 19–34.

Goldstein, B. J., G. M. Goss, R. Choi, D. Saur, B. Seidler, J. M. Hare, and N. Chaudhari, 2016, “Contribution of Polycomb Group Proteins to Olfactory Basal Stem Cell Self-Renewal in a Novel c-KIT+ Culture Model and In Vivo.”, *Development*, Vol. 143, No. 23, pp. 4394–4404.

Gonzales, K., L. Polak, I. Matos, M. T. Tierney, A. Gola, E. Wong, N. R. Infarinato, M. Nikolova, S. Luo, S. Liu, J. Novak, K. Lay, H. A. Pasolli, and E. Fuchs, 2021, “Stem Cells Expand Potency and Alter Tissue Fitness by Accumulating Diverse Epigenetic Memories.”, *Science*, Vol. 374, No. 6571, p. 2444.

Graziadei, P. P., and G. A. Graziadei, 1979, “Neurogenesis and Neuron Regeneration in the Olfactory System of Mammals I: Morphological Aspects of Differentiation and Structural Organization of The Olfactory Sensory Neurons.”, *Journal of Neurocytology*, Vol. 8, No. 1, pp. 1–18.

Green H., 1991, “Cultured Cells for The Treatment of Disease.”, *Scientific American*, Vol. 265, No. 5, pp. 96–102.

- Güler, K., 2021, *Identification of HB-EGF-Positive and HB-EGF-Responsive Cell Populations in the Zebrafish Olfactory Epithelium*, M.S. Thesis, Bogaziçi University.
- Hageman, J. H., M. C. Heinz, K. Kretzschmar, J. Van Der Vaart, H. Clevers, and H. Snippert, 2020, “Intestinal Regeneration: Regulation by the Microenvironment.”, *Developmental Cell*, Vol. 54, No. 4, pp. 435–446.
- Hansen, A., and E. Zeiske, 1998, “The Peripheral Olfactory Organ of The Zebrafish, *Danio rerio*: an Ultrastructural Study.”, *Chemical Senses*, Vol. 23, No. 1, pp. 39–48.
- Herrick, D. B., B. Lin, J. Peterson, N. Schnittke, and J. E. Schwob, 2017, “Notch1 Maintains Dormancy of Olfactory Horizontal Basal Cells, a Reserve Neural Stem Cell.”, *Proceedings of the National Academy of Sciences of the United States of America*, Vol. 114, No. 28, pp. 5589–5598.
- Holbrook, E. H., K. E. Szumowski, and J. E. Schwob, 1995, “An Immunochemical, Ultrastructural, and Developmental Characterization of The Horizontal Basal Cells of Rat Olfactory Epithelium.”, *The Journal of Comparative Neurology*, Vol. 363, No. 1, pp. 129–146.
- Hollborn, M., I. Iandiev, M. Seifert, U. E. Schnurrbusch, S. Wolf, P. Wiedemann, A. Bringmann, L. Kohen, 2006, “Expression of HB-EGF by Retinal Pigment Epithelial Cells in Vitreoretinal Proliferative Disease.”, *Current Eye Research*, Vol. 31, No. 10, pp. 863–874.

- Horsley, V., A. O. Aliprantis, L. Polak, L. H. Glimcher, and E. Fuchs, 2008, “NFATc1 balances quiescence and proliferation of skin stem cells.”, *Cell*, Vol. 132, No. 2, pp. 299–310.
- Hoxhaj, G., and B. D. Manning, 2020, “The PI3K-AKT Network at The Interface of Oncogenic Signalling and Cancer Metabolism.”, *Nature Reviews: Cancer*, Vol. 20, No. 2, pp. 74–88.
- Huard, J. M., S. L. Youngentob, B. J. Goldstein, M. B. Luskin, and J. E. Schwob, 1998, “Adult Olfactory Epithelium Contains Multipotent Progenitors That Give Rise to Neurons and Non-Neural cells.”, *The Journal of Comparative Neurology*, Vol. 400, No. 4, pp. 469–486.
- Huelsken, J., R. Vogel, B. Erdmann, G. Cotsarelis, and W. Birchmeier, 2001, “Beta-Catenin Controls Hair Follicle Morphogenesis and Stem Cell Differentiation In The Skin.”, *Cell*, Vol. 105, No. 4, pp. 533–545.
- Hung, K. W., H. W. Huang, C. C. Cho, S. C. Chang, and C. Yu, 2014, “Nuclear Magnetic Resonance Structure of The Cytoplasmic Tail of Heparin Binding EGF-Like Growth Factor (proHB-EGF-CT) Complexed With The Ubiquitin Homology Domain of Bcl-2-Associated Athanogene 1 From Mus Musculus (mBAG-1-UBH).”, *Biochemistry*, Vol. 53, No. 12, pp. 1935–1946.
- Inoki, K., Y. Li, T. Zhu, J. Wu, and K. L. Guan, 2002, “TSC2 Is Phosphorylated and Inhibited by Akt and Suppresses mTOR Signalling.”, *Nature Cell Biology*, Vol. 4, No. 9, pp. 648–657.

- Iqbal, T., and C. Byrd-Jacobs, 2010, “Rapid degeneration and regeneration of the zebrafish olfactory epithelium after triton X-100 application.”, *Chemical Senses*, Vol. 35, No. 5, pp. 351–361.
- Izumi, Y., M. Hirata, H. Hasuwa, R. Iwamoto, T. Umata, K. Miyado, Y. Tamai, T. Kurisaki, A. Sehara-Fujisawa, S. Ohno, and E. Mekada, 1998, “A Metalloprotease-Disintegrin, MDC9/Meltrin-Gamma/ADAM9 and PKC-Delta Are Involved in TPA-Induced Ectodomain Shedding of Membrane-Anchored Heparin-Binding EGF-Like Growth Factor.”, *The EMBO Journal*, Vol. 17, No. 24, pp. 7260–7272.
- Jeffries, M. A., L. E. McLane, L. Khandker, M. L. Mather, A. V. Evangelou, D. Kantak, J. N. Bourne, W. B. Macklin, and T. L. Wood, 2021, “mTOR Signaling Regulates Metabolic Function in Oligodendrocyte Precursor Cells and Promotes Efficient Brain Remyelination in the Cuprizone Model.”, *The Journal of Neuroscience*, Vol. 41, No. 40, pp. 8321–8337.
- Jiao, J., X. Huang, R. A. Feit-Leithman, R. L. Neve, W. Snider, D. A. Darrt, and D. F. Chen, 2005, “Bcl-2 Enhances Ca^{2+} Signaling to Support The Intrinsic Regenerative Capacity of CNS Axons.”, *The EMBO Journal*, Vol. 24, No. 5, pp. 1068–1078.
- Jin, K., X. O. Mao, G. Del Rio Guerra, L. Jin, and D. A. Greenberg, 2005, “Heparin-Binding Epidermal Growth Factor-Like Growth Factor Stimulates Cell Proliferation In Cerebral Cortical Cultures Through Phosphatidylinositol 3'-Kinase and Mitogen-Activated Protein Kinase.”, *Journal of Neuroscience Research*, Vol. 81, No. 4, pp. 497–505.

- Jin, K., Y. Sun, L. Xie, J. Childs, X. O. Mao, and D. A. Greenberg, 2004, “Post-Ischemic Administration of Heparin-Binding Epidermal Growth Factor-Like Growth Factor (HB-EGF) Reduces Infarct Size and Modifies Neurogenesis After Focal Cerebral Ischemia in The Rat.”, *Journal of Cerebral Blood Flow and Metabolism*, Vol. 24, No. 4, pp. 399–408.
- Kanitakis J., 2002, “Anatomy, Histology and Immunohistochemistry of Normal Human Skin.”, *European Journal of Dermatology*, Vol. 12, No. 4, pp. 390–401.
- Kempermann G., 2022, “What Is Adult Hippocampal Neurogenesis Good for?”, *Frontiers in Neuroscience*, Vol. 16, p. 852680.
- Kizil, C., J. Kaslin, V. Kroehne, and M. Brand, 2012, “Adult Neurogenesis and Brain Regeneration In Zebrafish.”, *Developmental Neurobiology*, Vol. 72, No. 3, pp. 429–461.
- Kocagöz, Y., 2021, *Cellular and Molecular Analysis of Regenerative Neurogenesis in The Zebrafish (Danio Rerio) Olfactory Epithelium*, Ph.D. Thesis, Boğaziçi University.
- Kocagöz, Y., M. C. Demirler, S. E. Eski, K. Güler, Z. Dokuzluoglu, and S. H. Fuss, 2022, “Disparate Progenitor Cell Populations Contribute to Maintenance and Repair Neurogenesis in The Zebrafish Olfactory Epithelium.”, *Cell and Tissue Research*, Vol. 388, No. 2, pp. 331–358.
- Koster, M. I., and D. R. Roop, 2007, “Mechanisms Regulating Epithelial Stratification.”, *Annual Review of Cell and Developmental Biology*, Vol. 23, pp. 93–113.

- Krolewski, R. C., A. Packard, A., and J. E. Schwob, 2013, “Global Expression Profiling of Globose Basal Cells and Neurogenic Progression Within The Olfactory Epithelium.”, *The Journal of Comparative Neurology*, Vol. 521, No. 4, pp. 833–859.
- Kyritsis, N., C. Kizil, and M. Brand, 2014, “Neuroinflammation and Central Nervous System Regeneration In Vertebrates.”, *Trends in Cell Biology*, Vol. 24, No. 2, pp. 128–135.
- Lavoie, H., J. Gagnon, and M. Therrien, 2020, “ERK Signalling: A Master Regulator of Cell Behaviour, Life and Fate.”, *Nature Reviews: Molecular Cell Biology*, Vol. 21, No. 10, pp. 607–632.
- Lee, J. H., and E. L. Rawlins, 2018, “Developmental Mechanisms and Adult Stem Cells For Therapeutic Lung Regeneration.”, *Developmental Biology*, Vol. 433, No. 2, pp. 166–176.
- Leung, C. T., P. A. Coulombe, and R. R. Reed, 2007, “Contribution of Olfactory Neural Stem Cells to Tissue Maintenance and Regeneration.”, *Nature Neuroscience*, Vol. 10, No. 6, pp. 720–726.
- Lie, D. C., S. A. Colamarino, H. J. Song, L. Desire, H. Mira, A. Consiglio, E. S. Lein, S. Jessberger, H. Lansford, A. R. Dearie, and F. H. Gage, 2005, “Wnt Signalling Regulates Adult Hippocampal Neurogenesis.”, *Nature*, Vol. 437, No. 7063, pp. 1370–1375.

- Lin, B., J. H. Coleman, J. N. Peterson, M. J. Zunitich, W. Jang, D. B. Herrick, and J. E. Schwob, 2017, “Injury Induces Endogenous Reprogramming and Dedifferentiation of Neuronal Progenitors to Multipotency.”, *Cell Stem Cell*, Vol. 21, No. 6, pp. 761–774.
- Lust, K., and E. M. Tanaka, 2019, “A Comparative Perspective on Brain Regeneration in Amphibians and Teleost Fish.”, *Developmental Neurobiology*, Vol. 79, No. 5, pp. 424–436.
- Mackay-Sim, A., and P. W. Kittel, 1991, “On the Life Span of Olfactory Receptor Neurons.”, *The European Journal of Neuroscience*, Vol. 3, No. 3, pp. 209–215.
- Magrassi, L., K. Leto, and F. Rossi, 2013, “Lifespan of Neurons Is Uncoupled From Organismal Lifespan.”, *Proceedings of the National Academy of Sciences of the United States of America*, Vol. 110, No. 11, pp. 4374–4379.
- Maik-Rachline, G., A. Hacoheh-Lev-Ran, and R. Seger, 2019, “Nuclear ERK: Mechanism of Translocation, Substrates, and Role in Cancer.”, *International Journal of Molecular Sciences*, Vol. 20, No. 5, p. 1194.
- Mamane, Y., E. Petroulakis, L. Rong, K. Yoshida, L. W. Ler, and N. Sonenberg, 2004, “eIF4E—From Translation to Transformation.”, *Oncogene*, Vol. 23, No. 18, pp. 3172–3179.
- Manglapus, G. L., S. L. Youngentob, and J. E. Schwob, 2004, Expression Patterns of Basic Helix-Loop-Helix Transcription Factors Define Subsets of Olfactory Progenitor Cells.”, *The Journal of Comparative Neurology*, Vol. 479, No. 2, pp. 216–233.

- Mascre, G., S. Dekoninck, B. Drogat, K. K. Youssef, S. Brohe, P. A. Sotiropoulou, B. D. Simons, and C. Blanpain, 2012, “Distinct Contribution of Stem and Progenitor Cells to Epidermal Maintenance.”, *Nature*, Vol. 489, No. 7415, pp. 257–262.
- Mathew, L. K., S. Sengupta, J. A. Franzosa, J. Perry, J. La Du, E. A. Andreasen, and R. L. Tanguay, 2009, “Comparative Expression Profiling Reveals an Essential Role for Raldh2 In Epimorphic Regeneration.”, *The Journal of Biological Chemistry*, Vol. 284, No. 48, pp. 33642–33653.
- Medema, R. H., G. J. Kops, J. L. Bos, and B. M. Burgering, 2000, “AFX-like Forkhead Transcription Factors Mediate Cell-Cycle Regulation by Ras and PKB Through p27kip1.”, *Nature*, Vol. 404, No. 6779, pp. 782–787.
- Mira, H., Z. Andreu, H. Suh, D. C. Lie, S. Jessberger, A. Consiglio, J. San Emeterio, R. Hortiguera, M. A. Marques-Torres, K. Nakashima, D. Colak, M. Götz, I. Farinas, and F. H. Gage, 2010, “Signaling Through BMPRII Regulates Quiescence and Long-Term Activity of Neural Stem Cells in The Adult Hippocampus.”, *Cell Stem Cell*, Vol. 7, No. 1, pp. 78–89.
- Morrison D. K., 2012, “MAP Kinase Pathways.”, *Cold Spring Harbor Perspectives in Biology*, Vol. 4, No. 11, p. 11254.
- Najm, F. J., M. Madhavan, A. Zaremba, E. Shick, R. T. Karl, D. C. Factor, T. E. Miller, Z. S. Nevin, C. Kantor, A. Sargent, K. L. Quick, D. M. Schlatter, H. Tang, R. Papoian, K. R. Brimacombe, M. Shen, M. B. Boxer, A. Jadhav, A. P. Robinson, J. R. Podojil, ... P. J. Tesar, 2015, “Drug-Based Modulation of

Endogenous Stem Cells Promotes Functional Remyelination In Vivo.”, *Nature*, Vol. 522, No. 7555, pp. 216–220.

Napoli, I., L. A. Noon, S. Ribeiro, A. P. Kerai, S. Parrinello, L. H. Rosenberg, M. J. Collins, M. C. Harrisingh, I. J. White, A. Woodhoo, and A. C. Lloyd, 2012, “A Central Role For The ERK-Signaling Pathway In Controlling Schwann Cell Plasticity and Peripheral Nerve Regeneration In Vivo.”, *Neuron*, Vol. 73, No. 4, pp. 729–742.

Niimura, Y., and M. Nei, 2005, “Evolutionary Dynamics of Olfactory Receptor Genes In Fishes and Tetrapods.”, *Proceedings of The National Academy of Sciences of The United States of America*, Vol. 102, No. 17, pp. 6039–6044.

Normanno, N., A. De Luca, C. Bianco, L. Strizzi, M. Mancino, M. R. Maiello, A. Carotenuto, G. De Feo, F. Caponigro, and D. S. Salomon, 2006, “Epidermal Growth Factor Receptor (EGFR) Signaling in Cancer.”, *Gene*, Vol. 366, No. 1, pp. 2–16.

Oyagi, A., N. Morimoto, J. Hamanaka, M. Ishiguro, K. Tsuruma, M. Shimazawa, and H. Hara, 2011, “Forebrain Specific Heparin-Binding Epidermal Growth Factor- Like Growth Factor Knockout Mice Show Exacerbated Ischemia and Reperfusion Injury.”, *Neuroscience*, Vol. 185, pp. 116–124.

Packard, A., N. Schnittke, R. A. Romano, S. Sinha, and J. E. Schwob, 2011, “DeltaNp63 Regulates Stem Cell Dynamics in The Mammalian Olfactory Epithelium.”, *The Journal of Neuroscience*, Vol. 31, No. 24, pp. 8748–8759.

- Paton, J. A., and F. N. Nottebohm, 1984, “Neurons Generated in The Adult Brain Are Recruited into Functional Circuits.”, *Science*, Vol. 225, No. 4666, pp. 1046–1048.
- Pellegrini, G., E. Dellambra, O. Golisano, E. Martinelli, I. Fantozzi, S. Bondanza, D. Ponzin, F. McKeon, and M. De Luca, 2001, “p63 Identifies Keratinocyte Stem Cells.”, *Proceedings of the National Academy of Sciences of the United States of America*, Vol. 98, No. 6, pp. 3156–3161.
- Peterson, J., B. Lin, C. M. Barrios-Camacho, D. B. Herrick, E. H. Holbrook, W. Jang, J. H. Coleman, and J. E. Schwob, 2019, “Activating a Reserve Neural Stem Cell Population In Vitro Enables Engraftment and Multipotency after Transplantation.”, *Stem Cell Reports*, Vol. 12, No. 4, pp. 680–695.
- Pons-Espinal, M., C. Gasperini, M. J. Marzi, C. Braccia, A. Armirotti, A. Potzsch, T. L. Walker, K. Fabel, F. Nicassio, G. Kempermann, and D. De Pietri Tonelli, 2019, “MiR-135a-5p Is Critical for Exercise-Induced Adult Neurogenesis.”, *Stem Cell Reports*, Vol. 12, No. 6, pp. 1298–1312.
- Potten C. S., 1975, “Epidermal Cell Production Rates.”, *The Journal of Investigative Dermatology*, Vol. 65, No. 6, pp. 488–500.
- Pourmorady, A., and S. Lomvardas, 2022, “Olfactory Receptor Choice: A Case Study For Gene Regulation In A Multi-Enhancer System.”, *Current Opinion in Genetics & Development*, Vol. 72, pp. 101–109.
- Rochat, A., K. Kobayashi, and Y. Barrandon, 1994, “Location of Stem Cells of Human Hair Follicles by Clonal Analysis.”, *Cell*, Vol. 76, No. 6, pp. 1063–1073.

- Rock, J. R., X. Gao, Y. Xue, S. H. Randell, Y. Y. Kong, and B. L. Hogan, 2011, “Notch-Dependent Differentiation of Adult Airway Basal Stem Cells.”, *Cell Stem Cell*, Vol. 8, No. 6, pp. 639–648.
- Schindelin, J., I. Arganda-Carreras, E. Frise, V. Kaynig, M. Longair, T. Pietzsch, . . . A. Cardona, 2012, “Fiji: an Open-Source Platform for Biological-Image Analysis.”, *Nature Methods*, Vol. 9, No. 7, pp. 676–682.
- Schlessinger J., 2000, “Cell Signaling by Receptor Tyrosine Kinases.”, *Cell*, Vol. 103, No. 2, pp. 211–225.
- Schnittke, N., D. B. Herrick, B. Lin, J. Peterson, J. H. Coleman, A. I. Packard, W. Jang, and J. E. Schwob, 2015, “Transcription Factor p63 Controls The Reserve Status But Not The Stemness of Horizontal Basal Cells in The Olfactory Epithelium.”, *Proceedings of the National Academy of Sciences of the United States of America*, Vol. 112, No. 36, pp. 5068–5077.
- Schwartz Levey, M., D. M. Chikaraishi, and J. S. Kauer, 1991, “Characterization of Potential Precursor Populations in The Mouse Olfactory Epithelium Using Immunocytochemistry and Autoradiography.”, *The Journal of Neuroscience*, Vol. 11, No. 11, pp. 3556–3564.
- Schwob J. E., 2002, “Neural regeneration and the peripheral olfactory system.”, *The Anatomical Record*, Vol. 269, No. 1, pp. 33–49.

- Schwob, J. E., W. Jang, E. H. Holbrook, B. Lin, D. B. Herrick, J. N. Peterson, and J. Hewitt Coleman, 2017, "Stem and Progenitor Cells of the Mammalian Olfactory Epithelium: Taking Poietic License.", *The Journal of Comparative Neurology*, Vol. 525, No. 4, pp. 1034–1054.
- Schwob, J. E., S. L. Youngentob, and R. C. Mezza, 1995, "Reconstitution of The Rat Olfactory Epithelium After Methyl Bromide-Induced Lesion.", *The Journal of Comparative Neurology*, Vol. 359, No. 1, pp. 15–37.
- Seib, D. R., N. S. Corsini, K. Ellwanger, C. Plaas, A. Mateos, C. Pitzer, C. Niehrs, T. Celikel, and A. Martin-Villalba, 2013, "Loss of Dickkopf-1 Restores Neurogenesis in Old Age and Counteracts Cognitive Decline.", *Cell Stem Cell*, Vol. 12, No. 2, pp. 204–214.
- Shirakata, Y., R. Kimura, D. Nanba, R. Iwamoto, S. Tokumaru, C. Morimoto, K. Yokota, M. Nakamura, K. Sayama, E. Mekada, S. Higashiyama, and K. Hashimoto, 2005, "Heparin-Binding EGF-Like Growth Factor Accelerates Keratinocyte Migration and Skin Wound Healing.", *Journal of Cell Science*, Vol. 118, No. 11, pp. 2363–2370.
- Singh, A. M., D. Reynolds, T. Cliff, S. Ohtsuka, A. L. Mattheyses, Y. Sun, L. Menendez, M. Kulik, and S. Dalton, 2012, "Signaling Network Crosstalk in Human Pluripotent Cells: A Smad2/3-Regulated Switch that Controls the Balance Between Self- Renewal and Differentiation.", *Cell Stem Cell*, Vol. 10, No. 3, pp. 312–326.
- Skeen, J. E., P. T. Bhaskar, C. C. Chen, W. S. Chen, X. D. Peng, V. Nogueira, A. Hahn-Windgassen, H. Kiyokawa, and N. Hay, 2006, "Akt Deficiency Impairs

- Normal Cell Proliferation and Suppresses Oncogenesis In a p53-Independent and mTORC1- Dependent Manner.”, *Cancer Cell*, Vol. 10, No. 4, pp. 269–280.
- Sokpor, G., E. Abbas, J. Rosenbusch, J. F. Staiger, and T. Tuoc, 2018, “Transcriptional and Epigenetic Control of Mammalian Olfactory Epithelium Development.”, *Molecular Neurobiology*, Vol. 55, No. 11, pp. 8306–8327.
- Strotmann, J., and H. Breer, 2006, “Formation of Glomerular Maps in the Olfactory System.”, *Seminars in Cell & Developmental Biology*, Vol. 17, No. 4, pp. 402–410.
- Sueda, R., I. Imayoshi, Y. Harima, and R. Kageyama, 2019, “High Hes1 Expression and Resultant Ascl1 Suppression Regulate Quiescent vs. Active Neural Stem Cells in the Adult Mouse Brain.”, *Genes & Development*, Vol. 33, No. 10, pp. 511–523.
- Sun, B. K., Z. Siprashvili, and P. A. Khavari, 2014, “Advances in Skin Grafting and Treatment of Cutaneous Wounds.”, *Science*, Vol. 346, No. 6212, pp. 941–945.
- Suzuki, J., K. Yoshizaki, T. Kobayashi, N. Osumi, 2013, “Neural Crest-Derived Horizontal Basal Cells as Tissue Stem Cells in The Adult Olfactory Epithelium.”, *Neuroscience Research*, Vol. 75, No. 2, pp. 112–120.
- Suzuki, M., A. Satoh, H. Ide, and K. Tamura, 2007, “Transgenic *Xenopus* with prx1 Limb Enhancer Reveals Crucial Contribution of MEK/ERK and PI3K/AKT Pathways In Blastema Formation During Limb Regeneration.”, *Developmental Biology*, Vol. 304, No. 2, pp. 675–686.

- Theriault, F. M., H. N. Nuthall, Z. Dong, R. Lo, F. Barnabe-Heider, F. D. Miller, and S. Stifani, 2005, “Role for Runx1 in The Proliferation and Neuronal Differentiation of Selected Progenitor Cells In The Mammalian Nervous System.”, *The Journal of Neuroscience*, Vol. 25, No. 8, pp. 2050–2061.
- Torres-Paz, J., and K. E. Whitlock, 2014, “Olfactory Sensory System Develops from Coordinated Movements Within the Neural Plate.”, *Developmental Dynamics*, Vol. 243, No. 12, pp. 1619–1631.
- Trejo, J. L., E. Carro, and I. Torres-Aleman, 2001, “Circulating Insulin-Like Growth Factor I Mediates Exercise-Induced Increases in The Number of New Neurons In The Adult Hippocampus.”, *The Journal of Neuroscience*, Vol. 21, No. 5, pp. 1628–1634.
- Van Landeghem, L., J. Chevalier, M. M. Mahe, T. Wedel, P. Urvil, P. Derkinderen, T. Savidge, and M. Neunlist, 2011, “Enteric Glia Promote Intestinal Mucosal Healing via Activation of Focal Adhesion Kinase and Release of proEGF.”, *American Journal of Physiology: Gastrointestinal and Liver Physiology*, Vol. 300, No. 6, pp. 976–987.
- Varadarajan, S. G., J. L. Hunyara, N. R. Hamilton, A. L. Kolodkin, and A. D. Huberman, 2022, “Central Nervous System Regeneration.”, *Cell*, Vol. 185, No. 1, pp. 77–94.
- Verhaagen, J., A. B. Oestreicher, W. H. Gispen, and F. L. Margolis, 1989, “The Expression of the Growth Associated Protein B50/GAP43 In The Olfactory

- System of Neonatal and Adult Rats.”, *The Journal of Neuroscience*, Vol. 9, No. 2, pp. 683–691.
- Vlahos, C. J., W. F. Matter, K. Y. Hui, and R. F. Brown, 1994, “A specific Inhibitor of Phosphatidylinositol 3-Kinase, 2-(4-morpholinyl)-8-phenyl-4H-1-benzopyran-4-one (LY294002).”, *The Journal of Biological Chemistry*, Vol. 269, No. 7, pp. 5241–5248.
- Wan, J., R. Ramachandran, and D. Goldman, 2012, “HB-EGF Is Necessary and Sufficient for Müller Glia Dedifferentiation and Retina Regeneration.”, *Developmental Cell*, Vol. 22, No. 2, pp. 334–347.
- Wang, E., and C. A. Higgins, 2020, “Immune Cell Regulation of The Hair Cycle.”, *Experimental Dermatology*, Vol. 29, No. 3, pp. 322–333.
- Watson, J. K., S. Rulands, A. C. Wilkinson, A. Wuidart, M. Ousset, A. Van Keymeulen, B. Göttgens, C. Blanpain, B. D. Simons, and E. L. Rawlins, 2015, “Clonal Dynamics Reveal Two Distinct Populations of Basal Cells in Slow-Turnover Airway Epithelium.”, *Cell Reports*, Vol. 12, No. 1, pp. 90–101.
- Weiler, E., and A. I. Farbman, 1998, “Supporting Cell Proliferation In The Olfactory Epithelium Decreases Postnatally.”, *Glia*, Vol. 22, No. 4, pp. 315–328.
- Wen, X., L. Jiao, and H. Tan, 2022, “MAPK/ERK Pathway as a Central Regulator in Vertebrate Organ Regeneration.”, *International Journal of Molecular Sciences*, Vol. 23, No. 3, p. 1464.

- Wu, Q., X. Xu, X. Miao, X. Bao, X. Li, L. Xiang, W. Wang, S. Du, Y. Lu, X. Wang, D. Yang, J. Zhang, X. Shen, F. Li, S. Lu, Y. Fan, S. Xu, Z. Chen, Y. Wang, H. Teng, . . . Z. Huang, 2022, YAP Signaling in Horizontal Basal Cells Promotes the Regeneration of Olfactory Epithelium After Injury.”, *Stem Cell Reports*, Vol. 17, No. 3, pp. 664–677.
- Xiao, J. H., X. Feng, W. Di, Z. H. Peng, L. A. Li, P. Chambon, and J. J. Voorhees, 1999, “Identification of Heparin-Binding EGF-Like Growth Factor As A Target in Intercellular Regulation of Epidermal Basal Cell Growth by Suprabasal Retinoic Acid Receptors.”, *The EMBO Journal*, Vol. 18, No. 6, pp. 1539–1548.
- Xie, J., and R. Weiskirchen, 2020, “What Does the “AKT” Stand for in the Name “AKT Kinase?” Some Historical Comments.”, *Frontiers in Oncology*, Vol. 10, p. 1329.
- Xue, W., Y. Zhao, Z. Xiao, X. Wu, D. Ma, J. Han, X. Li, X. Xue, Y. Yang, Y. Fang, C. Fan, S. Liu, B. Xu, S. Han, B. Chen, H. Zhang, Y. Fan, W. Liu, Q. Dong, and J. Dai, 2020, “Epidermal Growth Factor Receptor-Extracellular-Regulated Kinase Blockade Upregulates TRIM32 Signaling Cascade and Promotes Neurogenesis After Spinal Cord Injury.”, *Stem Cells*, Vol. 38, No. 1, pp. 118–133.
- Yang, A., R. Schweitzer, D. Sun, M. Kaghad, N. Walker, R. T. Bronson, C. Tabin, A. Sharpe, D. Caput, C. Crum, and F. McKeon, 1999, “p63 Is Essential For Regenerative Proliferation in Limb, Craniofacial and Epithelial Development.”, *Nature*, Vol. 398, No. 6729, pp. 714–718.

- Yin, J., and F. S. Yu, 2009, “ERK1/2 Mediate Wounding and G-Protein-Coupled Receptor Ligands-Induced EGFR Activation via Regulating ADAM17 and HB-EGF Shedding.”, *Investigative Ophthalmology & Visual Science*, Vol. 50, No. 1, pp. 132–139.
- Zepp, J. A., and E. E. Morrissey, 2019, “Cellular Crosstalk in The Development and Regeneration of The Respiratory System.”, *Nature Reviews: Molecular Cell Biology*, Vol. 20, No. 9, pp. 551–566.
- Zhang, W., and H. T. Liu, 2002, “MAPK Signal Pathways in The Regulation of Cell Proliferation in Mammalian Cells.”, *Cell Research*, Vol. 12, No. 1, pp. 9–18.
- Zhou, B. P., Y. Liao, W. Xia, B. Spohn, M. H. Lee, and M. C. Hung, 2001, “Cytoplasmic Localization of p21Cip1/WAF1 by Akt-Induced Phosphorylation in HER-2/Neu-Overexpressing Cells.”, *Nature Cell Biology*, Vol. 3, No. 3, pp. 245–252.
- Zhou, Y., A. M. Bond, J. E. Shade, Y. Zhu, C. O. Davis, X. Wang, Y. Su, K. J. Yoon, A. T. Phan, W. J. Chen, J. H. Oh, N. Marsh-Armstrong, K. Atabai, G. L. Ming, and H. Song, 2018, “Autocrine Mfge8 Signaling Prevents Developmental Exhaustion of the Adult Neural Stem Cell Pool.”, *Cell Stem Cell*, Vol. 23, No. 3, pp. 444–452.
- Zimmermann, S., and K. Moelling, K, 1999, “Phosphorylation and Regulation of Raf by Akt (Protein Kinase B).”, *Science*, Vol. 286, No. 5445, pp. 1741–1744.

Zocher, S., S. Schilling, A. N. Grzyb, V. S. Adusumilli, J. Bogado Lopes, S. Günther, R. W. Overall, Y. Winter, and G. Kempermann, 2020, “Early-Life Environmental Enrichment Generates Persistent Individualized Behavior in Mice.”, *Science Advances*, Vol. 6, No. 35, p.1478.

APPENDIX A: EQUIPMENT AND SUPPLIES

Table A.1. Equipment and Supplies.

EQUIPMENT	COMPANY
-20°C Freezer	Uğur, Turkey
-80°C Freezer, Farma 723	Uğur, Turkey
4°C Room	Birikim Elektrik, Turkey
Aquatic Habitats	Pentair Aquatic, USA
Oven	Nüve, Turkey
Capillary glass (1.00 mm ´ 0.75 mm ´ 10”)	Warner Instruments, USA
Jar	VWR, USA
Confocal Microscope, SP5-AOBS	Leica Microsystems, Germany
Confocal Microscope, TCS SP8	Leica Microsystems, Germany
Cryostat CM3050S	Leica Microsystems, Germany
PAP pen	Leica Biosystems, Germany
Forceps, FST	Dumont, Switzerland
Eppendorf Tube	Eppendorf, Germany
Humidity chamber	
Pasteur Pipette	
Glass Slides - Superfrost® Plus	Thermo Scientific, USA
Thermomixer	Eppendorf, Germany
Microinjector, FemtoJet	Eppendorf, Germany
Oil Microinjector	Narishige, Japan
Orbital shaker, Rotamax 120	Heidolph, Germany
P-97 Micropipette Puller	Sutter Instrument, Co., USA
pH-meter	Mettler Toledo, Switzerland
Stereomicroscope	Zeiss, Germany
Vortex - Genie 2	Scientific Industries, Inc., USA
U-100 insulin needle (30G)	Beckon Dickinson, USA

APPENDIX B: SOLUTIONS, BUFFERS, ANTIBODIES

Table B.1. Solutions, Buffers, Antibodies.

1% Triton X-100 Solution	
150 mM Tris-HCl (pH = 9)	
3% BSA Solution	
4% Paraformaldehyde (PFA) Solution	
1 X PBS	
1 X PBS-T	
10 X PBS	
Click-IT Detection Kit	Thermo
Tricaine	Sigma
Triton X-100, A4975	Appllichem
Phenol Red, A7615,01001	Appllichem
Optimum Cutting Temperature Compound (OCT), 4583	Sakura Finetek
DAPI (0,1 g/L)	Thermo
Alexa488 antibody (anti-rabbit)	Thermofischer, USA
Cy3 antibody (anti-mouse)	Jackson Immuno
Cy2 (mouse anti-rat)	Jackson Immuno
Cy5 (rabbit anti-mouse)	Jackson Immuno
Anti-mouse-HuC/D antibody, 16A11, 1661237	Life Technologies, USA
Anti-BrdU	Abcam Cat no:Ab6236
pERK antibody (rabbit; Cell signaling)	4370S
PCNA antibody (mouse; O84M4776)	Sigma-Aldrich
pAKT antibody (rabbit; Cell signaling)	2965S